2017

Compromising the 20S Proteasome Activates a Quality Control Pathway to Mitigate Proteotoxic Stress

Irit Shachrai

COMPROMISING THE 20S PROTEASOME ACTIVATES A QUALITY COTROL PATHWAY TO MITIGATE PROTEOTOXIC STRESS

A Thesis Presented to the Faculty of

The Rockefeller University

in Partial Fulfillment of the Requirements for

the degree of Doctor of Philosophy

by

Irit Shachrai

June 2017

COMPROMISING THE 20S PROTEASOME ACTIVATES A QUALITY COTROL PATHWAY TO MITIGATE PROTEOTOXIC STRESS

Irit Shachrai, Ph.D.

The Rockefeller University 2017

The regulation of the ubiquitin-proteasome system (UPS) has been the subject of a vast body of work because of its implication in normal development and a wide range of diseases. The UPS controls the degradation of a large number of cellular proteins and thereby regulates essential cellular processes critical for cellular adaptation and more. Amongst the main processes are removal of mis-folded and potentially toxic proteins, cell's loss of protein quality control is often associated with muscle atrophy and neurodegenerative diseases. The proteasome is subject to tight regulation, as many different proteins govern its transcription, assembly, stability and activity. Consequently, its regulation is extremely complex and even further complicated by the fact that all the above events are responsive to changing cellular environment and different pathophysiological conditions. Although the proteasome has been studied extensively, much still remains unknown, especially missing is a detailed mechanism as to how its complexed and multi-phased assembly adapts to proteotoxic stress.

In this thesis I used a proteasome impaired genetic background to screen for suppressors of proteotoxic stress which modify proteasomes adaptive tress response. To my surprise I identified a core 20S subunit of the proteasome, $\alpha 1$ subunit. This finding uncovered its functional interaction with a yet un-characterized regulator of proteasome

stability in *Drosophila,* Ecm29 (CG8858). Whereas much is known of proteasome stress response at the level of its expression, very little is known of adaptive responses through alternative assembly. The results of this thesis suggest a new mechanism for proteasome stress adaption through modified assembly. To date most studies of proteasome regulation focused on the regulatory particle as master regulator and overlooked participation of the proteasome core particle in regulatory function. This thesis exemplifies the significance of the core particle, specifically its α ring, as an integral entity in the regulation of protein degradation by the proteasome. The overall findings demonstrate vitality of the proteasomes as active players in the response to proteotoxic stress. Furthermore, they define regulation of proteasome assembly as a mechanism to control suitable protein turnover and healthy cellular function.

Dedicated to my grandmothers Fruma Shor and

Miriam Shachrai, my heart and brain

Acknowledgements

I would first like to convey my deep gratitude for my mentor and head of lab, Hermann Steller, for his leadership and support. My first day in lab started with stepping through the open door to your office and throughout my entire journey that door never closed. Your guidance and advice on how to communicate, think and develop an idea, complemented with your thoughtful listening and insight, got me through all the hurdles of a graduate student. As I take the last steps in this journey, I know I will leave with a profound sense of possibility thanks to you.

The Steller lab is filled with brilliant and kind people, and I thank them all past and present. Above all I would like to acknowledge Sigi Benjamin-Hong, for not only sharing your profound scientific wisdom but also for sharing your home and heart with me at times of trouble. Starting my days next to Sigi, and my south lab confidant Ainoha Perez Garijo was the best part of my day and this work would not have been possible without both of you. Ainoha, thank you for teaching me how to "Ainoha it". I am also especially grateful to Joe Rodriguez, you are a library of knowledge and body of warmth and compassion, your un-wavering will to help and guide is a model we should all aspire to. Yetis Gultekin, thank you for reminding me how scientific excitement looks like and for all those moments of joy and laughter I got to share with you and Sandra Jones, my wonderful bay mate. The work of the entire technical staff was invaluable but especially the hard work of Olga Matthews, thank you for your sweet presence and apple plates. A special nod to Yaron Fuchs, it might not have been a smooth ride for us in the beginning but what a soothing harbor and loyal friend I found in you.

I would like to thank my committee members Michael Young and Shai Shaham. I thank you for your support and guidance, thoughtful advice, direction and solutions during more difficult patches of the project. I would also like to thank my external examiner Mary Baylies from MSKCC for imparting her time and knowledge for me. Special thanks to the Dean's office and all its members, your generous support and care for students is priceless.

This work is not only a work of the mind but also of the heart and I thank all my friends for bolstering my heart. Stefanie Gersrberger, what can I say that you don't already know since you are my left half brain. Gianna Triller and Sasha Jereb, whether through an ocean apart or simply a wall separating us, your emanating warmth and helping hand always kept me going. Ivana Socoloff, so many years and so many good times to be thankful for but it is especially the hard times that I am thankful for facing together with you, I love you for your tough critique and soft heart. Karen Boyer, it is our time as roommates in apartment 10 that pushed us to face new mountains but it is our time as friends that will get us to the peak, you and Jay Grabowski are a corner stone of comfort and support.

Last but always first in my heart, my loving parents, Avigdor and Zipora, thank you for not only giving me life but more than that for giving me a future I could fill with dreams. Thanks to you building a wonderful home, a place to always come back to, I could spread my wings and never waver. Thank you for my dear sister Yael, brother Eyal, their partners Elad and Michal, and kids Yuval, Alma, Or, Omer and Daniel, for all the love you gave me and smiles you put on my face.

Table of Contents

List of Figures

List of Tables

1. Introduction

1.1 The Ubiquitin Proteasome System

The cellular protein pool is under continuous change and its regulation is crucial for normal cellular function. Loss of protein homeostasis has been implicated in many pathological conditions, most noted cancer, aging, muscle atrophy and a plethora of neurodegenerative diseases. The UPS is the primary degradation system that mediates the degradation of short-lived regulatory proteins and the removal of damaged soluble proteins. The UPS is involved in a diverse array of biological processes, including cell-cycle progression, DNA repair, apoptosis, immune response, signal transduction, transcription, metabolism, protein quality control and developmental programs.

As proteasome-mediated degradation plays a key role in essentially all cellular processes, its own regulation is primal for preserving cellular homeostasis. Proteasome activity is regulated at several levels: from its expression levels to the rate of assembly and stability, further fine-tuned by its localization and conformation changes due to post-translational modifications and binding of different accessory proteins and activators. Given the diversity and complexity of proteasome regulation, marked by a growing number of proteasome associated proteins being identified, it is becoming clear that the proteasome is more than just a static funnel for degradation as once imagined but rather a dynamic player in shaping the cellular proteomic profile.

1.1.2 Proteasomes and the ubiquitin pathway

Proteins are targeted for degradation by the proteasomes with a ubiquitin tag, covalently attached to lysine residues in substrate proteins. Ubiquitin (Ub) conjugation is ATP dependent and is achieved via an enzymatic cascade involving three distinct classes of enzymes: E1 (Ub-activating enzyme) hydrolases ATP and forms a thioester-linked conjugate between itself and ubiquitin; E2 (Ub-conjugating enzyme) receives ubiquitin from E1 and forms a similar thioester bond; and E3 (Ub ligase) binds both E2 and the substrate, mediating ubiquitin transfer to the substrate (Glickman and Ciechanover, 2002). Sub sequential reactions link additional ubiquitin molecules to the primary ubiquitin via internal ubiquitin lysines, thus creating a ubiquitin chain. A chain of at least four ubiquitins linked via lysine 48 is the classical recognition motif for proteasomal degradation (Thrower et al., 2000). Though other linkage types exist they are mostly used for signal propagation at different pathways rather than as a degradation signal. De-ubiquitinating enzymes (DUBs) remove polyubiquitin from proteasome substrates before substrates are translocated into the proteasome to rejoin the free ubiquitin pool. Substrate specificity is mostly achieved through the E3 enzyme (Finley, 2009). The most common and best understood E3 ligases are the Cullin-RING Ub ligases, they form a complex with F-box proteins which mediate substrate binding. The versatility of the Cullin proteins and their binding partners facilitates the recognition and ubiquitination of a large number of diverse proteins (Glickman and Ciechanover, 2002). Additionally, tissue specific expression of the Ub ligases contributes to substrate specificity, for example the muscle specific E3 ligases:

Muscle RING Finger 1 (MuRF1) and the Muscle atrophy F-box (MAFbx) (Bodine et al., 2001).

1.1.3 Proteasome Structure

Protein degradation is a vital process of life but when left un-checked it presents a major threat. Cells have developed several mechanisms to ensure specific activity of their proteases. The proteasome is a multi-subunit protease, uniquely controlled by its structure and composition. Protein degradation is contained in a hollow cylinder with sequestered active sites. The 26S eukaryotic proteasome is composed of the catalytic particle (CP,20S) capped by either one or two regulatory particles (RP,19S). (Kunjappu and Hochstrasser, 2014) (Figure 1.1). The CP is composed of four stacked hepta-heteromeric rings, forming a barrel shape structure. All proteasomes are composed of two related types of subunits, α subunits which form the two outer rings and β subunits which form the two inner rings. The β rings enclose an inner chamber in which the proteolytic activity is contained and carried by three dedicated β subunits: β1, β2 and β5. Each of these subunits convey site specificity to a broad range of peptide sequences, but are different from each other in their preferred site. Each of these subunits has a specific activity and are classified as caspase-like (β1), trypsin-like (β2) and chymotrypsin-like (β5) proteases (Arendt and Hochstrasser, 1997). The protein is sequentially degraded into small peptides, which upon exit into the cytoplasm are rapidly removed by amino-proteases.

Substrates gain entry to the core particle's interior through a gated axial channel formed by the N-termini of the α subunits (Rabl et al., 2008). For proteolysis to take place the proteasome must assume an open gate conformation. The α subunit tail is evolutionary

conserved between species however its sequence differs between the seven subtypes. Mutant analysis revealed that not all α subunits N-termini contribute to this gate in the same level of importance (Groll et al., 2000; Tian et al., 2011). For example, α3 mutants in comparison to α7 mutants are more deleterious to gate closure and functioning proteasome activity. Interestingly, the importance of the tails in the gate function correlates with their evolutionary conservation, as is exemplified by α3 and α7 subunits.

Even in the open gate conformation, the pore is still too narrow. For proteins to enter the catalytic chamber, they must first unfold and be freed of their ubiquitin tag, both events are highly regulated involving the RP as well as additional accessory proteins. The α subunits interact with the regulatory complex to control the opening and closing of the gated pore. The RP is divided into two sub-particles, the base and the lid (Figure 1.1). The base is made of 6 ATPases (Rpt1-6) forming a ring that sits on top of the CP, and three proteins, Rpn1, Rpn2 and Rpn13. The lid is composed of Rpn3,5-9,11,12 and 15 with Rpn10 sitting at the interface between the lid and base (Murata et al., 2009). Some of the base subunits capture ubiquitylated proteins either directly or through proteins that contain both UBL (ubiquitin-like) domains and UBA (ubiquitin-associated) domains. The one known function of the lid involves Rpn11 in de-ubiquitinating the substrates prior to entry into the channel. The function of other lid subunits is still un-known. The ATPase ring provides energy and assist in substrate unfolding and mechanical opening of the CP gate. The pockets formed between two adjacent α subunits serve as docking site for the C-termini tails of the Rpt proteins, hence playing an important regulatory and structural role in the gate configuration and the holo-complex stability (Tian et al., 2011). Some of the Rpt subunits contain a unique motif at their C-terminus, termed HbYX (hydrophobic-

tyrosine-X) motif, which mediates binding to the alpha pocket and subsequent gate conformational changes (Smith et al., 2007). Later studies have shown that multiple regulators and interacting proteins of the 20S proteasome also possess an HbYX motif that inserts into these same surface pockets between the α subunits and can induce gate opening (Dange et al., 2011; Kusmierczyk et al., 2011; Yu et al., 2010).

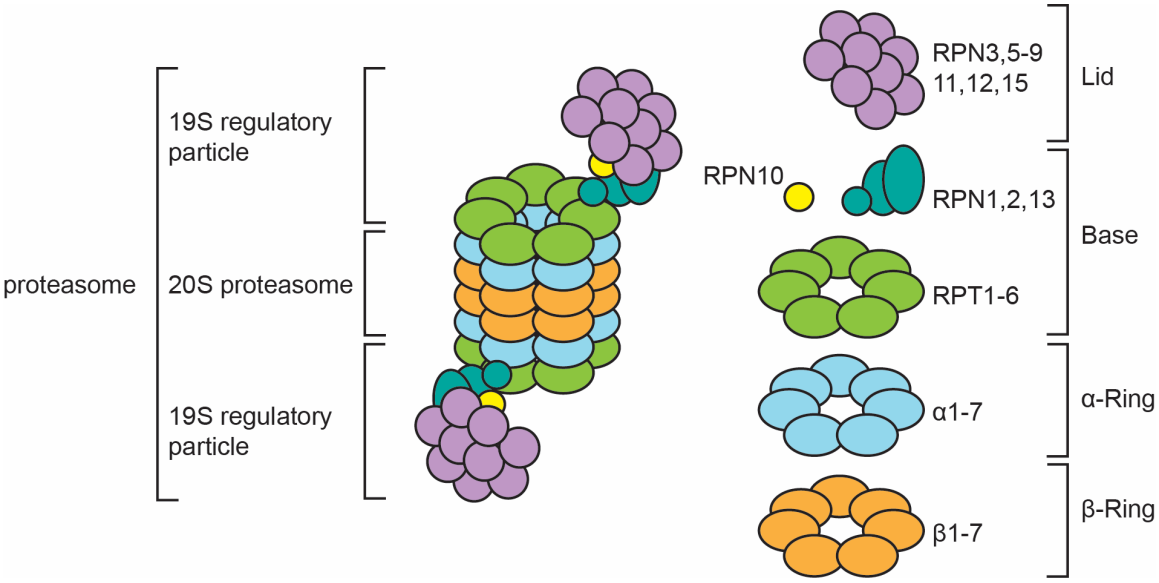

Figure 1.1. Subunit composition and structure of the proteasome. The 26S proteasome consists of two particles, the 20S core particle with catalytic function and the 19S regulatory particle. The 20S particle is built of four hepta-oligomeric rings, two outer α subunits ring (blue) and two inner β subunits ring (orange). The RP is made of two sub-complexes, the lid (purple) and base (green). The base is composed of both RPT and RPN subunits whereas the lid from RPN only. RPN10 (yellow) is found at the base–lid interface. Not depicted in this diagram are the various proteasome associating proteins as they are not proteasome stoichiometric subunits. Picture adapted from (Murata et al., 2009).

1.1.4 26S Proteasome assembly

The 20S proteasome assembly proceeds through an ordered series of intermediates with step-wise addition of subunits (Figure 1.2). Assembly initiates with the progressive assembly of the α ring on top of which the β ring is later formed, together they make a half CP. In the final step two half CP attach through the β subunits and form the complete core particle (Zwickl et al., 1994). In mammalian cells, systematic knockdowns of individual subunits suggested that β2 and β7 are the first and last β subunit added to the α ring respectively (Hirano et al., 2008). Free β subunits are synthesized with a C-terminal pro-peptide, rendering them inactive as proteases. This appendage is not found inside the mature proteasome so β subunits can be active in proteolysis. This mechanism prevents dis-regulated proteolysis by immature proteasomes. β7 incorporation stimulates the autocatalytic processing of the β-propeptides marking the final step in proteasome maturation (Li et al., 2007; Ramos, 2004).

An important gap in our current knowledge is whether RP assembly depends on the CP as template or whether it occurs independently of the CP. There are conflicting reports on this question, but it is possible that both mechanisms contribute to RP assembly. Previous studies in yeast suggested that Rpt ring assembly is guided in part by a pre-existing CP (Kusmierczyk et al., 2008; Park et al., 2009; Roelofs et al., 2009). This model supports RP assembly in a modular way. One subset of Rpt subunits assembles directly on the CP, including Rpt4 and Rpt6, and the corresponding mutants show the strongest assembly phenotype (Hendil et al., 2009; Park et al., 2009). Another group of Rpt subunits, including Rpt1, Rpt2 and Rpt5, is thought to initially assemble freely of the CP into a base intermediate called BP1, which later incorporates onto the existing RP-CP intermediate.

Of particular importance to this model is that both α subunit mutants and Rpt mutants show the accumulation of Rpt ring assembly intermediates. Further support is provided by the alternative proteasome lacking α3 which resulted in alternative RP intermediates (Kusmierczyk et al., 2011). Cells lacking α3 still form intact proteasomes however they also display many more types of different 19S intermediates. Interestingly, the tail of Rpt6, key subunit in promoting 19S assembly, was found to specifically cross-link with α3.

In contrast Kim and DeMartino showed that Rpt subunits with a 26S assembly defect (C-terminal truncation) were still found in intact 19S. Intact 19S was also found when 20S content was reduced by β5 RNAi; the RNAi reduced β5 content by more than 90% and proteasome activity in cell extracts by ~75% (Kim and DeMartino, 2011). These results support a model in which 20S is not an obligatory template for 19S assembly. However, the Rpts in question were Rpt3 and Rpt5, which belong to the subset of proteins that assembles into BP intermediates freely of 20S. Additionally, it is possible that the lid spontaneously attaches to the base when the base is in access due to assembly disruption. Order and timing of Rpt assembly is regulated by a set of four RP chaperones (Roelofs et al., 2009). A detailed mechanism of how the RP chaperones interact with the CP is still missing and additional studies are needed to shed light on this intricate assembly program.

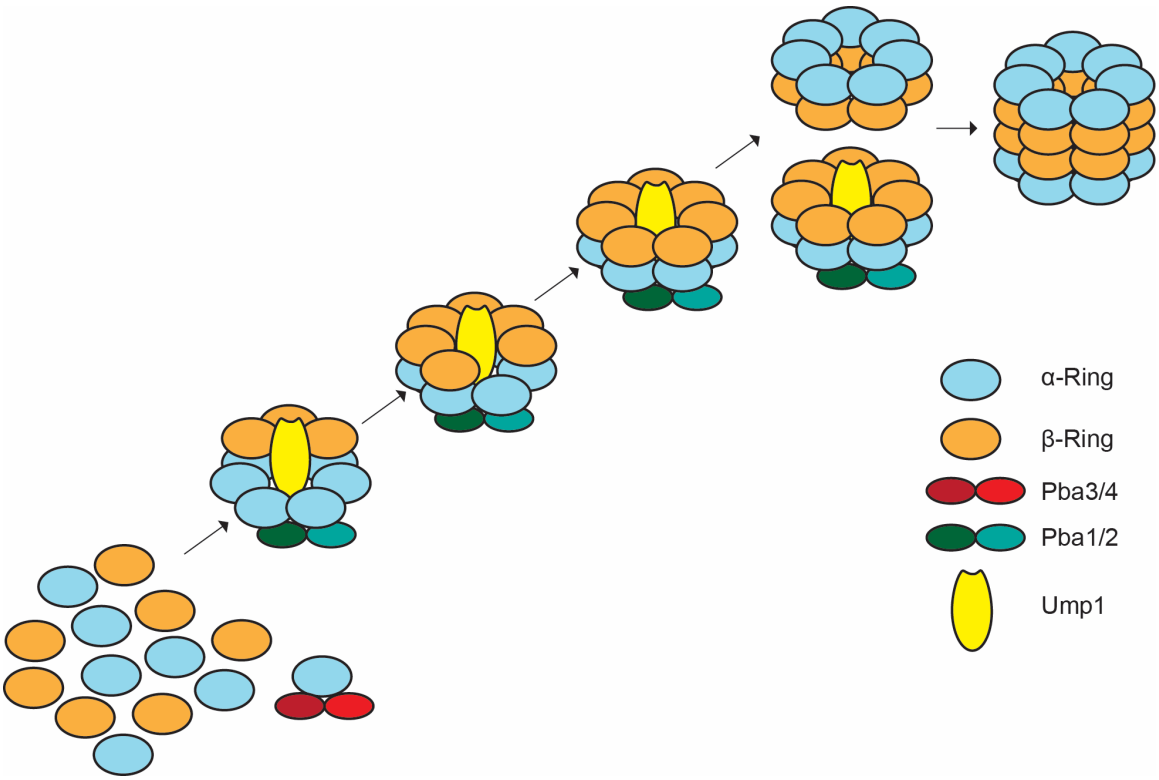

Figure 1.2. Core particle assembly is a multi-step process. α ring (blue) assembly starts with α5 with the aid of Pba3-Pba4 (red) chaperone dimer, followed by integration of α4 and α3 also guided by Pba3-Pba4. Pba1-Pba2 (green) provides scaffold for ring formation and prevent off-pathway interactions of two α subunit rings. β ring (orange) assembly is orchestrated on top of the formed α ring with the aid of Ump1 (yellow), starting with the addition of β2, β3 and β4. The last one to be incorporated is β7. Ump1 presides over this check point to prevent premature association of two half core particles. The dimerization of the half-proteasomes forms the pre-holoproteasome that is still immature. CP maturation is achieved by the autocatalytic processing of the β subunit propeptides and the degradation of the Ump1 chaperone. The Pba1-Pba2 chaperone also manages the maturation step and is supposedly degraded by the mature 20S. This process yields a functional CP competent for protein degradation. Picture adapted from (Kunjappu and Hochstrasser, 2014).

1.1.5 20S assembly chaperones

α subunits possess the intrinsic ability to self-assemble, but for efficient and correct assembly dedicated chaperones are recruited (Gerards et al., 1997; 1998; YAO et al., 1999). These chaperones interact with intermediates to guide assembly in an organized and timely fashioned manner but are not found on the mature proteasome. Dedicated 20S chaperones have been identified and studied in archaea, yeasts and mammals; although functionally related they are not orthologues (Hirano et al., 2005; Kusmierczyk et al., 2008; 2011). The first 20S assembly chaperone to be identified was Ump1 in yeast (called hUMP1 or POMP1 in humans), continuing with the identification of the heterodimeric chaperones Pba1-Pba2 (human PAC1-PAC2, PbaA-PbaB the only chaperone to be found in archaea) and Pba3-Pba4 (human PAC3/PAC4). Two additional factors, Blm10 and Ecm29, have been proposed to have roles in 20S proteasome assembly, but they are also thought to have other functions. The assembly chaperones can act slightly differently in different species: for instance in mammals, it has been shown that Ump1 can inhibit dimerization of two half particles but not in yeasts (Ramos et al., 1998; Witt et al., 2000). These differences are evident in their mutant phenotypes, which exhibit stronger phenotypes in mammals than in yeasts. Under normal conditions, their absence only has minimal effects on organismal growth despite slower and aberrant proteasome assembly, suggesting compensatory pathways and adaptation mechanisms. But when proteasome function is compromised by other mutants or environmental conditions, their absence is strongly deleterious or even lethal (Kusmierczyk et al., 2008; 2011; Ramos et al., 1998). Many mechanistic details of assembly factors function remain unknown and even less is known in Drosophila, where no 20S chaperones have been identified yet.

Ump1 was first identified as a chaperone needed to orchestrate β-subunit processing and 20S proteasome maturation (Ramos et al., 1998). β5 propeptide is normally thought essential for proteasome assembly and cell viability with the exception of when Ump1 is also deleted. Based on these data, β5 propeptide interacts with Ump1 to facilitate its auto-cleavage thus Ump1 is no longer needed in its absence. Years later an added function was described by Li *et al.,* showing that high levels of β7 can suppress defects associated with loss of the β5 propeptide and that this suppression requires the β7 C-tail to enhance 20S half-mer dimerization (Li et al., 2007). Overall Ump1 presides an assembly checkpoint; by inhibiting half CP dimerization and 20S maturation until all β subunits are properly incorporated.

PAC1–PAC2 heterodimer was first identified by its interaction with α-ring intermediates in human cells (Hirano et al., 2005). Knockdown led to compromised proteasome assembly and the accumulation of aberrant α-ring dimers indicating it was needed to prevent the off-pathway interaction of two α-subunit rings. Loss of Pba2 also led to the accumulation of poly-ubiquitinated proteins pointing to a proteotoxic stress (Le Tallec et al., 2007). PAC1 knockout mice are embryonic lethal, however yeast deleted for either one or both Pba1 and Pba2 show no growth defects. Though their absence does aggravate the phenotypic defects of other UPS genes mutants such as α3 and Rpn4, remarkably deletion of either one of them suppresses the growth defect of ΔUmp1 (Li et al., 2007). Interestingly, these chaperones possess C-terminal HbYX motifs like Rpt proteins and the recently identified proteasome activator, PI31 (Bader et al., 2011). The Pba1 and Pba2 HbYX motifs both contribute to chaperone function and proteasome precursor binding (Kusmierczyk et al., 2011).

Pba3-Pba4 serves as a scaffold on which α ring assembly is guided in a specific order, especially ensuring that the α3 subunit is positioned between the α2 and α4 subunits in the ring (Kusmierczyk et al., 2008). Knockdown of the mammalian PAC3 or deletion of either Pba3 or Pba4 resulted in retarded growth and proteasome assembly defects (Kusmierczyk et al., 2008; Le Tallec et al., 2007). Velichutina and colleagues showed in yeasts that in the absence of the chaperone dimer Pba3-Pba4 or α3 subunit, alternative proteasomes can be created with α4 as a substitute for α3 subunit (Velichutina et al., 2004). Recently, such proteasomes were also found in human cells (Padmanabhan et al., 2016). These alternative proteasomes can be formed naturally, albeit at a slower pace than the canonical proteasomes, suggesting that proteasome-dedicated chaperones provide structural flexibility of the proteasome depending on cellular environment. Interestingly, it has been shown that they have an advantage under specific stresses such as high metal and oxidative stress (Kusmierczyk et al., 2011). Moreover, chronic oxidative stress may alter proteasome assembly such that assembly of α4-α4 proteasomes is favored. Such proteasomes are expected to have a constitutively open α ring (Osmulski et al., 2009) and are thus better equipped to deal with high influx of damaged proteins. Additionally, the α4-α4 surface may interact differently with proteasome regulatory factors such as the RP and others.

1.1.6 Regulation of CP-RP interaction

The 20S is normally found in a latent form with a closed gate. A closed gate prevents the majority of proteins from entering the catalytic chamber to be degraded. Evading this mechanism are small peptides and partially un-folded proteins. The binding

of the regulatory particle is primary for gate opening. In the past year a cohort of high resolution structural analyses of the human proteasome reported the surprising observation that despite engagement of the RP ATPase with the CP outer ring, the CP gate remained closed (Chen et al., 2016; Huang et al., 2016; Schweitzer et al., 2016). The 26S can assume 4 different confirmations of which only one has an open gate. In the three closed confirmations only Rpt 3 and Rpt2 (Rpt5 in yeast) insert their tails into CP surface pockets. In the last active confirmation, all Rpt tails are inserted except Rpt4. Together with previous functional data (Kim and DeMartino, 2011; Lee et al., 2012b; Tian et al., 2011), it is now clear that not all subunits contribute to proteasome function symmetrically and some interactions might even contribute negatively. Since the capacity of the proteasome to degrade proteins depends crucially on RP-CP interaction and with so many factors affecting this interaction, it seems highly likely that this interface is subjected to complex regulation.

Though still not completely understood, there are some data supporting a model in which dynamic changes at distal points within the CP might regulate interactions occurring on the surface of the proteasome. Kusmierczyk and colleagues suggested that the archaeal chaperones PbaA-PbaB recognize immature 20S particles due to the presence of β subunits pro-peptides, implying that their binding is regulated allosterically by changes that are initiated at distant sites (Kusmierczyk et al., 2011). This model is supported by the observation that the chaperones bind stably to a 20S whose active sites are bound to inhibitors, mimicking an active proteolytic state of the propeptides (Kleijnen et al., 2007). Inhibition of proteasome active sites also stabilized 26S proteasomes, suggesting that the interface between the RP and the 20S proteasome dynamically changes depending on the

activities of the 20S proteasome. Interestingly, in yeast despite a lid assembly mutant of Rpn5, the base and 20S still assembled normally; however, they could not form a stable complex. It was proposed that the association of the lid with the base induces some conformational change in the base that strengthen and stabilize its association with the 20S proteasome (Isono et al., 2007).

Proteasome interacting proteins have been shown to regulate RP association with the 20S proteasome, most notably the Extracellular matrix 29 (Ecm29). Intact 26S proteasomes can be purified without ATP when Ecm29 is present, but ATP is required for maintaining a stable RP–CP interaction in the absence of this factor. This suggests that Ecm29 can stabilize the 26S proteasome complex (Kleijnen et al., 2007; Leggett et al., 2002). Ecm29 is a large protein of approximately 200 kDa with HEAT repeat motifs, repeats of α helices linked by a short loop, making it also a flexible one. Since it can bind to both the RP and the 20S proteasome in yeast it is likely that Ecm29 stabilizes 26S proteasomes by tethering the 20S proteasome to the RP. Ecm29 has a broader function and can act through several pathways (further details are outlined in Chapter 3). Another example of proteasome-stabilizer is a complex of p27, RPT4 and RPT5 which was found to enhance the proteolytic activity of the proteasome in mammalian cells by promoting the association of the RP and CP (Adams et al., 1997). However, the details of the mechanism in action remain unknown. Regulation of the RP-CP interface under stress adaptation has been mostly overlooked so far. But the increasing number of proteasome-interacting proteins suggests that 26S proteasomes are more diverse in their composition in response to various stimuli than previously assumed. The study of these proteins will lead to new perspectives on the dynamics of this uniquely complex machine.

1.1.7 Proteasome interacting proteins

In addition to the proteasome core subunits, many different proteins associate with the proteasome and influence its activity; some have been studied, but many more remain a mystery (Schmidt et al., 2005b). Interacting proteins are defined by their salt liability and sub-stoichiometric levels. Numerous well-documented examples illustrate how such proteins are changing views of proteasome function and regulation.

Several E3 ubiquitin ligases are found on proteasome, and in some cases this interaction was found to be important for their ligase activity (Chuang and Madura, 2005; Sakata et al., 2003; Seeger et al., 2003; Xie and Varshavsky, 2002). Ufd4 is an E3 ligase, which binds to the 26S proteasome through its N-terminal domain, presumably to Rpt4 and Rpt6. A truncated Ufd4, devoid of his N-terminal domain, can still catalyze ubiquitination of its substrates but does not promote their degradation (Xie and Varshavsky, 2002), indicating that for this E3 ligase both ubiquitination and proteasome association are crucial for degradation of its substrates. Parkin is a Ring ubiquitin ligase implicated in Parkinson disease. Although the pathogenesis of Parkinson is still not completely resolved, one of the disease associated mutations is in Parkin's binding domain to Rpn10 (Sakata et al., 2003). Detailed mechanism of the functional coupling between ubiquitination and degradation can provide better understanding of this disease.

Furthermore, some proteasome interacting proteins have similar roles to those of intrinsic subunits, like ubiquitin-binding, de-ubiquitination and unfolding. For example, in yeast, deletion of Rpn10, the only core subunit to be well-characterized as a receptor for ubiquitinated substrates, barely diminished cellular protein degradation. However, when coupled with a Rad23 deletion, global protein degradation was significantly impaired,

meaning that for some functions, associating proteins can complement core subunits. Rad 23 is part of a larger group of "shuttle" proteins, including Dsk2, Ddi1, the p97/cdc48Ufp1/Npl4 complex, and p62 (Madura, 2004). These proteins contain one or more of the domains capable of binding polyubiquitin (e.g., UBA domains) and N-terminal Ubl (ubiquitin-like) domains that reversibly bind to the RP. Such proteins likely serve as "shuttles" for delivery of poly-ubiquitinated proteins to the proteasome. Mutations in Ubiquilin2 (the human homologue of Dsk2), diminish proteasome activity and associate with the pathogenesis of ALS and dementia (Deng et al., 2011). Although the complexity of such regulation is not well understood, it might represent an important element in determining rate of degradation.

De-ubiquitination is a second important proteasome function supplemented by reversibly interacting proteins. Removal of polyubiquitin chains from substrates is a pre-requisite for proteasome-dependent degradation, however in some cases it can spare substrates from proteolysis. Premature substrate deubiquitination by Uch37, an intrinsic subunit of mammalian RP, actually prevented degradation (Guterman and Glickman, 2004). This mechanism further highlights the general notion that the proteasome actively participates in determining the fate of substrates that reach it. Uch37 does not remove ubiquitin chains in one group but rather shortens them (Lam et al., 1997). Simple truncation in ubiquitin chains might reduce their affinity to the proteasome, or alternatively edit molecules in a way that prevents degradation of lightly ubiquitinated substrates. Similarly yeast Ubp6 (and its mammalian orthologue Usp14) also cleave ubiquitin chains progressively (Guterman and Glickman, 2004). Ubp6 activity is greatly enhanced upon proteasome binding and deletion of its Ubl domain effectively neutralizes it completely. Remarkably, Ubp6 also appears to regulate general aspects of both proteasome and

ubiquitin homeostasis. Inactivation of Ubp6 resulted in a decrease of free ubiquitin which in turn up-regulated Ubp6 expression and its proteasome-associated fraction (Hanna et al., 2007) and additionally higher proteasome levels were marked. This observation suggests a transcription mediated response to ubiquitin stress (more on transcription regulation of the proteasome in section 1.1.9).

1.1.8 Alternative activators of the proteasome

20S proteasomes are known to associate with three, or even four, different families of activators that provide access to the central proteolytic chamber. 19S is the most common and conserved activator. The 19S activator requires ATP hydrolysis to promote the degradation of protein substrates and it mostly mediates degradation of ubiquitin-tagged proteins. The other two activator families are the 11S complexes (aka PA28, REGγ, PA26) and PA200/Blm10. These factors are less broadly conserved. While their substrates and biological functions are not as clear; the mechanisms they use to activate proteasomes have been characterized. Presumably, they have relatively specialized functions and enable largely unstructured proteins or peptides to pass through the degradation channel (Stadtmueller and Hill, 2011). Not too long ago, it was discovered that another form of the proteasome might exist in cells in which the AAA+ protein CDC48 (also known as p97 or VCP) serves as an additional ATPase cap (Barthelme and Sauer, 2012). Hybrid proteasomes that comprise a 19S regulatory particle on one end of the core particle and a different activator at the opposite end also exist, but it is not yet understood how the different caps act together (Cascio et al., 2002; Shibatani et al., 2006; Tanahashi et al., 2000).

After the RP the most intensively studied activator of the CP is proteasome activator PA28 (11S cap) (Förster et al., 2005). In contrast to the RP, PA28 lacks ATPase activity and the ability to bind ubiquitin conjugates. PA28 has been studied primarily in mammals. It is encoded within the MHC locus and is induced by interferon-γ. It is believed that PA28 optimizes efficient cell surface presentation of antigens by MHC class I molecules. It presumably does so by enhancing the cleavage specificity of certain antigens so they are more suited for MHC presentation (Cascio et al., 2002; Goldberg et al., 2002; Groettrup et al., 1996; Strehl et al., 2005), or/and by facilitating rapid exit of the peptide so it is not over-digested (Whitby et al., 2000). Regγ is similar in size to PA28, but is present in more organisms. Unlike PA28 it is not inducible. Since it has no ATPase activity to support unfolding, nor does it contain ubiquitin sensing receptors, it probably mediates the digestion of non-ubiquitinated targets (Masson et al., 2001). Although it is generally reported that 11S activators stimulate the hydrolysis of model peptide substrates but not full length proteins, REGγ has been implicated in the degradation of some naturally occurring unfolded proteins (Nie et al., 2010; Suzuki et al., 2009).

PA200, and its yeast orthologue Blm10 (no orthologue reported in Drosophila) are large and flexible owing to their HEAT-repeat motifs. These proteins assume a dome-shaped spiral atop the CP (Schmidt et al., 2005a). They differ from the 11S caps in that they bind the CP as a monomer, as opposed to the heptameric assemblies of the other two (Iwanczyk et al., 2006). Like 11S caps PA200 does not hydrolyze ATP, but its interaction with the CP disorders the α-ring gate and promotes entry of peptide substrates (Dange et al., 2011). Blm10/PA200 seems to be multi-functional as several reports describe its role as a proteasome assembly factor, activator, or quality-control factor (Dange et al., 2011;

Khor et al., 2006; Lopez et al., 2011; Ustrell et al., 2002). Blm10 has also been proposed to bind preferentially to 20S proteasomes with an open or disordered gate. CP mutants harboring α subunits with a truncated N-termini were found enriched with Blm10 – the same was observed a Ump1Δ mutant (Lehmann et al., 2008). These findings suggest a role for Blm10 in sequestering 20S proteasomes with a non-functional gates, thereby preventing uncontrolled substrate access to the catalytic chamber.

1.1.9 Transcription mediated regulation of the proteasome

Proteasome subunits are found in stoichiometric levels in the holocomplex, suggesting their biogenesis is transcriptionally regulated. Current knowledge regarding the basal rate of proteasome subunit biosynthesis is limited. It is believed that all core subunits are found in cells only in the context of their respective complex, the 20S or 19S. An exception is the 19S subunit Rpn10/S5a, which is also present in a free state in some cell types (Hendil et al., 2002; Piterman et al., 2014). Though information on physiological synthesis rate is lacking, numerous studies demonstrated a concerted upregulation of proteasome subunits in response to stress, uncovering a common signaling pathway regulating proteasome gene expression. The best studied transcriptional regulators of the proteasome are yeast Rpn4 and its mammalian counterpart Nrf1/Nrf2. Metazoan genomes apparently lack an Rpn4 orthologue, and neither a transcription factor nor a DNA regulatory element that regulates proteasome levels has been identified in higher eukaryotes. However, a concerted upregulation of UPS genes was observed in S2 Drosophila cell line upon RNAi-mediated knockdown of Rpn10/S5a or MG132 (proteasome inhibitor) treatment (Lundgren et al., 2005).

Rpn4 acts as a transcription factor, binding a unique sequence upstream to proteasomal genes termed PACE (proteasome associated control element), which stimulates their up-regulation (Mannhaupt et al., 1999). Rpn4 is a short-lived protein, whose degradation is ubiquitin dependent and regulated by the proteasome. Being a proteasomal substrate Rpn4 levels correlate with proteasome activity, making it part of a negative feedback loop which senses reduction in proteasome activity and in response elevates proteasomal genes expression (Xie and Varshavsky, 2001). Rpn4 by itself is regulated by stress factors. It was found that many stress-induced TFs recognize motifs upstream to the RPN4 gene, including factors related to oxidative stress, drug resistance, and heat shock. These findings suggest a possible role for proteasome upregulation under different stress conditions (Ma and Liu, 2010).

Besides common regulatory pathways, an intriguing study suggested that overexpression of a proteasome subunits, β5 or β1, may upregulate the level of other subunits, as well as proteasome assembly and activity (Chondrogianni et al., 2003; 2005). Increased amount of assembled proteasomse conferred enhanced survival following treatment with oxidants, primarily through a higher rate of degradation (Chondrogianni et al., 2005). Additional support regarding auto-regulation of proteasome subunits comes from the work of Wojcik and DeMartino in S2 Drosophila cell line (Wójcik and DeMartino, 2002). RNAi silencing of different proteasomal genes (β5, Rpt1, Rpt2, Rpt5, Rpn2, and Rpn12) resulted in mRNA induction of non-targeted proteasome subunits. These results and others (Meiners et al., 2003) show a concerted regulation of proteasome genes in response to proteasome inhibition, however not all subunits respond equally, suggesting a different regulation between different proteasome subunits.

1.1.10 Tissue specific proteasomes

The proteasome has specialized itself in some tissues by adapting tissue-specific subunits. Vertebrates encode four additional catalytic β-subunits: three interferon (IFN)gamma-inducible β1i, β2i, β5i defining the immunoproteasome (Kloetzel, 2004; Tanaka and Kasahara, 1998) and one thymus-specific β5t subunit defining the thymoproteasome (Murata et al., 2007). These alternative proteasomes have key roles in acquired immunity by altering antigen processing. The immunoproteasome preferable catalytic activities are chymotrypsin-like and trypsin-like activities, generating peptides which are suited for optimal presentation by MHC class I molecules (Kloetzel, 2004; Rock et al., 2004). The reduced chymotrypsin-like activity of the thymoproteasome favorably contributes to production of a unique peptide repertoire in the thymus (Murata et al., 2007; 2008).

Duplication of 20S subunits is also observed in the Drosophila testis. In Drosophila melanogaster, 13 of the 28 CP proteasome subunits are found to have testis-specific isoforms and in some cases they even have distinct functions (Belote et al., 1998; Ma et al., 2002; Zhong and Belote, 2007). For example, proteasome subunit alpha6 testis-specific (α6T), is required for spermatogenesis (Zhong and Belote, 2007). The canonical α6 can compensate for α6t deletion, but it still does not exclude the need for a specialized proteasome and the idea that the testis specific proteasome is somewhat different from the constitutive one.

1.1.11 Proteasome sub-cellular localization

Yeast proteasomes are mainly nuclear (Wilkinson et al., 1998), while mammalian proteasomes can be distributed both in the nucleus and cytoplasm, but are often concentrated in the nucleus as well (Reits et al., 1997). The 26S proteasome is synthesized within the cytoplasm and partly imported into the nucleus through the nuclear pore complex (Nederlof et al., 1995; Wendler et al., 2004), whereas the active transport of proteasomes from the nucleus to the cytoplasm has not been observed. Indication as to where assembly steps occur can be asserted from sub-cellular localization of the assembly chaperones. Early assembly chaperones, Pba1-Pba2 and Pba3-Pba4 are primarily cytoplasmic, whereas the late assembly chaperone, Ump1, is predominantly nuclear (Huh et al., 2003). This pattern supports a model in which CP assembly is initiated in the cytoplasm with final maturation steps occurring in the nucleus (Lehmann et al., 2002). Several proteasome subunits have nuclear localization sequences (NLSs), and a possible way to regulate localization of either mature proteasomes or assembly intermediates may be by modifying accessibility of these sequences (Nederlof et al., 1995; Tanaka et al., 1990). The fact that only a fraction of proteasome subunits bear an NLS suggests that for most of the subunits, transport into the nucleus requires prior formation of either mature proteasomes or proteasomal sub-particles.

Proteasome localization can also be modified by both extrinsic and intrinsic signals. A gradual shift of proteasome localization from the nucleus to the cytoplasm has been previously reported in both yeast and human cell lines under conditions of overgrowth or nutritional depletion (Laporte et al., 2008; Machiels et al., 1995). DNA damage response illustrates local recruitment of proteasomes to double-stranded DNA break sites and DNA

damage proteins (Krogan et al., 2004). Nerve synapses and testis exemplify how proteasome localization serves an active role in cellular function. During neuronal excitation, GFP-tagged proteasomes translocate on actin networks to synaptic spines, actively altering the synaptic proteomic profile (Bingol and Schuman, 2006). Furthermore it appears that proteasome localization can be regulated by post translational modification, as is the case for CaMKIIα phosphorylation of the proteasome in synaptic translocation (Bingol and Schuman, 2006) or Rpt2 myristoylation in determining cytoplasmic versus nuclear localization in yeast (Kimura et al., 2012). Such level of regulation distinguishes proteasome localization, highlighting its importance and specificity as opposed to a random diffusion process. Testis spermatogenesis involves massive cellular remodeling mediated by the proteasome (Zhong and Belote, 2007). Proteasome movement is critical for spermatogenesis, so much so that disrupted localization can yield sterile males (Ma et al., 2002).

1.2 Muscle atrophy: roles and regulation

Maintaining protein homeostasis (proteostasis) is a critical factor in preventing cellular dysfunction and propagating many disease states. Functional proteostasis is achieved by a balance between protein synthesis and degradation, although the latter is more often associated with pathological states than with normal cellular functioning. Atrophy is defined as a decrease in the size of a tissue or organ due to cellular shrinkage; this decrease in cell size is caused by the loss of organelles, cytoplasm and proteins. Un-controlled excessive protein degradation can be detrimental for skeletal muscle, and is the principle machinery behind muscle atrophy and weakness. This view is supported by the fact that activation of proteolysis is a feature of a number of pathologies, including cancer (cachexia), sepsis, renal failure (uremia), acquired immune deficiency syndrome, diabetes mellitus, aging (sarcopenia), disuse and denervation (Kandarian and Jackman, 2006; Lecker et al., 2006; Mitch and Goldberg, 1996). While aberrant chronic activation of proteolysis is damaging in disease states, long-term viability and maintenance of any organ system requires regular protein turnover and in muscle, when regulated, can even be beneficial.

Skeletal muscle is of unique importance when considering the necessity for properly functioning proteolytic systems. The maintenance of healthy muscles is crucial for preventing metabolic disorders, maintaining healthy aging and providing energy to vital organs during stress conditions. Skeletal muscle serves two essential functions, a contractile function for locomotion/maintenance of posture and a metabolic function as the protein reservoir of the body. The myofibers that make up the muscle consist primarily of myofibrillar proteins. These proteins assume a precise organization of contractile units

called the sarcomere, which are the force units behind locomotion (Hwang and Sykes, 2015; Knöll and Marston, 2012). The sarcomere consists of thick myosin filaments that can slide over thin actin filaments. Both types of filaments contain additional regulatory proteins and together they also serve as the major protein reservoir of the body. Upon fasting, once hepatic glycogen stores are depleted, muscle protein degradation releases amino acids which serve as building blocks for new protein synthesis in the body and are oxidized for energy production (Bell et al., 2016). Skeletal muscles are continuously challenged by mechanical, heat, and oxidative stress. These events increase protein damage and require efficient protein turnover to maintain optimal functioning. Furthermore, skeletal muscle repair and regeneration requires extensive remodeling through cycles of protein degradation and synthesis (Chen and Goldhamer, 2003; Dey et al., 2015). These examples illustrate the necessity of proteolysis in skeletal muscle.

Muscle proteostasis is a transcriptionally regulated process with a common transcriptional program carried by 'atrogenes' in various catabolic conditions (Lecker et al., 2004). 'Atrogenes' are genes identified as regulators of muscle mass whose expression is modified in different atrophy conditions, regardless of whether they promote protein degradation or prevent synthesis. Two major signaling pathways instruct muscle atrophy and growth. One is mediated by the forkhead box O (FoxO) transcription factors which are inactivated by Akt when the IGF-1/PI3K signaling pathway is active (Sandri et al., 2004; Stitt et al., 2004). The second regulatory pathway involves the transcription factor NF-kB, which is known to mediate signaling by TNF-α in the inflammatory response, this pathway activates the cachexia response to cancer (Cai et al., 2004). Intriguingly, these different pathways crosstalk and modulate one another at different levels to coordinate homeostatic

balance between protein synthesis and degradation simultaneously. Eventually, muscle proteolysis proceeds through either of these proteolytic systems: caspase mediated proteolysis, autophagy and the ubiquitin proteasome system (UPS), the latter considered the main driving force behind muscle atrophy.

1.2.1 Proteasome-mediated proteolysis in muscle

The UPS is responsible for degrading the majority of cellular proteins (Rock et al., 1994). A hallmark feature of the UPS is its ability to target specific proteins for degradation in a temporally highly regulated manner, through the coordinated activity of ubiquitin ligase and deubiquitinating enzymes. The significant dependence of muscle atrophy on the UPS became clear as a remarkable number of these enzymes have been implicated in muscle atrophy and identified as 'atrogenes' (see table 1.1 for UPS genes identified as 'atrogenes'). Among the strongly induced genes were also polyubiquitins and various subunits of the proteasome.

Table 1.1 UPS identified as 'atrogenes' by their loss of function phenotype.

UPS Gene	Experimental Model	Phenotype of Loss of Function	Regulation
Atrogin-1/MafBx	Knockout	Protection from atrophy induced by denervation (Bodine et al., 2001)	Upregulated in many catabolic conditions
Cbl-b	Knockout	Protection from unloading-induced atrophy (Nakao et al., 2009)	Upregulated upon unloading
Cul3-KLHL20	Skeletal muscle specific knockout	Increased diabetes-associated muscle atrophy (Liu et al., 2016)	Unknown
Fbxo21/SMART	Knockdown	Resistant to denervation-induced atrophy (Milan et al., 2015)	Upregulated in denervation and fasting
Fbxo30/MUSA1	Knockdown	Resistant to Smad knockout induced atrophy (Sartori et al., 2013)	Upregulated upon denervation and fasting
MuRF1/Trim63	Knockout	Protection from atrophy induced by denervation (Bodine et al., 2001) or glucocorticoids (Baehr et al., 2011)	Upregulated in many catabolic conditions
Nedd4–1	Knockout	Protection from atrophy induced by denervation (Koncarevic et al., 2007)	Upregulated upon unloading or denervation
SCF-Fbxo40	Knockdown	Thicker myofibers (Shi et al., 2011)	Upregulated upon denervation
Traf6	Muscle-specific inactivation, knockdown	Protection from atrophy induced by cancer cachexia, denervation (Paul et al., 2010), fasting (Paul et al., 2012), or glucocorticoids (Sun et al., 2014)	Upregulated in many catabolic conditions
Trim32	Knockout, shRNA knockdown	Premature senescence and sarcopenia (Kudryashova et al., 2012), Protection from atrophy induced by fasting (Cohen et al., 2012)	Unknown
Trim72	Knockout	Enhanced myogenesis (Lee et al., 2010)	Unknown
USP19	Knockout,knockdown	Protection from atrophy induced by denervation, glucocorticoids (Bédard et al., 2015), Increased myoblast fusion (Wiles et al., 2015)	Upregulated in many catabolic conditions

Adapted from (Bilodeau et al., 2016).

UPS genes have been implicated as 'atrogenes' in a multitude of muscle wasting conditions, including cancer (Baracos et al., 1995), fasting (Medina et al., 1995; 1991; Wing and Goldberg, 1993), denervation (Furuno et al., 1990; Medina et al., 1991; 1995), acidosis (Mitch et al., 1994), and sepsis (Tiao et al., 1994; Voisin et al., 1996). Initial studies to suggest a role for proteasome dependent degradation in the muscle were carried in incubated muscles where proteolysis, as measured by tyrosine release, was not reduced by lysosomal inhibition or by calpain inhibitors (calcium dependent proteases). However, ATP depletion greatly reduced proteolytic rates. Furthermore, in many of these conditions there was a concomitant increase of mRNA levels of ubiquitin and proteaosomal subunits, as well as ubiquitin-conjugated proteins (Baracos et al., 1995; Medina et al., 1991; 1995). The advent of the proteasome inhibitors, MG132 and LLN, provided a more direct assay of proteasome dependent proteolysis (Tawa et al., 1997). Proteolysis was reduced by 50% in incubated rat muscles upon treatment with these inhibitors, with no change in protein synthesis. Proteasome inhibition was further confirmed by accumulation of poly-ubiquitinated proteins. Their efficacy in inhibiting proteolysis was even more evident in muscles under catabolic conditions including denervation, hyperthyroidism, and sepsis. Enhanced proteolysis was blocked by 70%-100% when rats were treated with inhibitors.

A key finding in establishing the role UPS plays in muscle atrophy was the identification of muscle specific E3 ubiquitin ligases (Bodine et al., 2001; Gomes et al., 2001). Bodine et al., performed transcript profiling (mRNA comparison) to identify genes regulated upon immobilization. Although many genes were up regulated in immobilization model, only a small subset was regulated in additional models of denervation and unweighting, indicating their universality as markers of atrophy. These genes were MuRF1 (Muscle RING Finger 1) and MAFbx (Muscle atrophy F-box). Atrophy upon denervation

was attenuated by 56% and 36% at 14 days in MAFbx knockout mice and MuRF1 knockout mice respectively. Myosin heavy chains (MYH) were also significantly spared in MuRF1$^{-/-}$ mice treated with glucocorticoids and fasting MuRF1 mutant mice (Baehr et al., 2011; Clarke et al., 2007; Cohen et al., 2009). Moreover, MuRF1 was found in physical association with MYH and functioned as its E3-ligase *in vitro*. MuRF1 was also reported in the degradation of other muscle structural proteins, including troponin I, actin, myosin binding protein C and myosin light chains 1 and 2 (Cohen et al., 2009; Kedar et al., 2004; Polge et al., 2011). Gomes and colleagues used cDNA microarrays to identify MAFbx, named atrogin-1. Atrogin 1 expression was induced by more than 9-fold in fasting muscle, its mRNA was also markedly increased in atrophy related to diabetes, cancer and renal failure. Cloning and structure of MAFbx characterized it as an F-box protein found in the SCF complex. It was strongly induced even before muscle weight loss was detected and maintained at high levels as proteolysis accelerated, suggesting a role in both initiation and maintenance of the proteolysis. Remarkably, in age-related atrophy (sarcopenia), inducing these UPS genes delayed aging symptoms by maintaining protein quality control (Demontis and Perrimon, 2010; Edström et al., 2006). These findings further underline the importance of balanced proteasome activity, of which too high or too low can be detrimental.

Though far less established some UPS genes have been linked to atrophy through regulation of protein synthesis. MAFbx was found to bind and ubiquitinate eIF3-f (eukaryotic translation initiation factor 3 subunit F), as well as MyoD both *in vivo* and *in vitro* (Lagirand-Cantaloube et al., 2008; Tintignac et al., 2005). MyoD is a transcription factor required for myogenic stem cell and expression of eIF3-f, an important activator of protein synthesis. Genetic activation of eIF3-f was sufficient to cause hypertrophy and to

block atrophy in myotubes, reversed by ectopic expression of MAFbx. Conversely, MAFbx knock down prevented eIF3-f degradation sparing myotubes atrophy. Silencing USP19, a de-ubiquitinating enzyme, increased expression of myofibrillar protein due to up-regulation of the myogenic transcription factor Myogenin, though how it does so is still unclear (Sundaram et al., 2009). In agreement, USP19 knockout mice showed reduced atrophy in response to glucocorticoid or denervation; however muscle protein synthesis was similar to control mice (Bédard et al., 2015). MuRF1 and MAFbx expression was reduced in USP19 knockout, suggesting reduced proteolysis could account for muscle sparing.

1.2.2 Autophagy/lysosome mediated proteolysis in muscle

Autophagy is one of the major protein degradative pathways within virtually all cells of the body. Autophagy is a highly conserved homeostatic mechanism that is used for the degradation and recycling of long-lived proteins and organelles. It involves formation of membrane bound vesicles (termed autophagosomes) followed by their fusion with lysosomes where degradation takes place (Mizushima and Komatsu, 2011). Several studies over the past decade have indicated that excessive autophagy aggravates muscle wasting and contributes to muscle weakness (Dobrowolny et al., 2008; Mammucari et al., 2007; Wang et al., 2005; Zhao et al., 2007). Autophagosome accumulation has been observed in various myopathies (Malicdan et al., 2008). However, it could be activated as part of a stress response as basal autophagy is also necessary to maintain muscle mass and actually prevent atrophy.

During aging, muscle stem-cell regenerative function declines, mainly due to irreversible senescence of muscle satellite cells (Tang and Rando, 2014). Muscle stem cells preserve their regenerative capacity through autophagy-mediated proteostasis as a cellular quality control mechanism. Physiological decline of autophagy in old satellite cells or its genetic impairment in young cells, resulted in toxic cellular waste accumulation, mitochondrial dysfunction and oxidative stress together resulting in entry into senescence (García-Prat et al., 2016). Moreover, mice deficient of Atg7 or Atg5, autophagy related gene, showed a 20–40% age-dependent reduction in muscle fiber cross-sectional area and formation of protein aggregates (Masiero et al., 2009; Raben et al., 2010). Loss of muscle mass in $Atg7^{-/-}$ mice was also accompanied by corresponding decrease in force generation. An interesting link between autophagy and aging was recently described in *Drosophila*, where the maintenance of a normal autophagic flux in aged muscles was found to induce a beneficial extension of lifespan (Demontis and Perrimon, 2010). Loss of muscle proteostasis evident by protein aggregation and muscle weakness precedes aging of other tissues and contributes to life span decrease. Remarkably, increased activity of the transcription factor FOXO and its target 4E-BP in skeletal muscle was sufficient to prevent accumulation of protein aggregates and extend life span at least in part by promoting the basal autophagy. Taken together, these studies highlight the necessity for basal autophagy in muscle mass maintenance.

In addition, there is some evidence for an essential role for autophagy in exercise-induced muscle growth. However, the effects of acute and chronic exercise on the autophagic response in skeletal muscle cells appear to be inconclusive. Mechanical stress and the simultaneous production of ROS during physical exercise culminate in damaged cellular components and the need for their removal (Moylan and Reid, 2007). Ultra-

endurance runners show signs of increased autophagic activity evident by elevated expression and formation of autophagy complexes (Jamart et al., 2012a; 2012b). Studies in mice complemented these data, showing that not only was autophagy induced during short-term exercise but lack thereof hindered muscle performance (Grumati et al., 2011; He et al., 2012; Møller et al., 2015). On the other hand Kim and colleagues observed reduced expression of autophagy related genes, whereas MURF-1 which is involved in proteasome-mediated degradation was significantly increased (Kim et al., 2012). Conflicting reports were also observed after chronic exercise, with some studies depicting rise in autophagy markers (Lira et al., 2010) and some a decline (Grumati et al., 2011). It is possible that exercise intensity level, muscle type and metabolic state of the muscle (AMP/ATP reservoir) determine which degradation pathway will be induced (Schwalm et al., 2015).

1.2.3 Caspase-mediated proteolysis in muscle

Caspases (cysteine-aspartic proteases) are a family of proteolytic enzymes that are most commonly known for their role in initiating apoptosis. Despite their common association with cell death, caspase-mediated signaling events have been linked to a diverse array of vital cell tasks, which are independent of inducing apoptosis (Fuchs and Steller, 2011). Though caspases have been linked to muscle growth and maintenance by modulating stem cell commitment and differentiation (Dick et al., 2015; Fernando et al., 2002; Murray et al., 2008), their role in promoting muscle atrophy is limited. One possible mechanism of caspase involvement in muscle stress adaptation is through regulation of autophagy and proteasome-mediated protein degradation. In Drosophila oogenesis, death

caspase-1 (DCP-1), has been shown to promote autophagy by cleaving and inhibiting the key autophagy suppressing protein SesB (DeVorkin et al., 2014). In catabolic conditions, such as sepsis, cancer and uremia, initial breakdown of actomyosin by caspase-3 triggered sequential degradation by the UPS (Du et al., 2004). Coordinated regulation of proteasome activity by caspase-3 was observed in myoblast differentiation to myotubes (Wang et al., 2010a). In myoblast Rpt5 (19S proteasome subunits) cleavage decreased proteasome activity, whereas cleavage of Rpt2 and Rpt6 in myotubes increased activity. Mutation of the respective caspase-3 cleavage sites resulted in the expected corresponding change in proteasome activity with a profound block in the differentiation program. Moreover, they found that in mice with a chronic kidney disease, a muscle wasting condition, there was cleavage of subunits Rpt2 and Rpt6 and stimulation of proteasome activity.

2. A screen for proteasome modifiers in muscle atrophy model

2.1 Summary

UPS function is important for muscle cell function at several levels. Muscle growth and contractile function require a high level of proteasome activity, evident by its importance to both maintenance of muscle architecture and mobility. When proteasome function is impaired, muscle atrophy occurs, accompanied by loss of striated sarcomeric architecture and patterned spacing of nuclei, erosion of neuromuscular junctions and cytoplasmic aggregates, but does not result in cell death. DTS5 and DTS7 are β subunit proteasome mutants which impair proteasome function. From a collection of 327 RNAi lines previously shown to cause rough eye when DTS5+DTS7 are expressed in the eye, I conducted a screen for genes that when knocked down rescue muscle atrophy. This screen resulted in the identification of 10 candidate genes of which 4 were further characterized for their impact on muscle architecture and proteasome activity. The screen culminated in the surprising revelation that α1 knockdown, a proteasome core subunit, restores proteasome activity in the background of the DTS5 mutant. This chapter summarizes key steps of the screen and initial characterization of candidate genes.

2.2 Introduction

Drosophila's genetic pliability and well-characterized musculature provide an excellent *in vivo* system to study the targeted effects of muscle proteasome inhibition. The larval body wall musculature is composed of a reiterated set of 30 defined muscles in each abdominal hemisegment (Bate, 1990; Beckett and Baylies, 2006). The development of these muscles is highly stereotyped, with each muscle cell achieving a specific orientation, a standard number of nuclei and innervation at NMJs of exacting size and placement. One way to investigate the *in vivo* regulation of the ubiquitin–proteasome pathway is to use a mutational approach to disrupt proteasome function. However, since this pathway is so vital for many critical cellular functions, the majority of proteasome null mutants are lethal. Thus, temperature-dependent conditional mutants have proven themselves very useful in studying the UPS. In *Drosophila*, two such mutants are DTS5 and DTS7, which carry a single-amino-acid substitution in the β6 and β2 subunits, respectively (Saville and Belote, 1993; Smyth and Belote, 1999). Their DTS nomenclature originates in their identification in a screen for dominant temperature-sensitive (DTS) lethal mutants, when expressed in whole organism (Holden and Suzuki, 1973). Though their mechanism of action is still unclear they have been widely used to specifically inhibit the *Drosophila* proteasome (Haas et al., 2007; Henchoz et al., 1996; Hériché et al., 2003; Huang et al., 2016; Zirin et al., 2015) These mutant proteasome subunits can be spatially targeted only to muscles using the GAL4-UAS system (Brand and Perrimon, 1993), and temporally targeted using the conditional GS (GeneSwitch) system (Osterwalder et al., 2001). This provides a methodology to investigate the temporal requirement of proteasome function specifically within the developing musculature.

2.3 Results

2.3.1 Targeted expression of proteasome mutants causes larval paralysis

The DTS mutations DTS5 and DTS7 result from single amino acid substitutions in the β6 and β2 subunits of the 20S proteasome respectively (Saville and Belote, 1993; Smyth and Belote, 1999). These mutant subunits have been shown to inhibit UPS-mediated protein degradation of known proteasome substrates (Neuburger et al., 2006; Schweisguth, 1999; Speese et al., 2003). Previous studies corroborated by work carried in the Steller lab by Dolors Ferres Marco showed that transgenic co-expression of both proteasome subunit mutants in the Drosophila eye using the GAL4-UAS system had a synergistic effect in blocking proteasome function (Belote and Fortier, 2002), evident by a rough eye phenotype. To target DTS-mediated proteasome inhibition spatially in muscle and temporally under experimental control, the Gene-Switch (GS) inducible expression system was used with the muscle-specific MHC (myosin heavy chain) driver (Osterwalder et al., 2001). The GS system ensures expression of mutants only when food is supplemented with the RU-486 inducer and only in tissues in which the driver is active. Since this system is highly sensitive to developmental variability, for comparable measurements of age-matched larvae I devised the experimental design presented in Figure 2.1. Initially, both mutant subunits were co-expressed in the musculature in the present study.

DTS expression was temporally targeted during the early third instar stage of larval development by transferring age-matched larvae to RU486-containing food (RU) or RU486-free food (control) for 24 h incubation at the DTS permissive temperature 28.3°C. To assess muscle function two parameters were measured: 1. Number of larvae crawling

on the vial wall out of total larvae placed in vial. 2. Motility on apple plates of those larvae remaining in yeast food. Expression of both DTS mutants resulted in roughly 50% reduction of larvae exiting the food compared to larvae grown on control food (Figure 2.2A). Furthermore, DTS expressing larvae looked wasted and did not pupate. When larvae were transferred onto apple plates, DTS larvae demonstrated near complete loss in their ability to crawl compared to the random crawling of control larvae. Only 1% of DTS expressing larvae showed movement. Given genetic constraints of expressing both DTS5 and DTS7, I tested whether expression of only DTS5 yields a comparable phenotype to co-expression of both DTS mutants. DTS5 expression alone was comparable in both parameters and sufficient to cause paralysis, hence from here on all experiments were carried with DTS5 alone. As a control for induction of the GS-UAS system and to categorize paralysis as specific to DTS induction I expressed GFP as an inherent gene. As expected when driving GFP expression using this system, no paralysis was observed compared to control. Independent of conditions or genetic background roughly 50% of larvae always remained inside the food. Some of these remaining larvae represent random crawling in and out of food. However, some were dead probably due to some toxicity issues with the inducer. I used RU-486 at concentration of 15μg/ml, which was the minimal dose to produce a robust activation of the system (GFP expression in majority of larvae) at minimal toxicity. A lower dose of 10 μg/ml did not activate system in high numbers and a higher dose of 20 μg/ml increased toxicity-induced death.

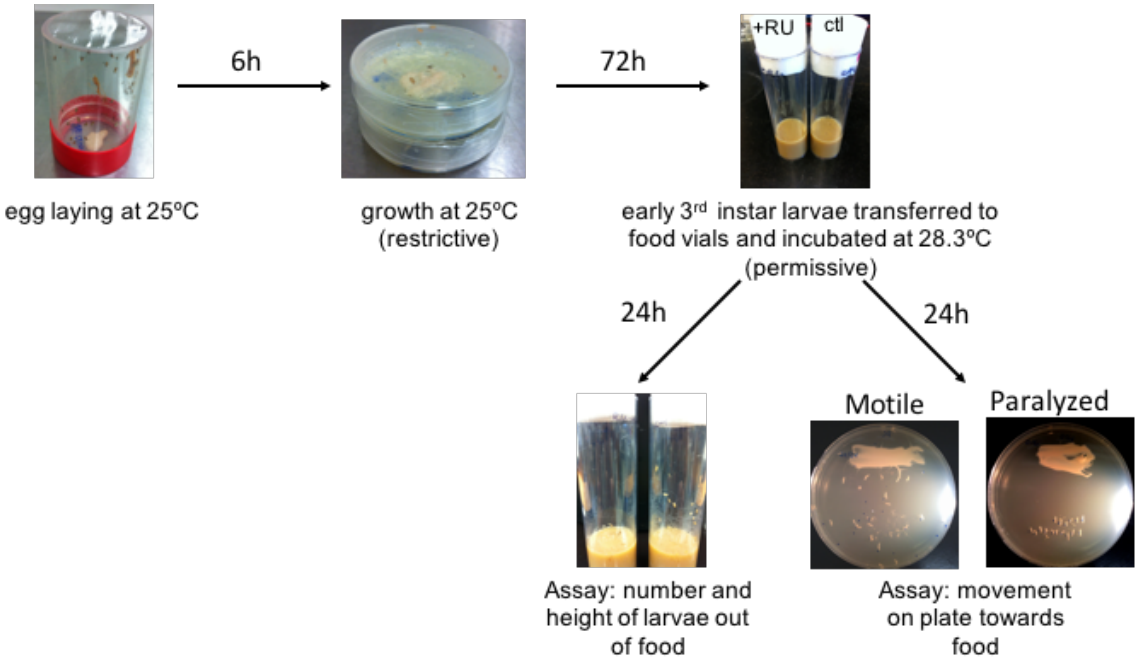

Figure 2.1 Scheme of experimental design and assays of larval paralysis. For age matching indicated crosses were carried in fly cages (50 females over 20 males) for the duration of 6 hours, followed by incubation of the egg laid plates at 25°C for additional 72 hours allowing eggs to mature into early third stage larvae. Larvae were collected into yeast food vials supplemented with RU-486 inducer versus mock supplementation as control. End point assay was analyzed by number of larvae crawling on vial wall and their movement on apple plates.

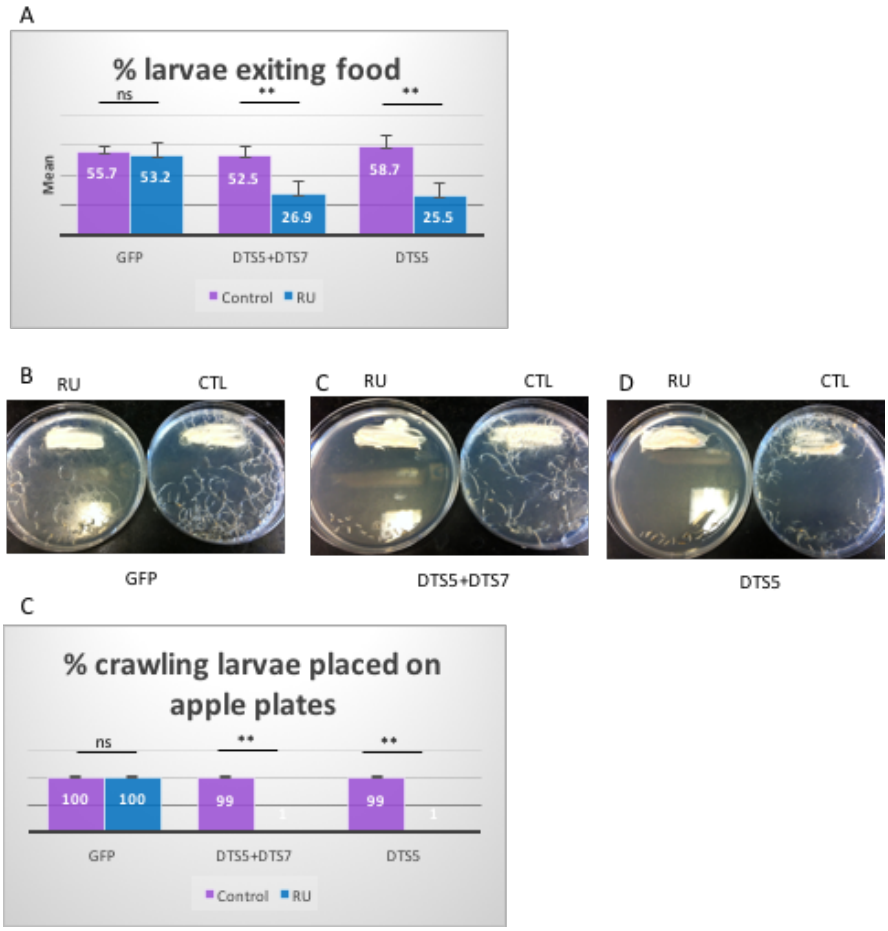

Figure 2.2 DTS expression results in larval paralysis. In both assays DTS expressing lines showed reduced movement compared to control, ranging from ~50% reduction in climbing to almost complete loss of motility on plates. A. Quantification of number of larvae exiting food as percentage of total larvae transferred into test tubes after 24 hours of growth in permissive temperature. Results collected of 5 independent trials over 200 larvae. B. Motility assay of larvae on apple plates. 20 larvae found in the yeast food of each test tube were placed on apple plates at experiment end point and monitored for their dispersion from start site (bottom of plate). C. Quantification of motility assayed in panel B. Results collected of 5 independent trials over 100 larvae. **P<0.001, Statistical analysis was performed with a two-tailed, paired, t test.

2.3.2. Proteasome function is required for muscle maintenance

The *Drosophila* larval musculature is formed during embryonic development by myoblast fusion, leading to formation of 30 unique multinucleated muscles per abdominal hemisegment (Bate, 1990; Beckett and Baylies, 2006). A subset of internal ventral longitudinal muscles, have been particularly well characterized. Each of these muscles, individually identifiable by position and size, contain a muscle-specific number of nuclei that are evenly distributed along the length of the syncitial cell. To directly assay the impact on the musculature, phalloidin (actin) and DAPI (4′,6-diamidino-2- phenylindole) (nuclear) staining was used to examine muscle architecture (Figure 2.3). Phalloidin labelling revealed striking muscle atrophy after 24 h induction of the DTS proteasome mutants (Figure 2.3C). Although muscle cell integrity and attachments were maintained, all muscles showed a dramatic reduction in cellular volume with a loss of the regular actin filaments cyto-architecture. Due to its large size muscle number 6 (VL3) was used for size measurements. On average width of muscle number 6 from wild-type larvae was 80 μm, whereas muscles of DTS5 expressing larvae demonstrated a 2.7-fold reduction on average (Figure 2.3D). In control muscle nuclei are often distributed in an organized manner along the length of the myotube, however DAPI staining revealed that in atrophied muscle nuclei were dramatically shifted and found in a disarrayed pattern, mostly clustering at muscle ends, near tendon insertion sites (see insets in figure 2.3C). Nonetheless there was no significant difference in nuclei number (Figure 2.3E), averaging 14 nuclei per wild-type muscle-6 and 13 per mutant muscle-6. Interestingly, this nuclear clustering phenotype recapitulates a pattern seen early in embryonic muscle development (Bate, 1990). Despite the prominent muscle atrophy and loss of nuclear spacing/localization, there was no sign

of apoptosis as evident by lack of staining for active caspase-3 (Figure 2.4). Thus, conditional inhibition of the proteasome disrupted muscle architecture within 24 h, but did not cause cellular degeneration. Preliminary results (more data on the matter in chapter 3) suggested activation of autophagy as muscle atrophy progressed. These results were obtained with an ATG8-dsRed transgene introduced to either wild-type or DTS5 strains. Atrophy induction in the DTS5 strain was accompanied by an average 2.7-fold increase in number of ATG8-dsRed cytoplasmic puncta. No statistical analysis was carried out since experiment was performed only once with 4 larvae. It is possible that autophagy underlines the mechanistic basis of distraught architecture caused by loss of proteasome function, yet this experiment was carried out only once.

To examine the time-course of the effects of proteasome inhibition, muscle structures were examined at timed intervals following induction of DTS5 proteasome mutant expression (Figure 2.3). Control muscles maintained a normal architecture with a clear striated sarcomeric pattern and organized nuclei along the myotube length at all time points: 6,12 and 24-hours post induction. At 6 hours after induction DTS5-expressing muscles were still comparable to control muscles with no gross morphological changes (Figure 2.3A). It is possible that not enough DTS5 mutant proteasomes have accumulated at this time point or that it takes much longer till perturbed proteasome function results in evident muscle atrophy. However, by 12 hours, muscles clearly began to reduce in width and loose nuclear pattern (Figure 2.3B). This coincided with a loss of the muscle striation pattern and sarcomeric boundaries were no longer clearly defined despite intense actin staining along the length of the muscle. At 24 hours after induction of DTS5 expression, there was a complete loss of the normal striated sarcomeric pattern.

To assess the specific effect of DTS expression on UPS function in muscle, larvae were stained with an antibody against poly-ubiquitinated proteins (FK-2 antibody; Figure 2.3). Accumulation of poly-ubiquitinated proteins is indicative of reduced protein degradation due to proteasome function impairment and elevation of proteotoxic stress. A marked accumulation of poly-ubiquitinated proteins was observed at the 24-hour time point in RU486-fed larvae compared with control (Figure 2.3C). As expected, poly-ubiquitinated proteins accumulated only in the targeted-muscles, but not in surrounding soma or other tissues. Poly-ubiquitinated proteins accumulated throughout the muscle cell, but the accumulation was most evident in perinuclear regions and punctate distribution (see inset figure 2.3C). It is important to note that RU-486 fed flies present mild increase in poly-ubiquitinated levels already at the 12-hour time point, preceding morphological changes of atrophy. This result alludes to the progress of events, most likely proteotoxic stress precedes atrophy induction and plays a role in its progression. These results demonstrate the ability to interfere with proteasome function *in vivo*, only in muscle cells and in a temporally controlled manner.

Figure 2.3 Time-course of muscle atrophy following DTS5 induction. A-C. Muscles were dissected and stained for phalloidin (actin), DAPI and poly-ubiquitinated proteins (FK-2) at the following time points respectively: 6, 12 and 24 hours after RU486 or control supplementation. No apparent morphological changes were seen after 6 hours, but progressive muscle atrophy and overt accumulation of poly-ubiquitinated proteins was observed onward. Scale bar 50μm. **D-E.** Quantification of muscle number 6 width and nuclei number respectively, at 24-hour time point. Statistical analysis was carried out on 3 independent experiments by taking measures of the muscle from 4 larvae per experiment, in total 12 muscles were quantified. **$P<0.001$, Statistical analysis was performed with a two-tailed, paired, t test.

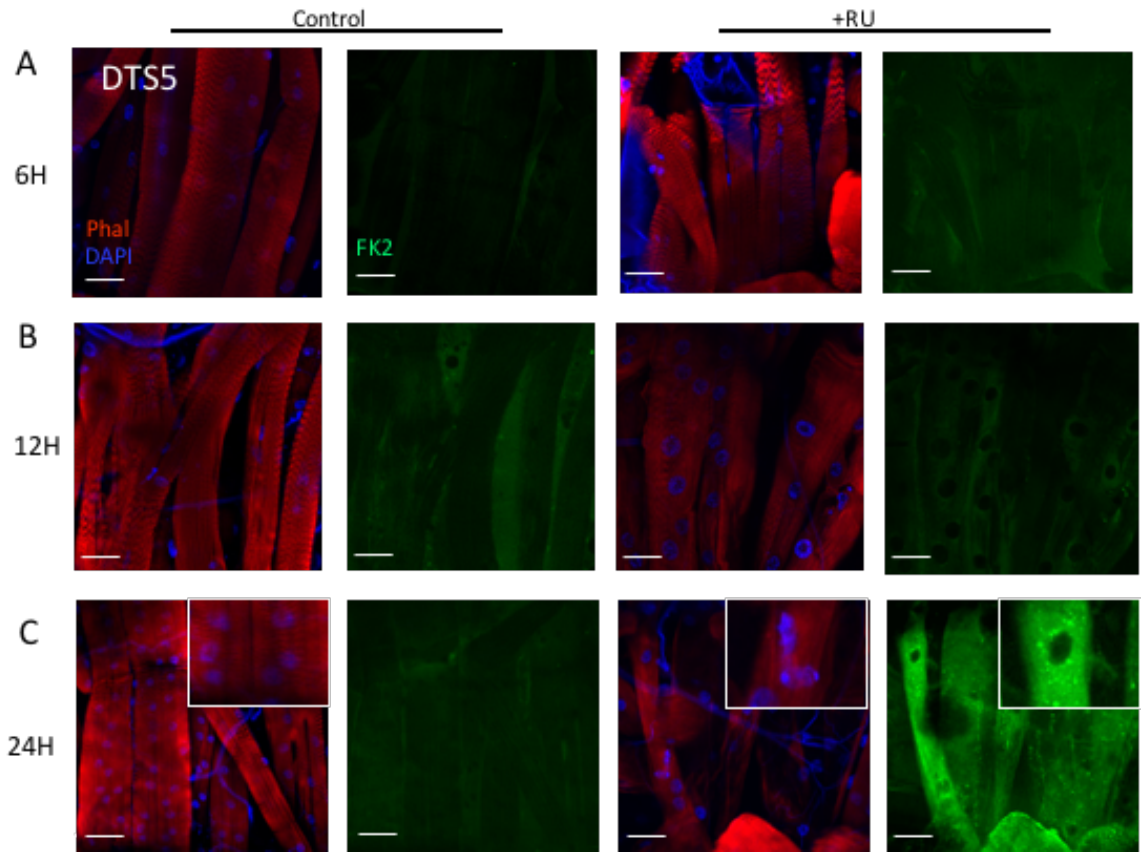
Control
+RU
A
DTS5
6H
Phal
DAPI
FK2
B
12H
C
24H

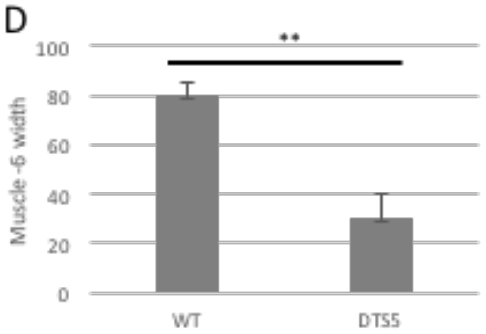
D
**
Muscle -6 width
100
80
60
40
20
0
WT
DTS5

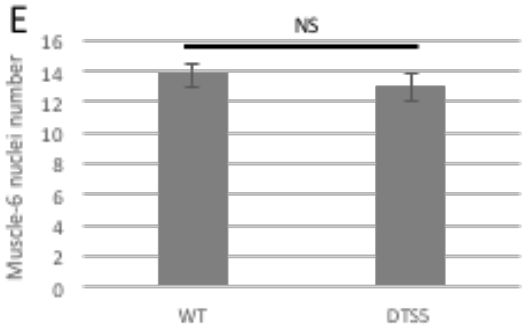
E
NS
Muscle-6 nuclei number
16
14
12
10
8
6
4
2
0
WT
DTS5

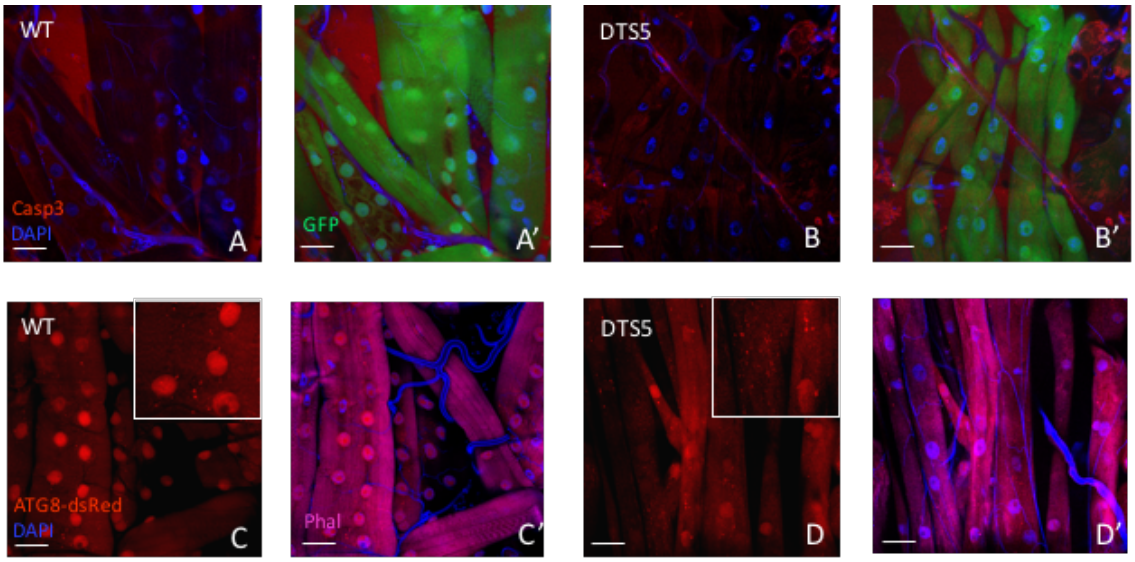

Figure 2.4 Muscle atrophy does not involve apoptotic program but trigger autophagy. A-B. Muscles were dissected at experiment end point and stained for active caspase-3. Negative staining in both wild-type and DTS5 expressing larvae indicate that observed atrophy does not proceed through induction of apoptosis. Note that muscles are marked by GFP. **C-D.** Transgenic flies expressing ATG8-dsRed in either WT or DTS5 background were dissected for muscles at experiment end point. Increased puncta in DTS5 strain mark autophagy induction.

2.3.3. Screen for modifiers of DTS5 induced muscle atrophy

To learn more about proteasome regulation in the muscle, I devised a screen to identify enhancers of proteasome activity which rescue larval paralysis when proteasome function is disturbed by the expression of the DTS5 proteasome mutant. I carried out this screen on 327 RNAi expressing lines, which were already identified as modifiers of the rough eye phenotype. The rough eye phenotype is the manifestation of DTS5 targeted expression in the eye. To score the rough eye phenotype females expressing DTS5 under a GMR (glass multiple reporter) driver were crossed with males expressing the respective RNAi (UAS-TRiP). The GMR-GAL4 driver is believed to be expressed from mid-third-instar stage through pupal development exclusively in all cells posterior to the morphogenetic furrow (MF) in differentiating eye discs (Freeman, 1996). Crosses were carried and propagated in 25°C and were subsequently transferred to the DTS5 permissive temperature 6 days after egg laying (AEL), 4 days before eclosing. Adults were collected during the first two days after hatching. Since gender may produce mild effects due to hormonal differences only males were compared (un-published observations). Additionally, only those with a Tm6B balancer on their third chromosomes were compared, since the Stubble marker can affect Notch signaling and thus enhance the rough eye phenotype independent of proteasome-related interaction. DTS5 expressing flies grown at 25°C for their entire life cycle developed normal looking eyes just like wild-type flies (Oregon-R) as expected from the temperature dependent nature of the DTS5 mutation (Figure 2.5A). However, flies transferred to 28.3°C at day 6 AEL developed a rough eye due to retinal cells degeneration, accompanied by reduced width of the eye and some necrotic tissue at its periphery.

To confirm that the rough eye phenotype was specific to retinal degeneration due to proteasome specific stress, I continued with the analysis of head sections. Heads were fixed and prepared by sucrose gradient prior to OCT embedding and cryostat sectioning. To establish retinal degeneration and deformed morphology, I stained sections with Chaoptin antibody (24B10). Chaoptin is a cell surface glycoprotein required for *Drosophila* photoreceptors (Reinke et al., 1988). Analysis of photoreceptor morphology was supplemented with counterstaining for ELAV to demarcate brain tissue. ELAV is an RNA-binding protein exclusively expressed in neurons and is important for the formation and maintenance of the nervous system (Koushika et al., 1996). DTS5 induction was damaging for photoreceptors which revealed a shorter, stacked morphology when stained for Chaoptin. ELAV staining was deformed and aggregated instead of running along the length of the photoreceptor. Additionally, nuclear DAPI staining moved distally, indicative of cell degeneration (Figure 2.1B). In vertical sections, there were gaps amidst the Chaoptin staining which might be accounted for by dead photoreceptors. However, ELAV expression and distribution was unaffected as GMR is not expressed in neurons.

I followed the same approach to validate proteasome de-regulation as the cause for observed degeneration. Proteasome inhibition should lead to impaired protein degradation and thus accumulation of poly-ubiquitinated proteins. Mono-ubiquitinated proteins are not specific targets for degradation and therefore can be disregarded. Prevalence of poly-ubiquitinated proteins was analyzed with FK2 antibody (Figure 2.5C). Enhanced FK2 staining in DTS5 strains confirmed that DTS5-expressing strains indeed experienced proteotoxic stress as expected from proteasome inhibition.

Finally, I analyzed the distribution of Rpt3 protein, subunit of the proteasome regulatory particle (Figure 2.5D). In DTS5 flies, Rpt3 staining was weaker with the

appearance of some aggregates. This observation may correlate with proteasome interference; however, it could also result from cellular degeneration. In the coming sections I address the distinction between disruption of proteasome activity and/or assembly. Overall DTS5 promoted retinal degeneration due to specific proreasome related proteotoxic stress.

Figure 2.5. DTS5 expression produces proteotoxic stress followed by retinal degeneration. A. DTS5 is a temperature sensitive mutant. GMR driven expression in permissive temperature manifests itself as a rough eye. **B-D.** Heads were fixed, dehydrated and embedded in OCT.cryosections were immunostained with the indicated antibodies and imaged by confocal microscopy. **B.** Staining with 24B10 (green) and ELAV (red) depict photoreceptors and neuronal tissues. To assess tissue architecture heads were cross-sectioned as well as vertically sectioned. **C.** FK2 (green) staining depicts accumulation of poly-ubiquitinated proteins. **D.** Rpt3 (green) used to represent proteasomes.

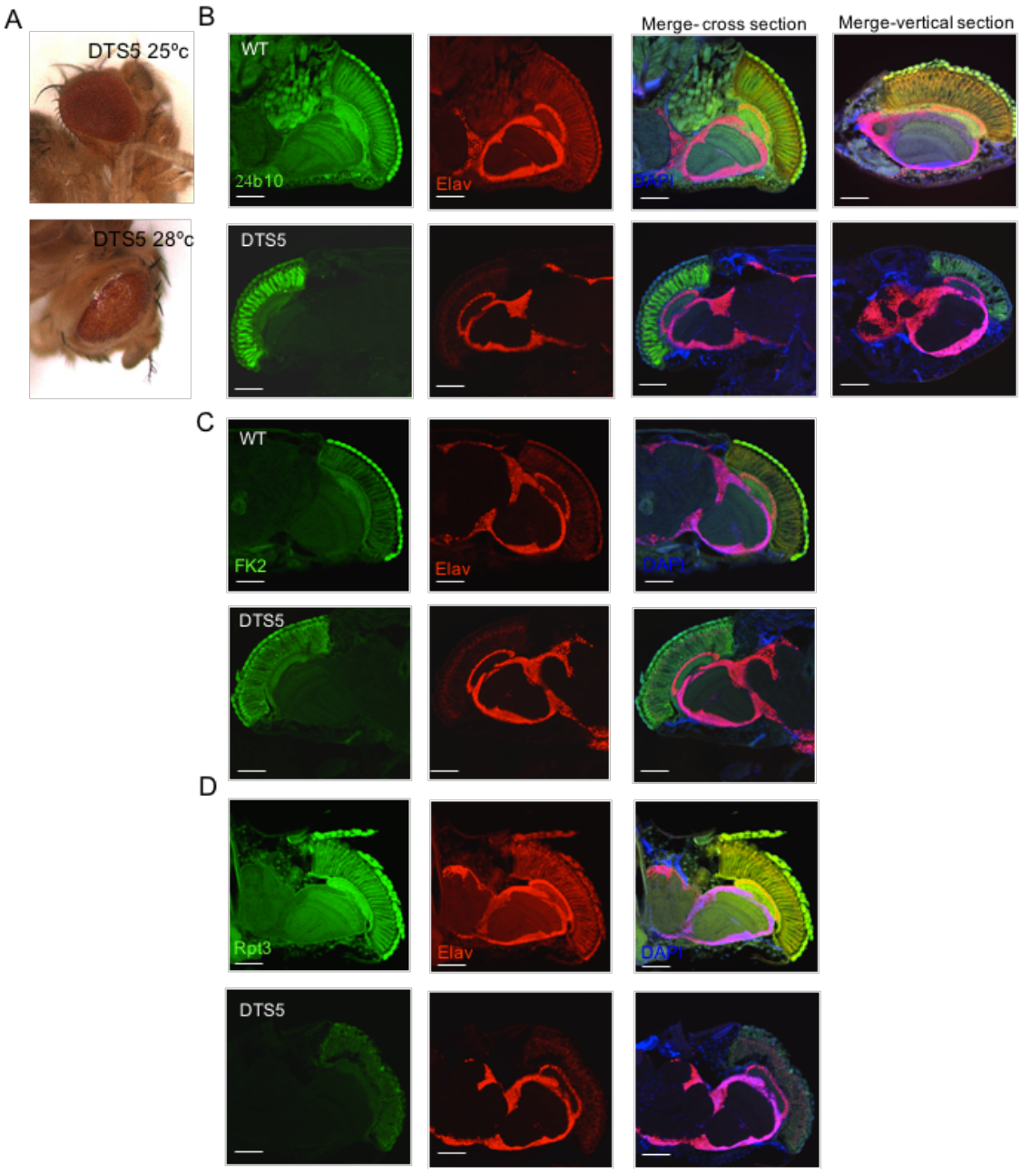
A
DTS5 25°c
DTS5 28°c
B
Merge- cross section
Merge-vertical section
WT
24b10
Elav
DAPI
DTS5
C
WT
FK2
Elav
DAPI
DTS5
D
Rpt3
Elav
DAPI
DTS5

Impaired proteasome function is lethal at early developmental stages, therefore DTS5 expression was targeted at the early third instar larvae stage by the combination of RU486 supplementation and transfer to permissive temperature at that specific developmental stage. However, DTS5 expression was still leaky, despite inducer absence, when combined with the MHC-GS driver. This resulted in a sick line with low eclosion rates, thus obstructing proper progression of the screen. This issue was resolved with an added preceding cross to the screen design. The DTS5 strain was first crossed with an RNAi target strain; followed by a subsequent cross between the suitable progenies and the MHC-GS driver to be screened for larval paralysis (see screen design in Figure 2.6). To follow DTS5 expression I recombined it with a UAS-GFP.

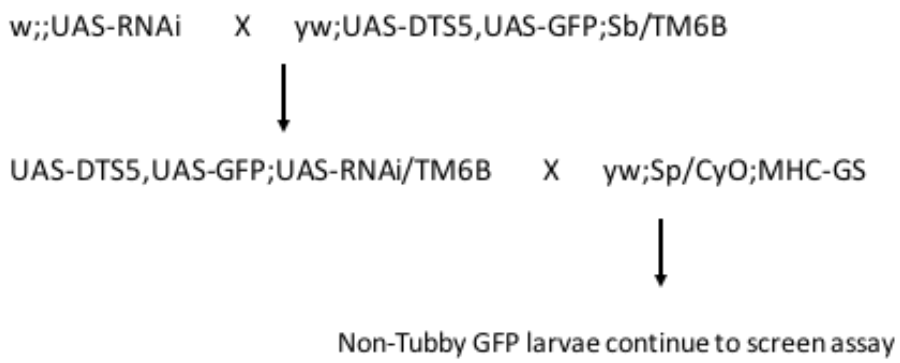

Figure 2.6. Crossing scheme to screen for modifiers of muscle atrophy

Of the 327 RNAi targets, 10 were suppressors of the DTS5 paralysis phenotype (Figure 2.7), 4 of which were further characterized for their effect on proteasome function until one candidate, α1 proteasome subunit, was chosen as the subject of my thesis.

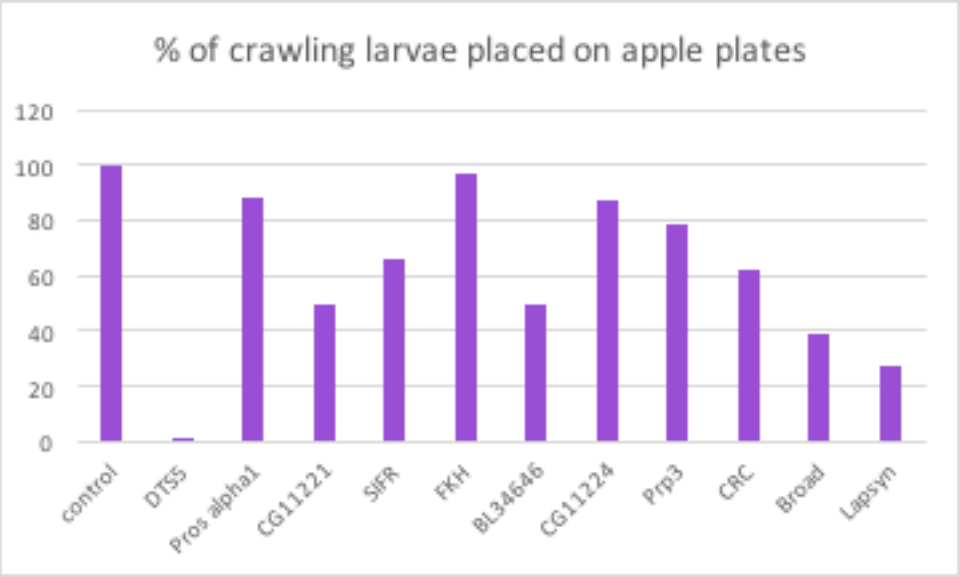

Figure 2.7. Candidate genes of proteasome modifiers. RNAi target genes identified as DTS5 induced muscle atrophy suppressors in screen. Percentage was calculated per genotype as number of crawling larvae per total larvae placed on apple plate.

2.3.4 Suppressors of DTS5-induced muscle atrophy

From the screen, four genes were selected for further characterization as to their specific proteasome related effects. In addition to their suppression of DTS5-induced paralysis, they were characterized by three more criteria: rough eye phenotype, *in vitro* proteasome activity, *in vivo* proteasome activity (summary in table 2.1).

This list of genes was chosen based on interest from preliminary literary data:

1. FKH (Forkhead) – this transcription factor plays a role in a variety of valuable processes such as cell cycle, metabolic regulation and development (salivary gland morphogenesis). The human orthologues, FOXO proteins, are known inducers of proteasome activity and promoters of muscle atrophy through the elevation of MuRF1 and MAFbx (muscle specific E3 ligases) [(Bodine et al., 2001),(Sandri et al., 2004)]. FOXOs expression usually correlates with enhanced muscle atrophy. One exception is in sarcopenia, where the induction of FOXO forcibly or through dietary restriction helps to delay ageing syndrome through improved protein degradation (Demontis and Perrimon, 2010).
2. CG11221 – to date very little is known of this uncharacterized gene. It was identified in a screen for regulators of glucose metabolism, where knockdown in the musculature resulted in hyperglycemia (Ugrankar et al., 2015). Based on domain prediction it contains serine/threonine kinase like domain (fly base IntelPro database).
3. SIFR – SIFamide Receptor, is a G-protein coupled receptor. It was previously shown through screen methodology that, when overexpressed, it can cause defects in early spermatogenesis (Schulz et al., 2004) and increase adult life span (Paik et

al., 2012). Though SIFR was never studied for proteasome related functions, both spermatogenesis and life span are dependent on proteasome regulation.

4. Pros α1- core subunit of the 20S proteasome particle (detailed description in introduction).

My aim was to identify proteasome regulators in muscle tissue, in which the proteasome plays a unique role in atrophy. Since I did not want to assume that each gene behaves similarly in different tissues, all modifiers identified in the previous rough eye screen were also screened for muscle phenotypes, whether they were identified as enhancers or suppressors of phenotype. As seen in Figure 2.8 knockdown of SIFR and α1 suppressed this phenotype and produced eyes comparable to normal controls. This recapitulated suppression seen in the muscle screen and expected from increase in proteasome activity. Knockdown of FKH did not rescue the rough eye phenotype and resembled that seen with DTS5 alone. Discrepancies between muscle and eye are possible due to tissue-specific interaction and likely different needs for proteasome activity in the tissues. Also, it is important to note that proteasome interference was carried in different developmental stages of the fly and each respective tissue. Targeted expression of CG11221 RNAi in the eye was lethal and did not yield adults at all. GMR is considered empirically to be expressed only in the eye and not expected to have effects on whole organism viability. However, several reports (Firth et al., 2006; Mallik and Lakhotia, 2009; 2014; Morris et al., 2006) reported lethality following expression of certain transgenes under GMR driver, notwithstanding the fact that eye is not essential for survival of the fly. An explanation to this observation can be found in a recent thorough study of GMR expression (Ray and Lakhotia, 2015) which showed that this driver is indeed expressed in

additional tissues, including a common set of specific neuronal cells in larval and pupal ventral and cerebral ganglia.

I next asked whether these proteins influence proteasome activity directly in muscle tissue. For this purpose, I employed two assays to measure proteasome activity using *in vitro* and *in vivo* methodology. I assayed proteasome activity in wild-type, DTS5 mutant, and the strains of DTS5 introduced with each target RNAi respectively. Flies were raised as described for the screen and samples were collected only from larvae fed on inducer at the permissive temperature. For *in vitro* activity assay muscle tissue from these larvae was lysed in a native lysis buffer containing ATP to preserve the 26S proteasome holocomplex. Differences in proteasome activity were detected by measuring the hydrolysis of a fluoregenic peptide. DTS5 induction reduced proteasome activity significantly by 40% compared to measured levels in wild-type. With the exception of CG11221 knockdown, knockdown of the other candidates increased proteasome activity by roughly 2-fold in comparison to the DTS5 strain. This observed increase even crossed the wild-type activity level, which may suggest some synergistic contribution, however this rise was not significant especially given the inherent noise in this assay (Figure 2.8). Activity levels remained low as in the DTS5 strain when CG11221 RNAi was introduced; possibly indicative of non-specific targets which are independent of proteasome activity. A similar trend was observed in analysis of *in vitro* proteasome activity from head samples of DTS5 mutants; inhibition of proteasome activity by DTS5 in the permissive temperature and suppression of DTS5-dependent inhibition by α1 knockdown (Figure 2.8C). However, the results obtained from head samples were statistically insignificant. In addition to inherent technical noise, some variability can be accounted for by low fraction of GMR-expressing

cells out of the whole head tissue, therefore measurements represent a mixed population. In summary RNA interference of α1, SIFR and FKH relieved DTS5 inhibition of proteasome activity.

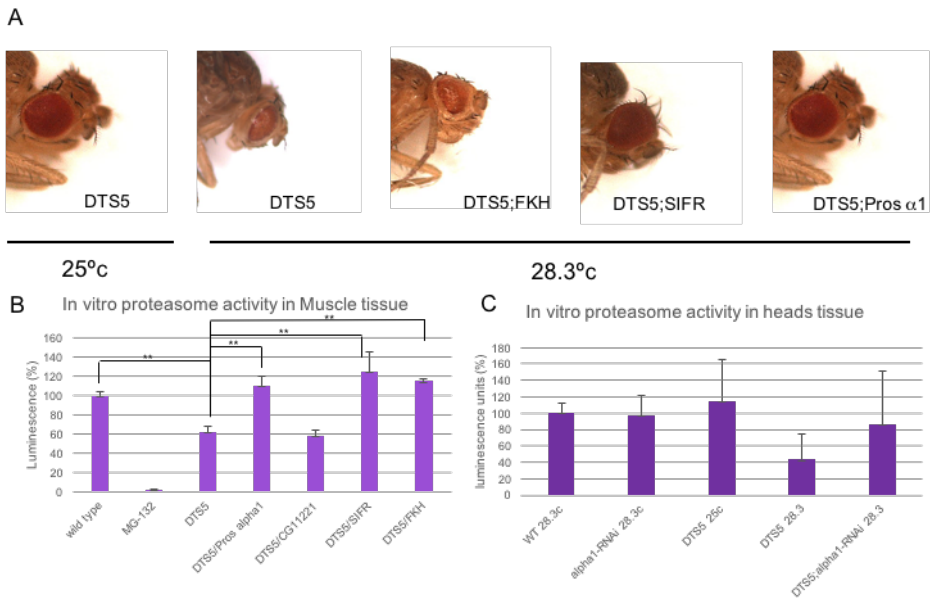

Figure 2.8. Candidate genes modify DTS5 dependent proteasome inhibition. A. Proteasome function is required for eye development and morphology. DTS5 is a temperature-sensitive mutant, expression at permissive temperature (28.3°C) results in a rough eye phenotype, which can be rescued by two candidate genes: SIFR and Pros α1. CG11221 is not shown since it was lethal for viability. DTS5 and RNAi were driven by the GMR driver. **B.** Muscle tissue from DTS5 strain displayed significant decrease in proteasome activity. With the exception of CG11221, knockdown of candidate proteins elevated proteasome activity significantly in comparison to the DTS5 strain (**P<0.001 n=3). Total protein (75 µg) was extracted from dissected muscle tissue of indicated genotype and proteasome activity was detected by measuring fluorogenic-peptide hydrolysis after 10 minutes. Measurements were normalized to wild-type and plotted as relative luminescence units. The standard deviation was measured from three independent repeats. MG-132, proteasome inhibitor was used to confirm specificity of read out. **C.** *In vitro* proteasome activity assay of head tissue (n=3).

The *in vitro* assay has a few caveats; in addition to variability it measures only chymotryptic activity and is not ubiquitin-dependent; therefore, it might measure also 20S activity and not exclusively 26S proteasome activity. To address this point, I used an *in vivo* assay to assess proteasome activity in the muscle tissue. This assay was adapted from (Neuburger et al., 2006) and monitors the degradation of a heat shock inducible fluorescent copy of a known target of the ubiquitin-proteasome pathway, the *Drosophila* Nintra protein. Unstable EGFP was constructed by fusing EGFP with a portion of Notch containing its PEST degradation signal, which is rich in ubiquitin dependent degradation motifs (Wesley and Saez, 2000), marking it as a target for proteasome dependent degradation. For *in vivo* imaging and following heat shock, the larvae muscles were dissected, fixed and stained for Phalloidin, DAPI and GFP (to enhance signal). When transgenic larvae were subjected to heat shock the EGFP-Nintra reporter protein is ubiquitously expressed, reaching peak fluorescence within 1 hour and then steadily diminishing until it is only weakly detectable after 4 hours (Figure 2.9C-D). This reduction in signal is proteasome dependent and specific to the un-stable EGFP-Nintra fusion. Stable GFP, without the Nintra fusion, demonstrated persistent GFP signal past 4 hours of HS induction; indicating it was not sensitive to proteasome dependent degradation at the time scale of the assay (Figure 2.9A-B). In the DTS5 strain the GFP signal significantly persisted 4 hours post induction, indicative of impaired proteasome activity (Figure 2.9E-F). Phalloidin staining confirmed that heat shock and the transgenic expression EGFP do not disturb muscle architecture, hence any observed atrophy is proteasome dependent as seen before. FKH, SIFR and Pros α1 (Figure 2.9G, H, I respectively) knockdown

effectively abrogated GFP persistence and DTS5-dependent proteasome inhibition; reduction in signal was significant in comparison to DTS5, 5-10 fold reduction on average, and comparable to levels seen in the wild-type strain (Figure 2.9K). As demonstrated by the *in vitro* measurements, CG11221 knockdown did not significantly restore proteasome activity. Yet, GFP induction was relatively reduced already at 1-hour post induction, therefore this result was inconclusive (Figure 2.9I,K).

In conclusion the screen was successful in identifying genes that modify proteasome activity. DTS5 inhibited proteasome activity which is required to maintain functional musculature and motility. Proteasome inhibition was relieved through depletion of either of these candidate proteins: FKH, SIFR and Pros α1.

Figure 2.9 DTS5 and candidate genes effect on *in vivo* proteasome activity. Larvae of all genotypes were subjected to 30 minutes heat shock at 37°C 20 hours after RU-486 feeding and transfer to permissive temperature. At indicated time points muscles were dissected, fixed and stained for Phalloidin, DAPI and GFP. **A-B.** *In vivo* induction of EGFP reporter transgene: Protein stability is marked by GFP signal persistence at 4-hours post heat shock. **C-D.** *In vivo* induction of EGFP-Nintra reporter transgene: GFP signal reduction by 4-hours post heat shock marks proteasome dependent degradation of un-stable protein. **E-F.** *In vivo* induction of EGFP-Nintra reporter transgene and DTS5 mutant: GFP signal dramatically persisted 4-hours post heat shock, indicative of inhibition in proteasome activity. **G-J.** *In vivo* induction of EGFP-Nintra reporter transgene, DTS5 mutant and respective RNAi: FKH, SIFR and α1 knockdown displayed GFP signal reduction 4-hours post heat shock indicative of functional proteasome activity. All images were taken with the same conditions of laser intensity and exposure. Scale bar 50 μm. **K.** Quantification of GFP signal. Bars represent the means of percent values 4-hours versus 1-hour post HS induction of each respective strain. Statistical analysis was carried out on a total of 12 larvae (images) from 3 independent experiments. **P<0.001 significance in comparison to DTS5 signal, with a two-tailed, paired, t test.

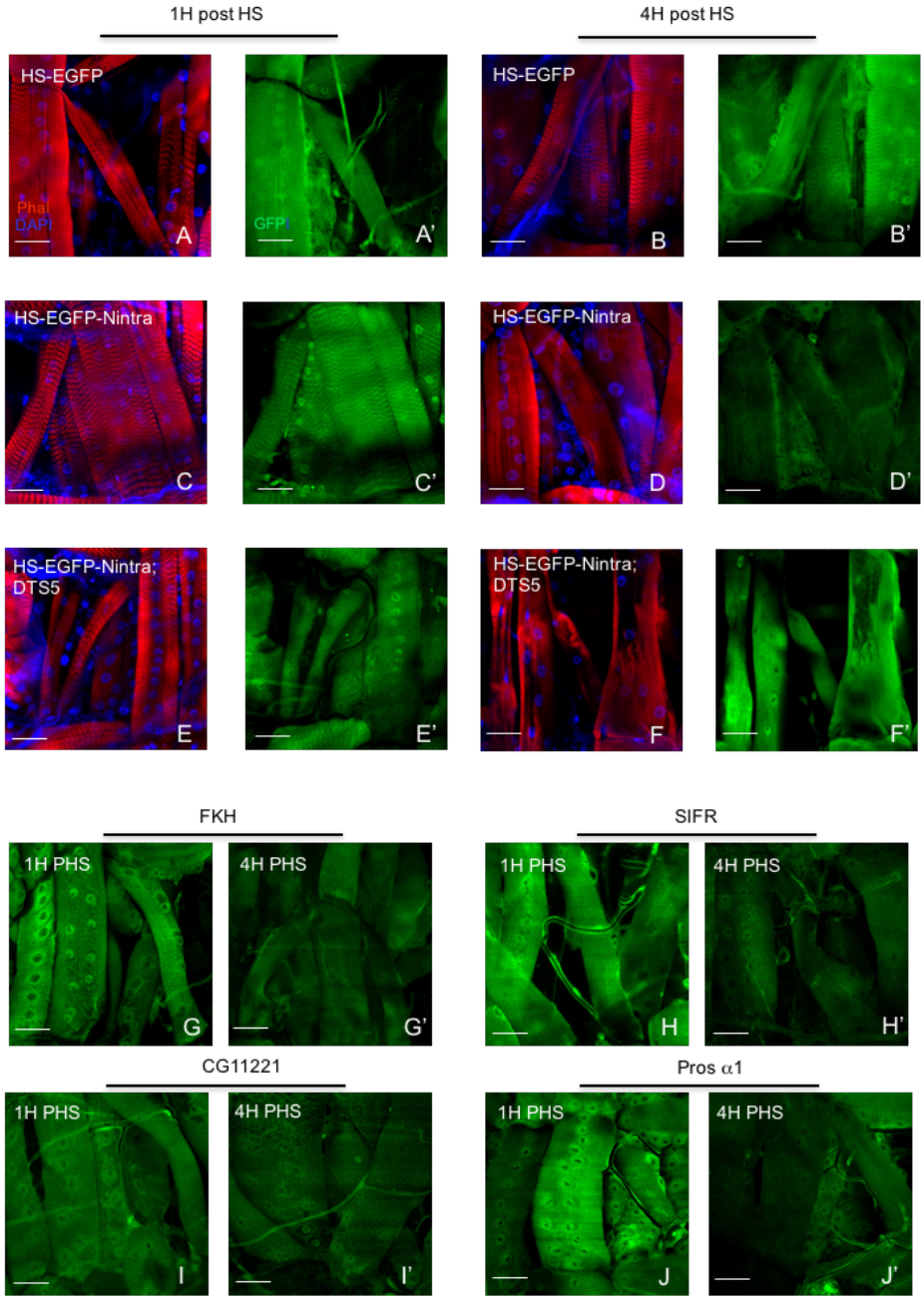
1H post HS
4H post HS
HS-EGFP
Phal
DAPI
A
GFP
A'
HS-EGFP
B
B'
HS-EGFP-Nintra
C
C'
HS-EGFP-Nintra
D
D'
HS-EGFP-Nintra;
DTS5
E
E'
HS-EGFP-Nintra;
DTS5
F
F'
FKH
SIFR
1H PHS
4H PHS
G
G'
H
H'
CG11221
Pros α1
I
I'
J
J'
K
Relative GFP levels
140
120
100
80
60
40
20
0
**
WT
DTS5
DTS5/Pros alpha1
DTS5/CG11221
DTS5/SIFR
DTS5/FKH

Table 2.1 Summary of candidate genes characterization. All results represent DTS5 induction at permissive temperature with knockdown of respective gene and are compared to DTS5 effect alone on the indicated tissue. The rough eye phenotype repeated at my hands.

	Paralysis	Rough eye	*In Vitro* proteasome activity In muscle	*In Vivo* proteasome activity In muscle
FKH	Suppress	Enhance	Increased	Increased
CG11221	Suppress	Enhance	Not Significant	Not Significant
SIFR	Suppress	Suppress	Increased	Increased
Pros alpha1	Suppress	Suppress	Increased	Increased

2.3.5 Knockdown validation of candidate genes

To validate specificity of the RNAi knockdowns, additional RNAi strains were tested. All α1 RNAi lines repeated their effect on paralysis suppression as their previously used counterpart α1-27557 (Figure 2.10A). However, of the FKH RNAi lines only the previously used FKH-33760 suppressed DTS5 induced paralysis (Figure 2.10A). This result may indicate non-specific off target effects or incompetence of the RNAi transgene. Therefore, I next checked expression levels of target proteins. To assess FKH expression levels I extracted protein for Western blot analysis with FKH antibody. Overall there was a substantial reduction in protein expression levels. Despite displaying a dramatic reduction

in protein levels, FKH-27072 strain did not suppress paralysis (Figure 2.10B). Immunofluorescence analysis with FKH antibody found reduced expression levels in strain FKH-33760 (Figure 2.10C), quantification of relative signal, normalized to DAPI levels, showed a 4-fold reduction compared to wild-type (not shown).

Due to lack of available antibody against α1, I performed RT-PCR in order to assess its expression levels. I extracted mRNA from wild-type and two different strains expressing α1-RNAi. All material was extracted from muscle-targeted α1-RNAi as knockdown of α1 is not viable at the whole organism level. This analysis revealed more mRNA in wild-type animal already at cycle 25 compared to either RNAi strain (Figure 2.10D). All α1 knockdown experiments in this thesis refer to strain 27557.

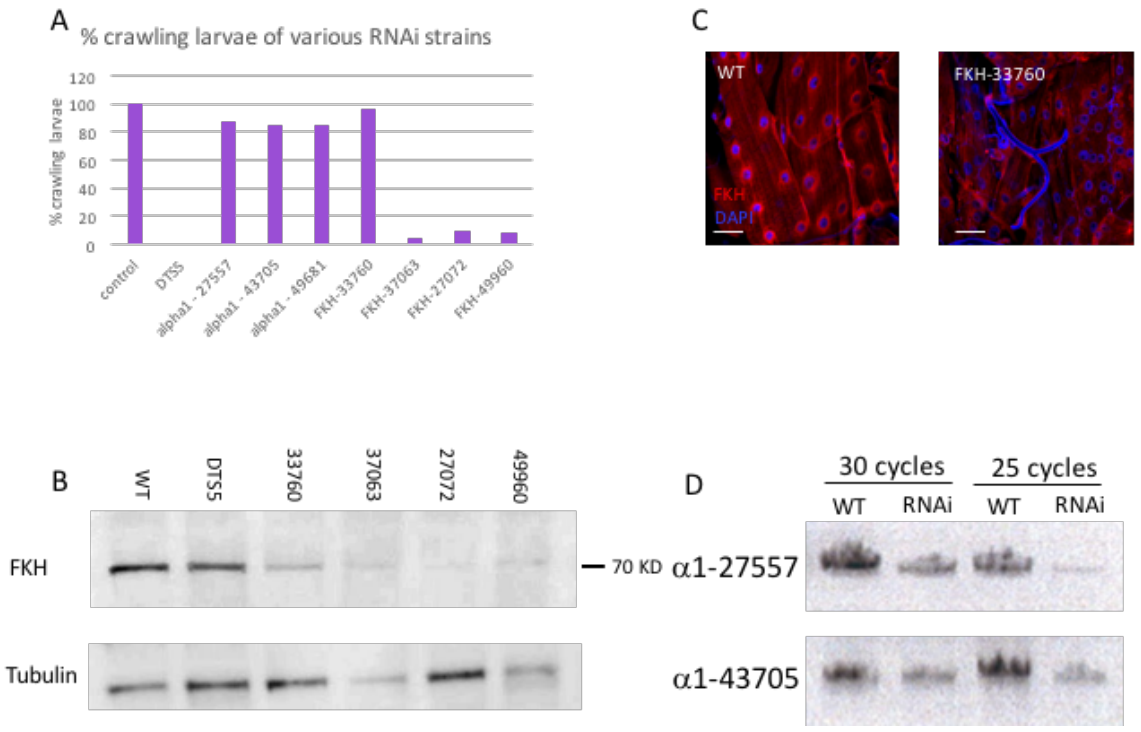

Figure 2.10 RNAi validation of target genes. A. In the crawling larvae assay all RNAi lines targeting α1 behaved similarly and recapitulated paralysis suppression, whereas of the FKH-targeting strains only FKH-33760. The percentage was calculated per genotype as number of crawling larvae per total larvae placed on apple plate. **B.** RNAi-dependent reduction in FKH expression levels was assessed by Western blotting of protein extracts from dissected muscle. Conclusion can be deducted only for lines 33760 and 27072 as loading control for the other two lines was not comparable to wild-type. α-tubulin protein levels served as loading control. **C.** Immunofluorescence analysis of fkh antibody revealed the reduction in protein levels in muscles of fkh-33760. Scale bar 50 μm. **D.** RT-PCR analysis of α1 transcripts collected from wild-type, α1-27557, α1-43705 larval muscles. More transcripts were detected in wild-type indicted that RNAi suppresses α1 expression.

2.4 Materials and Methods

Fly stocks

John Belote generously provided us with UAS-DTS5 and UAS-DTS7 strain (Belote and Fortier, 2002), as well as the hs-EGFP-Nintra lines used for the *in vivo* proteasome activity assay (Neuburger et al., 2006). MHC-GS driver was kindly given to us by Thomas Osterwalder and Haig Keshishian (Osterwalder et al., 2001). RNAi fly library was procured from Bloomington stock center. All stocks were in a yw or w^{1118} background and were cultured on cornmeal–molasses medium supplemented with 3% active yeast at indicated temperature or room temperature.

RU486 induction protocols and mobility assays

Larvae were raised on apple juice plates or in standard fly food to the desired age. Up to 10 mg/ml of RU486 (Mifepristone, Sigma) was dissolved in ethanol. For larval feeding, RU486 was diluted 26.6-fold from the working concentration in ethanol followed by 25-fold dilution in sterile water to get a final concentration of 15 μg/ml in 4% ethanol which was directly mixed in culture food. RU486 was allowed to saturate in the food overnight prior to larvae placement. For induction of the UAS transgene, staged third instar larvae were transferred into food containing RU486 or 4% ethanol alone (−RU486 control) for defined periods at 28.3°C, up to 24 h. Motility was expressed as the percentage of larvae climbing on vial walls or the percentage of mobile larvae on apple-juice/agar plates. Initial scoring of motility on apple plates was performed 6 hours following placement, however mobile larvae started crawling immediately whereas paralyzed larvae never regained

motility (not even after 24 hours), therefore for the majority of the experiments motility was scored immediately after larvae were placed on apple plates.

Muscle immunohistochemistry

Body wall muscles were dissected in PBS (130 mM NaCl, 7 mm Na_2HPO^4, 3 mm NaH_2PO_4, pH 7.0) as follows: third instar larvae were dissected along the dorsal midline, taking out body fat and secured flat with insect pins (Fine Science Tools) on silgard plates. Tissue was fixed in 4% formaldehyde in PBS for 30 min, rinsed three times with PBS for 5 min and afterwards transferred into Eppendorf tubes for the following steps. Tissue was permeabilized with PBT (PBS + 0.1% Triton X-100) for 15 min and rinsed twice with PBS for 10 min. Muscles were than incubated for 1 hour in blocking buffer (PBS, 1%BSA, 0.1% Triton X-100, 5% Normal Goat Serum and 5% Normal Donkey Serum purchase from Jackson ImmunoResearch) and incubated overnight on a shaker with primary antibody (diluted in blocking buffer) at 4°C. After rinsing with PBS, three times for 10 min, muscles were incubated on a shaker for 1 hour at room temperature with Alexa secondary antibody diluted 1:200 in PBS (Invitrogen) with 1:300 dilutions of TRITC-Phalloidin (Sigma), followed by PBS rinse, three times for 10 minutes, and mounted in Vectashield mounting medium with DAPI (Vector Laboratories). For poly-ubiquitin staining the mouse monoclonal antibody FK2 (Stressgen) was used at 1:500 dilution. For cleaved-caspase-3 staining a rabbit polyclonal anti-cleaved Caspase-3 (Asp175) antibody (Cell Signaling technology) was used at 1:100 dilution. For FKH staining rabbit polyclonal was used at 1:500 dilution (Acris). All pictures were taken with a Zeiss confocal microsocopy.

Head immunohistochemistry

Heads were cut off and collected in Eppendorf tube on dry ice. Prior to collection one eye was finely nicked with a scalpel to facilitate medium penetration into brain tissue. Tubes were incubated while spinning over night at 4°C with 4% paraformaldehyde in PBS. Following steps were carried while spinning at 4°C. Heads were rinsed in PBS, three times for 10 min, followed by tissue dehydration with sequential incubation for 20 min at increasing sucrose concentration: 5%, 10% and 20%. Incubation at 20% sucrose was carried out overnight. Heads were embedded in OCT (TissueTek) and frozen at -80°C over night. Cryostat sections were placed on slides and fixed with 0.5% paraformaldehyde for 30 min and rinsed with PBS. Steps of permeabilization, blocking and staining were carried out as described for muscle immuhistochemistry but were performed on slides using rinsle coverslips and in a humid chamber. 24B10 and Elav antibodies were procured from Developmental Studies Hybridoma Bank and used at 1:500 dilution. Rpt3 mouse monoclonal antibody was used at 1:100 dilution (Enzo). All pictures were taken with a Zeiss confocal microscopy.

In vitro proteasome activity assay

Dissected muscle tissue of 30 larvae per genotype was lysed in native lysis buffer: 50 mM Tris-HCl (pH 8.0), 5 mM MgCl2, 0.5 mM EDTA, 2 mM ATP (added fresh), 0.2% NP40 (added fresh), and homogenized using pellet pestle motor (Kontes). Protein concentration was measured in a Bradford assay. 75 μg protein was mixed at a 1:1 ratio with Proteasome-Glo chymotrypsin activity detection kit (Promega) at room temperature. Reactions were divided into three so each independent experiment represents an average of triplicates. All

reactions were conducted in a 96-well plate according to manufacturer's protocol. Measurements were read by a SpectraMax M-2 micro-plate reader (Molecular Devices).

In vivo proteasome activity assay

To assess the degradation of EGFP-Nintra in the presence of dominant proteasome mutants, females of genotype wP{hs-EGFP-Nintra}15(X) were crossed with males of pP{MHC-GeneSwitch}(3) and propagated for a stable line. Females of this stable line were later crossed with males of the different genotypes. Late third instar larvae were placed in pre-warmed small petri dishes containing apple-juice/agar supplemented with active yeast and heat-shocked by placing them in a 37°C water bath for 30 min. The larvae were then placed in a 25°C incubator and allowed to recover for 1 or 4 hours. Larvae were dissected for muscles and were prepared for immunohistochemistry as described in muscle immunohistochemistry. Since GFP gets somewhat bleached during the preparation polyclonal chicken anti-GFP was used at 1:1000 dilution (Aves) to strengthen signal. Fluorescence images were quantified using Image J software.

Western blot

Protein extracts were produced from dissected muscle tissue of 30 larvae, homogenized in lysis buffer (20mM Hepes pH7.6, 150 mM NaCl, 10% glycerol, 1% Triton X-100, 2mM EDTA, 1 mM DTT) and spun at 14,000 rpm for 15 minutes at 4°C. Protein concentration was determined by Bradford assay (Biorad). 10 μg of total protein was dissolved in SDS loading buffer and resolved on 4-20% Mini-PROTEAN TGX precast protein gel. Electrophoresis was carried for 1.5 hour at 100V voltage and protein transfer to immobilon-

P membrane (Milipore) for 1 hour at 100V voltage. Membranes were blocked with 5% milk in PBST (0.5% Tween20 in PBS) overnight at 4°C. Afterwards, samples were washed three times for 10 min in PBST and incubated with primary antibody for 1 to 2 hours at room temperature. Primary antibodies were diluted and kept in PBST supplemented with 0.02% Azide and 3% BSA. Following additional wash steps, membranes were incubated in HRP-conjugated secondary antibody (1:5000 dilution) for 1 hour and washed three more times with PBST before developing with ECL Western blotting detection reagent (Amersham) and Kodak Biomax MR film. Forkhead antibody was used at a dilution of 1:1000 (Acris).

RNA isolation and RT-PCR analysis

Total RNA was extracted by using Micro Total RNA purification system (Invitrogen) according to manufacturer's reccomendations. Dissected muscle tissue of 10-20 larvae was used to obtain RNA for RT-PCR reactions. The samples were collected on ice with 300 μl of Invitrogen lysis buffer and 3 μl of β-mercaptoethanol, ahomogenized with motorized pestle (Kontes) and subsequent RNA purification was continued with commercial kit (Invitrogen). Genomic DNA was removed with RQ1 DNase (Promega). RNA was used for RT-PCR reactions using the SuperScriptTM III One-Step RT-PCR System with Platinum Taq DNA polymerase (Invitrogen). For RT-PCR reaction Mastercycler Gradient PCR machine (Eppendorf) was programmed as follows: 50°C for 30 min, 94°C for 2 min and amplification steps of: 30 seconds of 94°C, 30 seconds of 60°C and 1 min of 68°C. Amplification was carried out for 25 and 30 cycles. Genomic DNA absence was verified with substituting RT/Taq mix with Taq DNA polymerase (Invitrogen).

3. Pros-α1 knockdown aids proteasome stability through Ecm29 chaperone recruitment

3.1 Summary

The Ubiquitin-Proteasome system catalyzes the degradation of most intracellular proteins. Although ubiquitination of proteins is the primary determinant of their stability, there is growing evidence that proteasome function is also regulated and it plays a key part in cellular homoeostasis. In this chapter, I describe the functional characterization of Pros-α1 in muscles and how its knockdown in stressed muscles mitigates proteotoxicity. I identified that DTS5 inhibits proteasome activity by facilitating the dis-assembly of the 26S holocomplex to its constituting particles, the 20S core particle and 19S regulatory particle. Pros-α1 knockdown promoted stable proteasomes by recruiting the Ecm29 chaperone. This genetic interaction was needed for restoring functional proteasome activity to maintain muscle architecture and motility. Although Ecm29 has been reported to regulate the proteasomal CP–RP interactions in yeast, its physiological role in *Drosophila* have not been characterized. In this chapter, I present the first functional study of Ecm29 in flies and the first one to characterize its role in proteasome regulation. These findings demonstrate a role for controlled proteolysis during muscle function and illuminate proteasome stability as a target of stress adaptation.

3.2 Introduction

Cells have evolved numerous and often overlapping homeostatic pathways to adapt to changes in their environment and to survive under adverse conditions. Ecm29 is a 205 kDa protein associated with the proteasome and was reported to regulate proteasome function via several mechanisms. Ecm29 was initially identified by its binding to yeast 26S proteasomes under low salt conditions, classifying it as an interacting protein rather than a stoichiometric subunit (Leggett et al., 2002). Like Blm10, Ecm29 is a HEAT-repeat protein and is conserved in yeast (Ecm29), humans (KIAA00368) and *Drosophila* (CG8858). These repeats characterize flexible proteins and are thought to be important for its function in binding both the RP on the one hand and CP on the other (Kajava et al., 2004).

Ecm29 can positively regulate proteasomes by stabilizing the 26S proteasome complex (Gorbea et al., 2004; Kleijnen et al., 2007; Leggett et al., 2002). It was shown to keep RP-CP complexes intact even in the absence of ATP, whereas when it was missing, ATP was needed to prevent dissociation of such complexes. In yeast extracts Ecm29 was found bound only to proteasome species which contained both RP and CP; an apparently unique property, that may reflect the requirement for both particles in stable association of Ecm29 to proteasomes (Leggett et al., 2002; Panasenko and Collart, 2011). Furthermore, evidence suggested that Ecm29 may function in proteasome quality control by either sequestering aberrantly formed proteasomes or repairing them. First, Ecm29 was purified with 26S proteasomes lacking β3 but still associated with a RP. These proteasomes were classified as immature due to the presence of unprocessed β5 (Lehmann et al., 2010). Reconstitution assays suggested that exogenous addition of Ecm29 was sufficient to drive

the maturation of the β5 subunit in these complexes. Additional reports confirmed Ecm29 preference to aberrant or mis-assembled proteasomes, these include proteasomes with mutant α or Rpt subunits (Lee et al., 2011; Park et al., 2011) and proteasomes assembled in the absence of Ump1 or Pac2 (Park et al., 2011). Ecm29 has pleiotropic effects; conflicting studies showed that it can either promote gate closure or opening (Kleijnen et al., 2007; Lee et al., 2011). Since Ecm29 was mostly studied under non-physiological conditions, these divergent observations may be explained by distinctive environmental conditions and/or association with alternative mutants in the existing studies. Ecm29 may function in the UPS pathway through additional mechanisms such as in maintaining proteasome integrity via the ubiquitin ligase Not4 (Panasenko and Collart, 2011), in playing a role in proteasome trafficking in mammalian axons (Hsu et al., 2015) and as proteasome adaptor protein in endocytic pathways (Gorbea et al., 2004; 2010). Despite the many intriguing observations linking Ecm29 to proteasomes, its exact mechanism of action remains uncertain. There is an existing gap in our understanding of what triggers Ecm29 recruitment to proteasomes, but the consent is that its ability to identify atypical or abnormal proteasomes is at the core of its function. Knowledge of Ecm29 function is largely derived from yeast and cell cultures analyses, therefore its physiological impact in insects and higher organisms is largely unknown. Nonetheless, it is considered a strong and evolutionarily conserved regulator of the proteasome.

3.3 Results

3.3.1 Pros-α1 characterization in eye and muscle models

The screen from Chapter 2 identified Pros-α1 (α1) knockdown as a suppressor of DTS5-dependent effects both in eye and muscle models. But two questions remained open which are addressed here:

1. Do pros-α1 levels specifically modify observed phenotypes?
2. How do α1 levels modify observed phenotypes independent of DTS5 stress?

The first question was addressed by overexpressing a α1 transgene (EP-α1) to complement reduced α1 levels due to RNAi expression. Overexpressing α1 in the DTS5;α1-RNAi strain abrogated suppression of the rough eye phenotype (Figure 3.1C). Additionally, immunofluorescence examination of OCT embedded heads revealed disrupted photoreceptor morphology and showed signs of retinal degeneration (Figure 3.1D, see inset). In conclusion, α1 levels were specifically responsible for modifying DTS5-dependent effects.

The second question was addressed in the muscle model, by applying RNA interference of α1 in a wild-type background. Despite α1 being a core subunit of the proteasome, these larvae displayed normal motility, not significantly different from wild type values, in the crawling assay (Figure 3.1I,L). I followed behavioral assays of larvae by examining changes at the molecular level. Even though there was no induction of paralysis, muscles still endured proteotoxic stress as presented in moderate accumulation of poly-ubiquitinated proteins (Figure 3.1J). Actin staining with phalloidin and DAPI displayed normal sarcomeric pattern and normal nuclei distribution with no signs of

atrophy (Figure 3.1J'). Photoreceptors were affected by α1 RNA interference in the same manner (Figure 3.1K). With no DTS5 expression, poly-ubiquitinated proteins rose in photoreceptors expressing α1 RNAi but not enough to initiate gross degeneration (Figure 3.1K'). I conclude that diminished α1 levels were not enough to activate a full muscle atrophy program or complete photoreceptor degeneration. Alternatively, distressed homeostasis was countered by triggering an adaptation response.

Figure 3.1 α1 role in stress and development. A-C. Shown is GMR-driven expression of indicated genotype at permissive temperatures. Overexpressing α1 over its RNAi re-suppressed α1-dependent rescue of DTS5-induced rough eye. **D-E.** Vertical sections of OCT embedded heads immunostained for 24B10 (green), ELAV (red) and DAPI (blue). Photoreceptors degeneration is dependent on α1 levels. **F-I.** Shown is MHC-GS driven expression of indicated genotype at permissive temperature. α1 RNAi expression is not sufficient to promote muscle atrophy in a wild-type background. **J.** α1 KD muscle stained for poly-ubiquitinated proteins (green) merged with Phalloidin (red) and DAPI (blue) in panel J'. Low α1 levels present some proteotoxic stress revealed by moderate accumulation of poly-ubiquitinated proteins but not sufficient to disturb muscle morphology. **K.** Cross sections of OCT embedded heads immunostained for FK2 (green) merged with ELAV (red) and DAPI (blue) in panel J'. Low α1 levels present some proteotoxic stress revealed by moderate accumulation of poly-ubiquitinated proteins but not sufficient to induce photoreceptor degeneration. **L.** Bars represent mean values from 5 independent experiments, 100 larvae in total. Percentage was calculated per genotype as number of crawling larvae per total larvae placed on apple plate. **P<0.001 two-tailed Student's t-test).

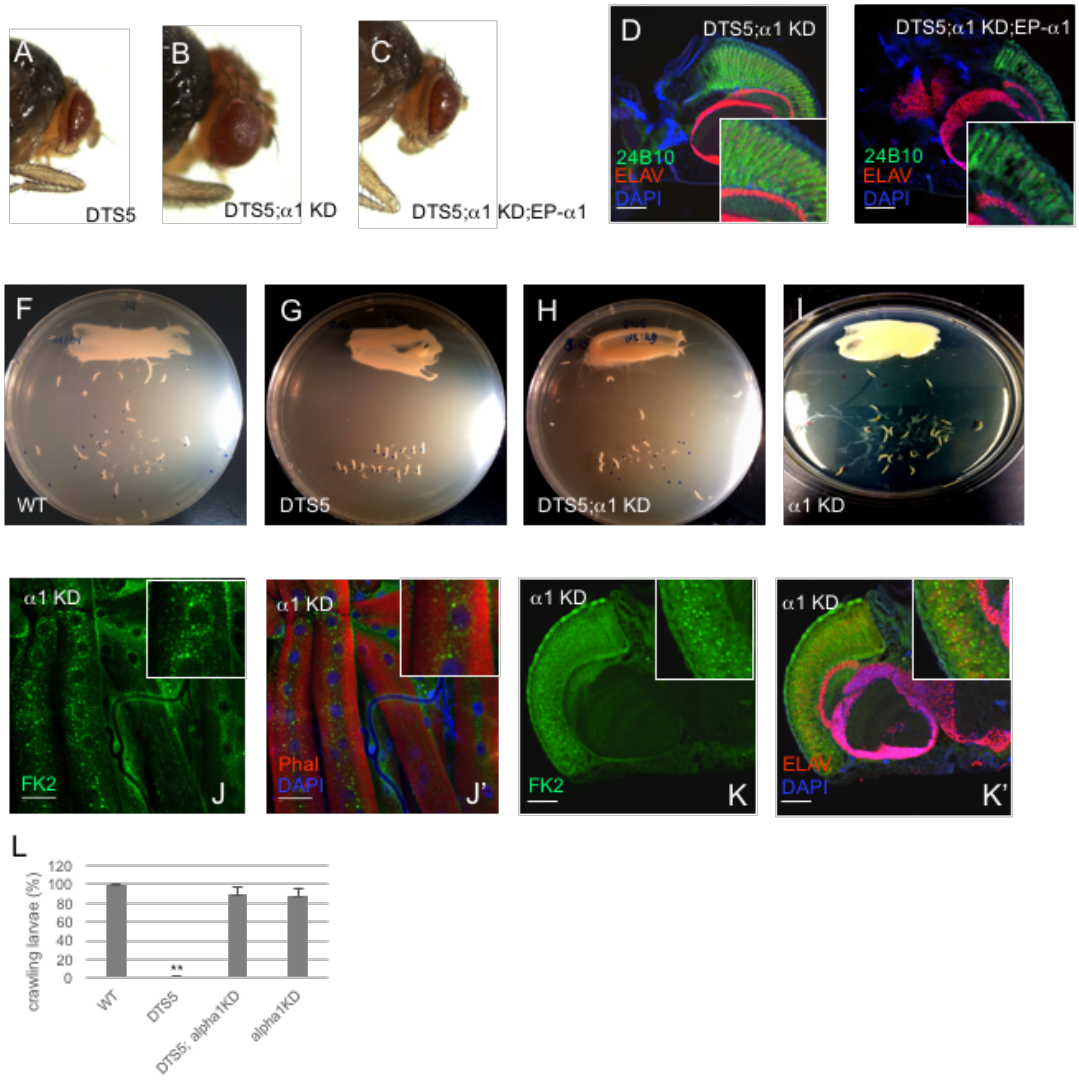
A
DTS5
B
DTS5;α1 KD
C
DTS5;α1 KD;EP-α1
D
DTS5;α1 KD
24B10
ELAV
DAPI
DTS5;α1 KD;EP-α1
24B10
ELAV
DAPI
F
WT
G
DTS5
H
DTS5;α1 KD
I
α1 KD
α1 KD
FK2
J
α1 KD
Phal
DAPI
J'
α1 KD
FK2
K
α1 KD
ELAV
DAPI
K'
L
crawling larvae (%)
120
100
80
60
40
20
0
**
WT
DTS5
DTS5; alpha1KD
alpha1KD

3.3.2 Atrophy salvage by α1 KD correlates with altered localization of proteasomes

Nature has evolved several mechanisms to detoxify intracellular protein aggregates that arise upon proteotoxic challenges. These include controlled deposition of misfolded proteins at distinct cellular sites, protein disaggregation and refolding by molecular chaperones and/or degradation of this toxic aggregates by the proteasome. To facilitate increased demand for degradation at specific sites, localized degradation is mediated by proteasome compartmentalization. Targeted proteasome deposition and transport are not only important in stress adaptation but are also vital for organismal development, especially for neuronal plasticity and sperm individualization.

To further explore molecular effects of the genetic interaction of DTS5 and α1 on proteasome localization, muscles were counterstained for the 19S RP subunit Rpt3. Proteasome assembly is initiated in the cytoplasm followed by transfer of its sub-particles to the nucleus where final stages of assembly are completed. Under normal growth of cells, the proteasome is usually found in the nucleus (Reits et al., 1997; Wilkinson et al., 1998). As expected Rpt3 showed predominant nuclear staining in wild-type flies (Figure 3.2A). Additionally, α1 knockdown flies also showed predominant nuclear staining (Figure 3.2D) demonstrating that they experience only mild proteotoxic stress. For flies expressing DTS5 and those introduced with α1 RNAi the Rpt3 staining pattern stood out. In flies experiencing DTS5-dependent proteotoxic stress, Rpt3 staining was mostly excluded from nuclei revealing an un-defined distribution pattern along the length of the muscle (Figure 3.2B). Proteasome subunits are usually expressed in stoichiometric quantities and are assumed to be fully incorporated into holo-proteasome particles with no free subunit

deposits. The appearance of an un-defined pattern led me to think that it could result from proteasome dis-assembly, therefore I continued with a more thorough examination of proteasome assembly using native gel assays in the following sections. Yet, it cannot be ruled out that the atrophy and its associated loss of architecture could account for this diffused pattern.

Especially intriguing was the observed pattern in flies expressing both DTS5 and the α1 RNAi (Figure 3.2C). Instead of a predominant nuclear staining, majority of the Rpt3 was now found in the cytoplasm. Staining was prevalently in the peri-nuclear compartment known to harbor the ER-Golgi network. Counterstaining for Rpt2, another 19S RP subunit, repeated same observations, reaffirming this result. Of special note is that the differential localization is observed only in muscle tissues, where expression of this genetic interaction is targeted. Soma tissue was comparable to wild-type and retained predominant nuclear localization of proteasomes (Figure 3.2C, see arrow).

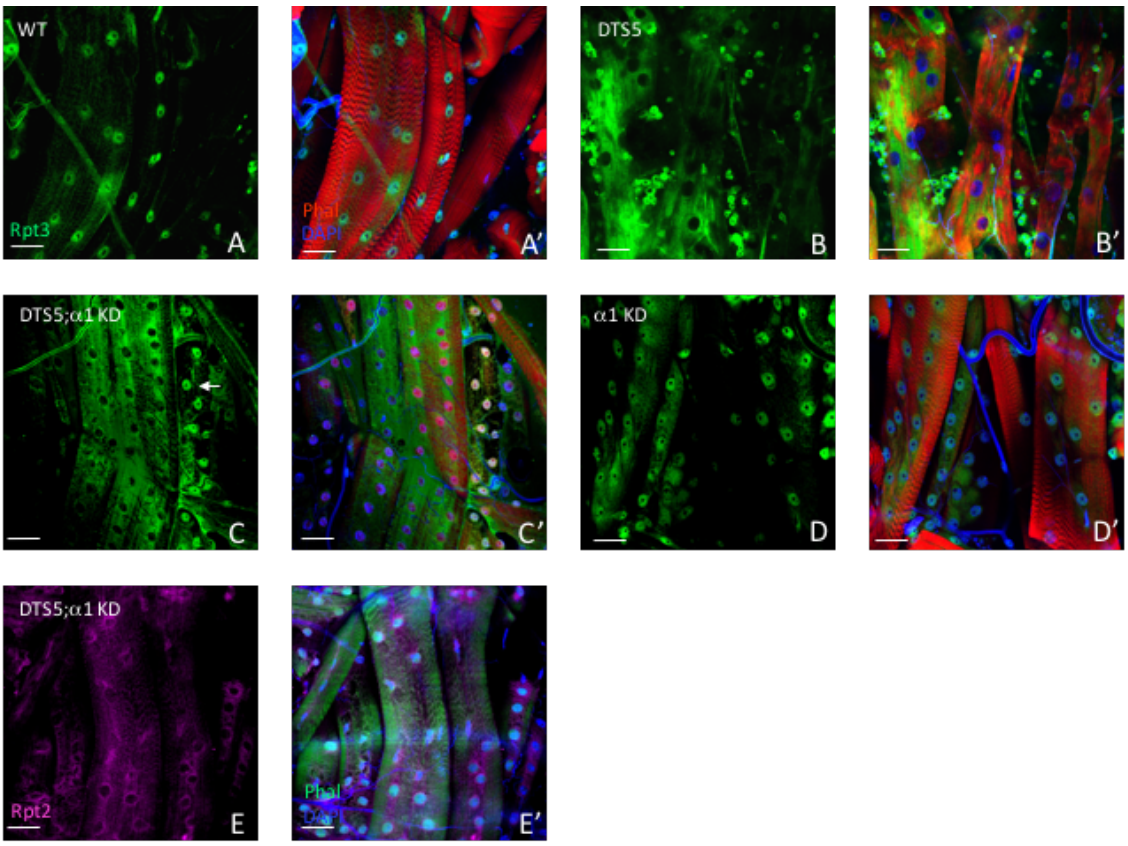

Figure 3.2 Distribution of proteasomes under proteotoxic stress and stress adaptation. Larvae were raised as described before, muscles were dissected at a 24-hour time point and counterstained for either Rpt3 or Rpt2 to visualize proteasomes. Prevalent nuclear staining of Rpt3 was observed in wild-type and α1 knockdown in muscle tissue, whereas in DTS5-expressing muscles Rpt3 staining was dispersed un-defined. Differential localization was seen in DTS5;α1-KD muscles, with prevalent peri-nuclear staining of Rpt3 in DTS5 and α1 RNAi-targeted muscle cells, as opposed to predominant nuclear staining in soma tissue (marked with arrow). **A-D** Left panels depict Rpt3 staining marked by green, right panels (**A'-D'**) depict the merge of Rpt3 staining with DAPI (blue) and Phalloidin (red). **E.** Left panel depicts Rpt2 staining marked by magenta, right panel (**E'**) depicts merge of Rpt2 staining with DAPI (blue) and Phalloidin (green).

Rpt3 alone is not enough to depict where active proteasomes may reside. In order to complete the picture, a 20S core particle marker was needed. Co-localization of 19S and 20S markers depict where active holo-proteasomes are found. For this purpose, I used transgenic flies expressing GFP-tagged α2 subunits from an endogenous promoter reconstructed with the genetic transgenes that I studied (Figure 3.3A-C). Proteasomes containing fused proteins exhibited normal function *in vivo* (Ma et al., 2002). In wild-type flies α2-GFP merged with the Rpt3 staining displaying the same nuclear pattern expected from functioning proteasomes in normal growth (Figure 3.3A). In DTS5 flies α2-GFP co-localized with Rpt3 in the same diffusive pattern depicted before (Figure 3.3B). In DTS5 flies constructed with α1 RNAi, α2-GFP was predominantly found in the nucleus, but abundant co-localization with the Rpt-3 signal was found primarily in the peri-nuclear domain (Figure 3.3C).

The peri-nuclear area is an intracellular site that exhibits high levels of ubiquitin-dependent proteolysis and is known to host molecular chaperones responsible for re-folding mis-folded aggregates and/or sorting them for cellular clearance pathways. Compartmentalized degradation could be one of the mechanisms that make these flies better equipped to cope with proteotoxic stress.

More rigorous examination of these observations was carried by inducing genetic clones using the Flp-FRT system (Golic and Lindquist, 1989; Harrison and Perrimon, 1993). This technology that allows for the spatial and temporal restriction of transgene expression relies on the use of the yeast site-specific recombinase, flipase (Flp) and its recognition target sequence (FRT). The Flp-out technique uses transgenes that are silenced by a transcriptional stop signal flanked by FRT sites that can be removed by the expression

of Flp to activate the gene of interest (Bischof and Basler, 2008; McLeod et al., 1986). Only progenitors in which flipase was active in would express the GAL4-UAS system. This genetic technique can be used to label single cells or multiple cells sharing a single progenitor. The Flp-FRT-dependent mitotic recombination results in genetic marking of clones, which express a transgene that is otherwise repressed in the adjacent wild-type non-recombined clones. This method provides a tool to study transformed tissues in the background of a phenotypically wild-type un-altered cells. To induce mosaic clones, I used the flipase under a heat-shock promoter (hs-FLP) for temporal control. Mosaic prevalence can be controlled by timing and duration of heat shock exposure, so that only a subset of progenitors will go through a flipase-FRT recombination. After Flp-FRT- dependent recombination, clones in which the stop signal was removed now express GAL4 under tubulin promoter and are genetically marked with ds-Red. Only ds-Red marked cells also drive expression of the DTS5 and α1-RNAi transgenes that are under GAL4-UAS control. Non-marked tissue is comparable to wild-type tissue. In line with the former results, ds-Red clones displayed aberrant Rpt3 localization whereas non-marked clones behaved similarly to wild-type revealing nuclear staining (Figure 3.3D). Rpt3 staining was aberrant but still not quite the same as seen beforehand. There are two possible explanations to this discrepancy. First this observation can be classified as a non-autonomous effect. With this method, transgenic clones may appear in other tissues such as brain. Albeit these random clones are not enough to effect whole organism viability and morphology, they could be enough to instruct dissimilar signal transduction in other tissues. Second in this model GAL4 is under a tubulin promoter and not MHC, which might explain altered expression.

Figure 3.3 26S proteasomes concentration in peri-nuclear sites correlates with stress-adaptation. A-C genetic backgrounds of: wild-type, DTS5 and DTS5;α1-KD respectively were constructed in flies expressing a transgenic GFP tagged α2 subunits (green, first to left column). Muscles were counterstained with anti-GFP to enhance signal, Rpt3 (red, second to left column), Phalloidin (magenta) and DAPI. Third to left column depicts a merge of green and red channels, marking co-localization of 20S (α2-GFP) and 19S (Rpt3) markers. Fourth column depict a merge including DAPI (blue) and Phalloidin (magenta). In wild-type tissue co-localization was observed primarily in the nucleus. In muscles derived from DTS5;α1-KD, α2 tagged proteins were found both in nucleus and cytoplasm but co-localized with Rpt3 primarily in peri-nuclear sites. **D.** Flp-FRT system was used to create clones expressing DTS5 and α1 RNAi, which were visualized with ds-Red marker (first left column) and counterstained for Rpt3 (green, second left column). Third and fourth column depict a merge without and with DAPI (blue) and Phalloidin (magenta) respectively. Clones displayed altered distribution as opposed to predominant nuclear staining in non-clonal muscles, indicating that localization pattern was likely dependent on transgenic expression of DTS5 and α1 RNAi.

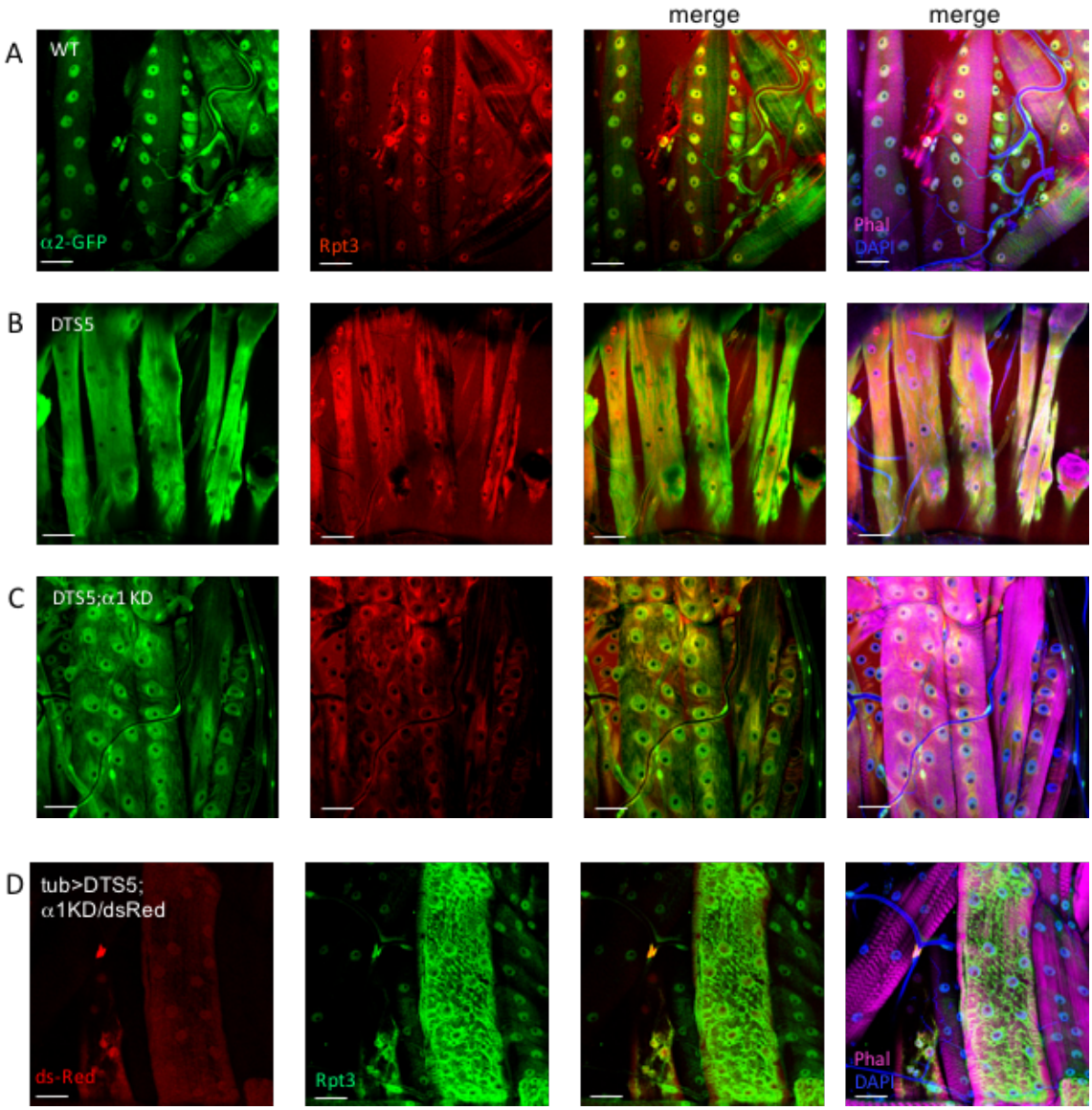
merge
merge
A
WT
α2-GFP
Rpt3
Phal
DAPI
B
DTS5
C
DTS5;α1 KD
D
tub>DTS5;
α1KD/dsRed
ds-Red
Rpt3
Phal
DAPI

3.3.3 Atrophy salvage is mediated by a general mechanism of compromised 20S proteasome complex

Recently Tsvetkov et al. showed that compromising 19S proteasome complex can protect cells against proteotoxic stress incurred by the proteasome inhibitors MG-132 or Bortezomib (Tsvetkov et al., 2015). They performed a screen on a collection of mutant human CML cells looking for resistance to proteasome inhibitors. Surprisingly, cells which had reduced expression of various 19S subunits, including both Rpt and Rpn subunits, were more resistant, however no mutants of 20S subunits were enriched in the screen. Strong reduction was cytotoxic but a modest reduction protected cells from inhibition. In light of this finding, I postulated that mitigating the DTS5 proteotoxic stress might not be a unique characteristic of α1 subunit and instead might represent a more general mechanism of compromising either the 20S complex or 19S complex.

I addressed this notion by expanding the screen to include almost all subunits of the α ring (α3 is not represented since it has no RNAi stock), some β ring subunits and both Rpn and Rpt representatives of the 19S particle. All α ring subunits except α6 were successful at rescuing larval paralysis (Figure 3.4A). Yet, β2 and β5 RNAi did not relieve atrophy. It is possible that their inability to relieve atrophy had to do with their catalytic function, thus they are needed in stoichiometric levels. Reduced expression of almost all of the 19S subunits, notwithstanding Rpn2, which exhibited moderate rescue, did not alleviate larval paralysis significantly (Figure 3.4B). I also tested the effect of knocking down α subunits for their ability to suppress the rough eye phenotype. Similarly, to what I

observed in regards to muscle atrophy, all α subunits RNAi reverted the eye phenotype back to normal, except α6.

In conclusion α1 action in the context of DTS5 stress is not exclusive but rather part of a general stress adaptation mechanism enlisted when compromising the 20S complex. The role of α6 does seem to be unique. The discrepancy in 19S role between my study and that of Tsvetkov and colleagues (Tsvetkov et al., 2015; 2017) can be explained by the mode of proteasome disruption that was used. In their study, they used proteasome inhibitors which target the catalytic activity of the proteasomes whereas I used a mutant form of a proteasome subunit, which could target other aspects of proteasome function such as assembly. Up to date the mechanism of action of DTS5 is largely unknown and is addressed in this thesis.

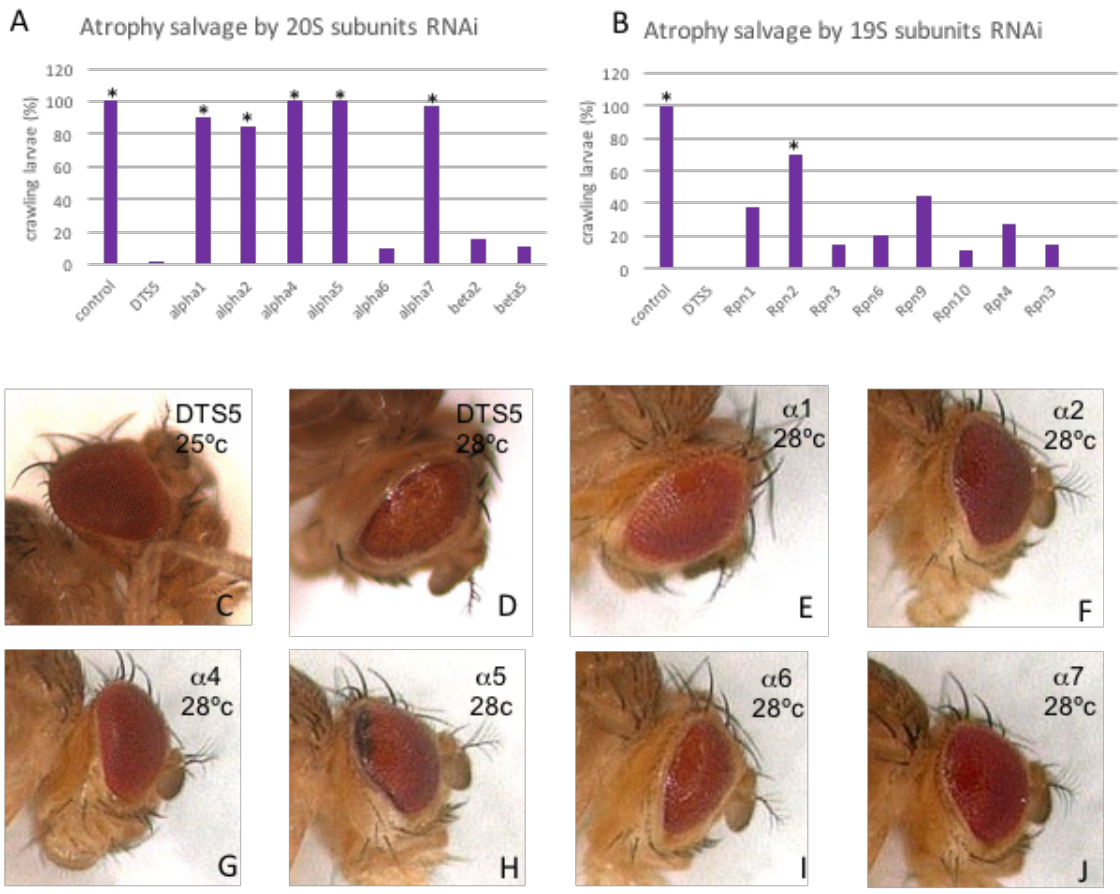

Figure 3.4 Atrophy is relieved when compromising the 20S complex but not 19S. A-B. Quantification of RNAi effects on DTS5 induced larval paralysis categorized by 20S and 19S subunits respectively. Percentage was calculated per genotype as number of crawling larvae per total larvae placed on apple plate. **C-J.** Analysis of rough eye phenotype as describe before. Flies were constructed with the GMR driver to promote transgenes expression.

3.3.4 Alternative compensatory mechanisms for proteasome inhibition

Proteasome activity is regulated at several levels to preserve homeostasis. Upon proteasome inhibition, a concerted de novo synthesis of all 26S proteasomal subunits with subsequent whole proteasome formation, was observed in several organisms (Li et al., 2011; London et al., 2004; Lundgren et al., 2005; Meiners et al., 2003; Mitsiades et al., 2002). A common regulatory pathway in response to reduced proteasome function or general stress is induction of transcription factors to elevate subunit abundance (Radhakrishnan et al., 2010; Steffen et al., 2010; Xie and Varshavsky, 2001). In *Drosophila* deletion of the Rpn10/S5a subunit or its depletion with RNA interference increased the level of 26S proteasome (Lundgren et al., 2003; Szlanka et al., 2003). Accordingly *Drosophila* cell lines lacking Rpn10/S5a showed only minor increases in ubiquitin conjugate levels with no observable loss of *in vivo* proteasome activity (Lundgren et al., 2003).

To investigate compensatory induction of proteasome subunits I performed Western blots assaying protein levels of the proteasome subunits Rpt3 and α7 (Figure 3.5A). It is believed that all proteasome subunits are expressed in comparable stoichiometric levels and are found in cells in the context of their respective complex with no free subunits. An exception to this rule is Rpn10/S5a which can be found in a free state (Piterman et al., 2014). Proteasome inhibition with DTS5 did not result in augmented abundance of these proteins. Like Rpn10/S5a depletion, proteasome interference with α1 RNAi presented mild proteotoxic stress with accumulation of poly-ubiquitinated proteins but no observable loss of proteasome activity (Lundgren et al., 2003), but it did not result

in increased expression of other proteasome subunits. In conclusion, it is unlikely that α1depletion restored proteasome activity in DTS5 flies through transcriptional regulation of proteasome subunits as no elevated expression was observed in its presence. If anything, expression levels seemed to decrease, but Tubulin levels were also reduced in that sample.

The UPS and autophagy are the two main systems involved in the regulation of protein homeostasis and housekeeping functions. The UPS presents a selective pathway for protein degradation, whereas autophagy is responsible for bulk destruction. These protein degradation pathways share some common regulators so they can act simultaneously and in conjunction to preserve protein homeostasis and quality control (Mammucari et al., 2007; Zhang et al., 2014; Zhao et al., 2014; 2015). Specifically, activated FoxO3 stimulated both proteasome and autophagy-dependent degradation to promote muscle atrophy (Zhao et al., 2014). The UPS acts constitutively as the first line of defense in the elimination of protein aggregates. But when proteasomal degradation is compromised, cells have been shown to recruit autophagy as a compensatory mechanism (Fusco et al., 2012; Kageyama et al., 2014; Pandey et al., 2007).

To explore if autophagy contributes to induced atrophy and/or its rescue I applied RNA interference of two autophagy key players, ATG4 and ATG13 (Figure 3.5B). ATG4 is responsible for LC3 processing in the elongation and expansion phase of the autophagosome (Satoo et al., 2009). ATG13 participates in the initiation and nucleation of the autophagosome (Alers et al., 2014). Depletion of autophagy components mildly rescued larval paralysis, though not statistically significant, denoting some contribution to autophagy activity in induced atrophy. As discussed in Chapter 2 muscle atrophy was accompanied with a mild elevation in ATG8 puncta, a sign for increased autophagy. On

the other hand, depletion of autophagy components from the DTS5;α1-RNAi strain did not impair paralysis suppression gained by expression of α1 RNAi. This observation implies that α1-RNAi did not rescue muscle atrophy through triggering compensatory autophagy and that another general mechanism is in play.

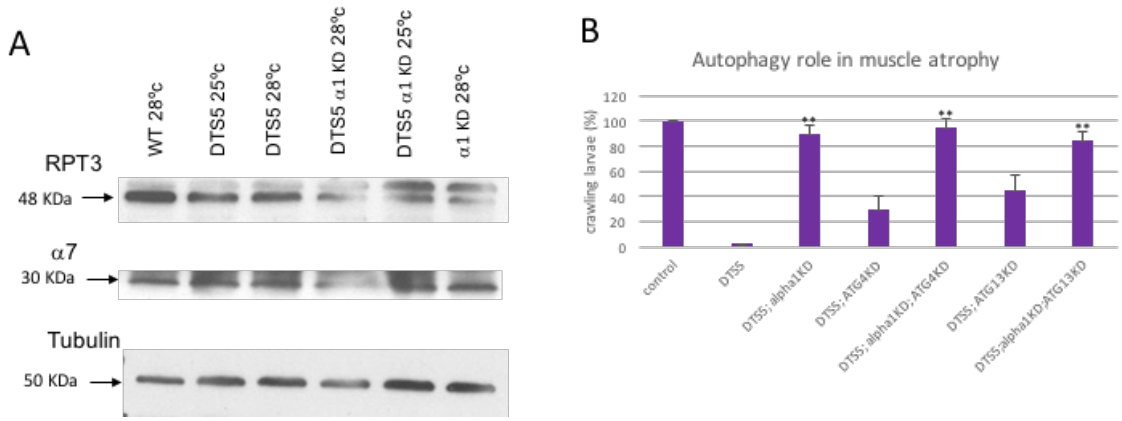

Figure 3.5 α1 knockdown does not mitigate proteasome inhibition through alternative compensatory mechanisms. A. Proteasome inhibition by DTS5 and its rescue by α1 do not enhance expression of proteasome subunits, as assessed by Western blotting for Rpt3 and α7 of protein extracts from dissected muscles. Tubulin protein levels served as loading control. **B.** Autophagy had insignificant contribution to DTS5 induced larval paralysis but was not required for α1 RNAi mechanism of action. Bars represent mean values from 3 independent experiments, 90 larvae in total. Percentage was calculated per genotype as number of crawling larvae per total larvae placed on apple plate. Significance measured in respect to DTS5 values **P<0.001 (two-tailed Student's t-test).

3.3.5 α1 knockdown alters 26S composition

Proteasome function is derived from the processivity of its catalytic activity and assembly rate. Despite the spread use of the DTS mutants as a standard model for proteasome disruption, their mechanism of action is not fully resolved. While it is clear that they impair proteasome activity, they could do so through two distinct mechanisms. First, they could perhaps directly inhibit the catalytic sites through allosteric effects, or alternatively attenuate 26S assembly. In fact, β2 and β6 assume at a unique position which stabilizes two half proteasomes together.

To examine whether DTS5 and α1 function relates to proteasome biogenesis, I examined proteasomal particles from muscle lysates resolved by non-denaturing PAGE (native gel), followed by immunoblotting. Native gel allows for fine resolution of the multiple species of the proteasome and analysis of ratio between proteasome holoenzymes (RP2-CP and RP-CP) to free CP, indicative of proteasome assembly (Elsasser et al., 2005). Dissected tissue was lysed in an ATP rich buffer to protect proteasome holoenzymes from dis-association. Membranes were immunoblotted with α7 (Figure 3.6A) to assess holoenzymes and free particles, and Rpt3 (Figure 3.6B), which can detect holoenzymes and RP assembly intermediates. DTS5 led to a dramatic reduction in 26S to 20S ratio and increased presence of free RP, revealing for the first time that DTS5 inhibits proteasomes due to reduced assembly.

One might expect RNA interference of α1 to weaken the interaction between the RP and CP and consequently lead to a reduction in the ratio of proteasome holoenzyme (RP_2-CP and RP-CP) to free CP. On the contrary, these proteasomes were found

predominantly in the holoenzyme form, and the level of free CP fell below detection limit (Figure 3.6). Among holoenzymes, the RP_2-CP species predominated over RP-CP whenever α1 RNAi was applied. I assume that stoichiometric imbalance in 20S subunits created an imbalance in favor of RP over CP, which led to preferential formation of RP_2-CP over RP-CP. Remarkably, α1 RNAi also accumulated RP assembly intermediates (Figure 3.6B). Together these observations suggest that a CP assembly defect did follow α1 depletion. However, formed holoenzymes were more stable so overall active proteasomes were present at higher levels in flies expressing RNAi, whether in a wild-type or DTS5 background, compared to wild-type or DTS5 at permissive temperature respectively. In conclusion, increased proteasome activity could be accounted for with increased stability of holoproteasomes.

In addition to the features described above, proteasomes from α1-RNAi flies also exhibited reduced electrophoretic mobility in native gels. This effect could be seen for both the RP-CP and RP_2-CP forms of the proteasome (Figure 3.6). The mobility shift pointed to a major structural difference. I hypothesized this structural difference might account for α1 role in mitigating proteotoxic stress and continued with this line of premise.

α1 mode of action on proteasome species was not unique to muscle tissue. Native gel was also used to resolve proteasome species of heads only tissue (Figure 3.6C-D). For holoenzyme analysis in heads I relied mostly on Rpt3 signal. α7 antibody is a more sensitive and less robust antibody and often failed in distinguishing holoenzyme species, especially in head samples. In this respect, increasing the sample size was beneficial although same amount of protein was loaded as in native gel with muscle tissue. Even though GMR is expressed only in a fraction of the cells in heads, it still remarkably

captured similar key observations as seen in the muscle analysis. In its permissive temperature proteasomes from the DTS5 strain were found mostly in a CP free, in line with proteasome dissociation. Moreover, proteasomes from α1-RNAi flies displayed reduced electrophoretic mobility, suggesting a general stress adaptation response.

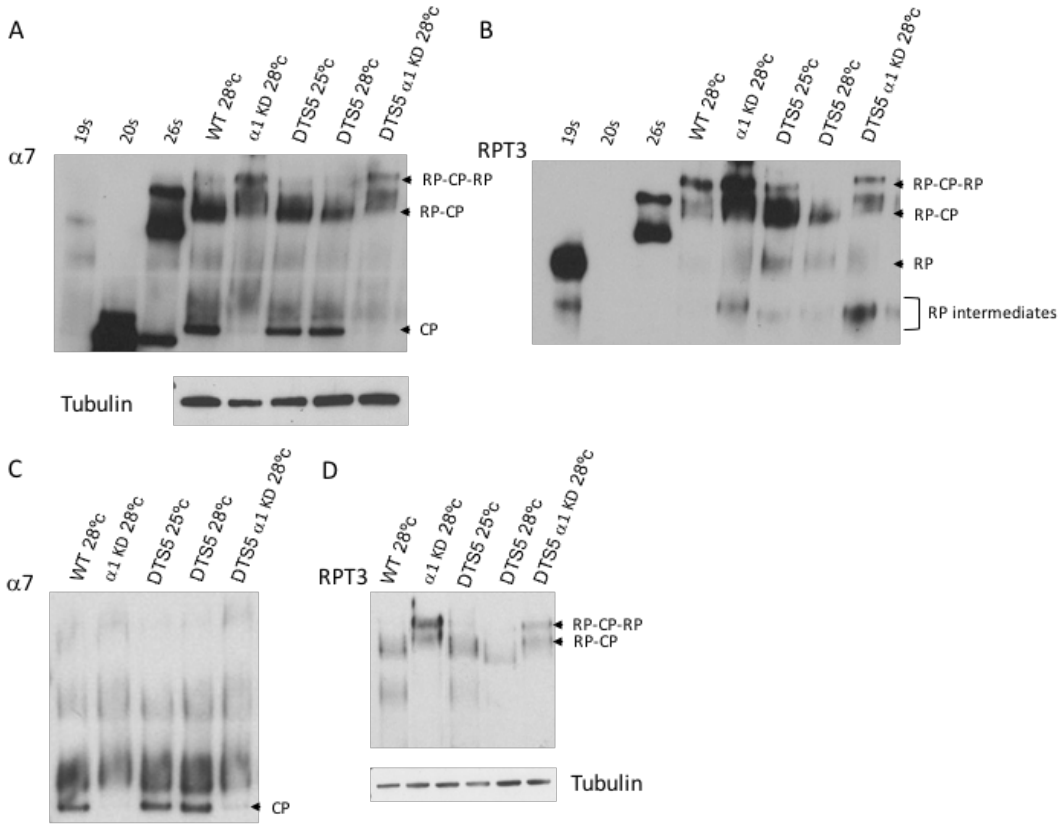

Figure 3.6 α1 knockdown promotes holoenzyme complex assembly. A-B. Protein extracts (25 μg) of dissected muscle tissue from indicated strains were resolved on native gels and subjected to immunoblot for subunit of the CP (α7) and subunit of the RP (Rpt3) respectively. **C-D.** As in **A-B** Proteasome species were assayed with native gel of protein extracts (25 μg) from head tissue. Free CP was examined with α7 and RP-CP with Rpt3. For control 10 μg of protein extracts was resolved on SDS-PAGE and immunoblotted for tubulin.

3.3.6 Identification of Ecm29 role in novel proteasome particles

α1-RNAi resistance to DTS5 proteotoxic stress suggested α1 reduction triggered an adaptation response to promote proteasome stability, that may account for structural changes depicted in the previous section. Based on the native gel observations I proposed proteasomes were modified by a regulatory protein that should comply with three key criteria:

I. Must be a large enough protein to account for significant mobility shift.

II. Bind to complexes composed of both RP and CP.

III. Support holoenzyme complexes.

Knowledge of proteasome regulators in *Drosophila* is limited to the 19SRP and PI31, whereas several regulatory complexes are known in mammals and yeast: PA28, PA200/Blm10, Usp14/Ubp6, KIAA00368/Ecm29. Ecm29 is the only one conserved in flies, sharing 18% identity with the yet un-characterized CG8858. Ecm29 stood out as a promising candidate as it fulfills all three criteria I predicted. First it is a very large protein, 205KDa, and has been shown to confer a mobility shift of proteasomes (Kleijnen et al., 2007; Park et al., 2011). Ecm29 is known to associate with the proteasome holoenzyme in preference to its sub-complexes, the RP and CP (Kleijnen et al., 2007; Leggett et al., 2002; Park et al., 2011). Moreover, Ecm29 has been implicated in supporting RP-CP association and stabilizing the proteasome holoenzyme (Kleijnen et al., 2007; Leggett et al., 2002; Lehmann et al., 2010; Park et al., 2011).

To better understand how CG8858 (from now on referred as Ecm29) might regulate proteasome function I used a hypomorphic P-element allele construct of this gene

(Ecm29^{MI482}). Ecm29 is known as a chaperone: under normal conditions loss of Ecm29 had no effect on organismal growth but when proteasome function was compromised its function was required (Haratake et al., 2016; La Mota-Peynado et al., 2013). I therefore examined Ecm29^{MI482} effect on Ecm29 expression both in wild-type background and when proteasome function was compromised by α1 depletion. Ecm29^{MI482}'s ability to deplete Ecm29 protein expression was confirmed both by Western blot (Figure 3.7A) and immunofluorescence (Figure 3.7B). While it seemed that α1 reduction led to upregulation in Ecm29 expression this observation was not consistent with the Western blot.

I next asked if Ecm29 depletion effected muscle atrophy and proteotoxic stress. As expected Ecm29 depletion by itself did not disrupt larval motility and muscle function, regardless of whether α1 was present at normal or reduced levels (Figure 3.7C). Nonetheless it did enhance accumulation of poly-ubiquitinated proteins which was even more enhanced when α1 was present at low levels (Figure 3.7D). This result signifies α1 and Ecm29 association in alleviating proteotoxic stress. The Ecm29^{MI482} effect was not enough to stop poly-ubiquitinated proteins from accumulating but was sufficient to prevent gross atrophy induction It will be interesting to see what would happen with a null form of Ecm29.

Figure 3.7 Ecm29 is not needed for normal muscle function. A-B Validation of the Ecm29^{MI482} mutant. **A.** Protein extracts from muscle tissue of the indicated strain were resolved on SDS-PAGE and immunoblotted for Ecm29. Ecm29^{MI482} disturb Ecm29 expression. Tubulin was used as loading control. **B.** Dissected muscles were fixed and immunoassayed against Ecm29. In line with the idea that Ecm29 has no function under normal conditions its signal was low in wild-type tissue (left panel) but enhanced upon α1 interference (middle panel). Enhanced signal was dependent on Ecm29 expression as Ecm29^{MI482} diminished that signal (right panel). **C.** RU-486 fed larvae of indicated genotype were placed on apple plates after 24-hours incubation in 28.3°C. Depletion of Ecm29 did not halt motility independent of α1 levels (middle and right panel). Quantification of motility in panel **C'.** Bars represent mean values from 5 independent experiments, 100 larvae in total. Percentage was calculated per genotype as number of crawling larvae per total larvae placed on apple plate. **D.** Muscles of larvae from panel C were assayed for poly-ubiquitinated protein accumulation with FK2 antibody. High levels of Ecm29 are required to diminish proteotoxic stress resulting from α1 interference, see Figure 3.1 for comparison (right panel), yet remaining Ecm29 expression was sufficient to prevent muscle atrophy and maintain normal muscle architecture.

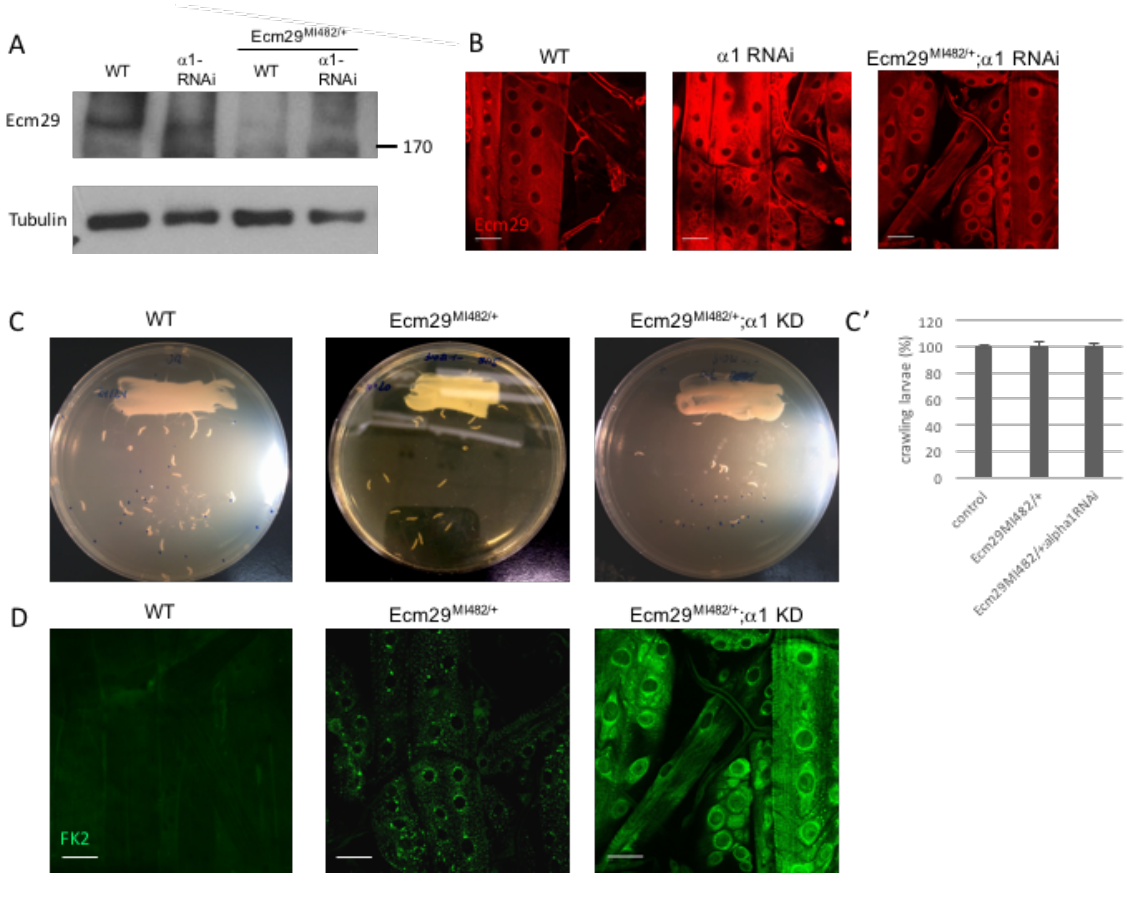
A
Ecm29MI482/+
WT
α1-RNAi
WT
α1-RNAi
Ecm29
170
Tubulin
B
WT
α1 RNAi
Ecm29MI482/+;α1 RNAi
Ecm29
C
WT
Ecm29MI482/+
Ecm29MI482/+;α1 KD
C′
crawling larvae (%)
120
100
80
60
40
20
0
control
Ecm29MI482/+
Ecm29MI482/+;alpha1RNAi
D
WT
Ecm29MI482/+
Ecm29MI482/+;α1 KD
FK2

After characterizing Ecm29 requirement in normal conditions I followed suit in DTS5-dependent proteotoxic stress. Ecm29^{MI482} expression significantly diminished the ability of α1 knockdown to rescue DTS5 induced larval paralysis (Figure 3.8A). Abolished rescue was not complete with still roughly 40% of larvae remaining motile (Figure 3.8A'). The DTS5 allele carries a wild-type Ecm29, which might account for preserved motility. For a more accurate genetic analysis of Ecm29 activity, I will employ two strategies for future experiments: DTS5 recombined with Ecm29^{MI482} and null Ecm29. I started in the construction of strains, for null strains applying the CRISPR method but they remain to be validated and therefore were not assayed yet. As expected from behavioral assays high levels of Ecm29 were needed for α1-RNAi to counter accumulation of poly-ubiquitinated proteins (Figure 3.8B). Larval paralysis followed deformed muscle architecture as presented before. Not surprisingly, by itself Ecm29^{MI482} had no effect on DTS5-dependent paralysis or poly-ubiquitin accumulation (Figure 3.8A-B, right column). These observations highlight both α1-RNAi and Ecm29's functional requirements in mitigating DTS5 proteotoxic stress.

I tested whether α1-RNAi and Ecm29 association was specifically related to proteasome activity with *in vivo* assay for proteasome activity (previously described in section 2.3.4). High levels of Ecm29 were needed for α1-RNAi to relieve DTS5-dependent inhibition of proteasome activity. In short, the combined action of α1 RNA interference and Ecm29 function was needed to sustain proteasome activity required for normal function of muscles.

Figure 3.8 α1 RNAi requires Ecm29 to suppress DTS5 dependent stress. A. Following RU-486 feeding and 24-hours incubation in 28.3°C larvae of indicated strain were assayed for their movement on apple plates. High levels of Ecm29 were needed for α1-RNAi to suppress DTS5 dependent larval paralysis (third column). **A'.** Bars represent mean values from 5 independent experiments, 100 larvae in total. Percentage was calculated per genotype as number of crawling larvae per total larvae placed on apple plate. Significance in respect to wild-type motility (Figure 3.7C') **P<0.001, statistical analysis was performed with a two-tailed paired t test. **B.** Muscles of larvae from panel A were assayed for poly-ubiquitinated protein accumulation with FK2 antibody. $Ecm29^{MI482}$ de-suppress accumulation of poly-ubiquitinated proteins observed in DTS5/α1-RNAi strains (middle panels). **C.** *In vivo* proteasome activity of indicated strains reveal Ecm29 prerequisite for α1-RNAi to relieve DTS5 inhibition of proteasome activity. Analysis was carried out as described Figure 2.9, GFP signal persistence at 4-hours post heat shock depict inhibition of *in vivo* proteasome activity. **C'.** Quantification of GFP signal. Bars represent the means of percent values 4-hours versus 1-hour post HS induction of each respective strain. Statistical analysis was carried out on a total of 12 larvae (images) from 3 independent experiments. **P<0.001 significance in comparison to WT signal, with a two-tailed, paired, t test.

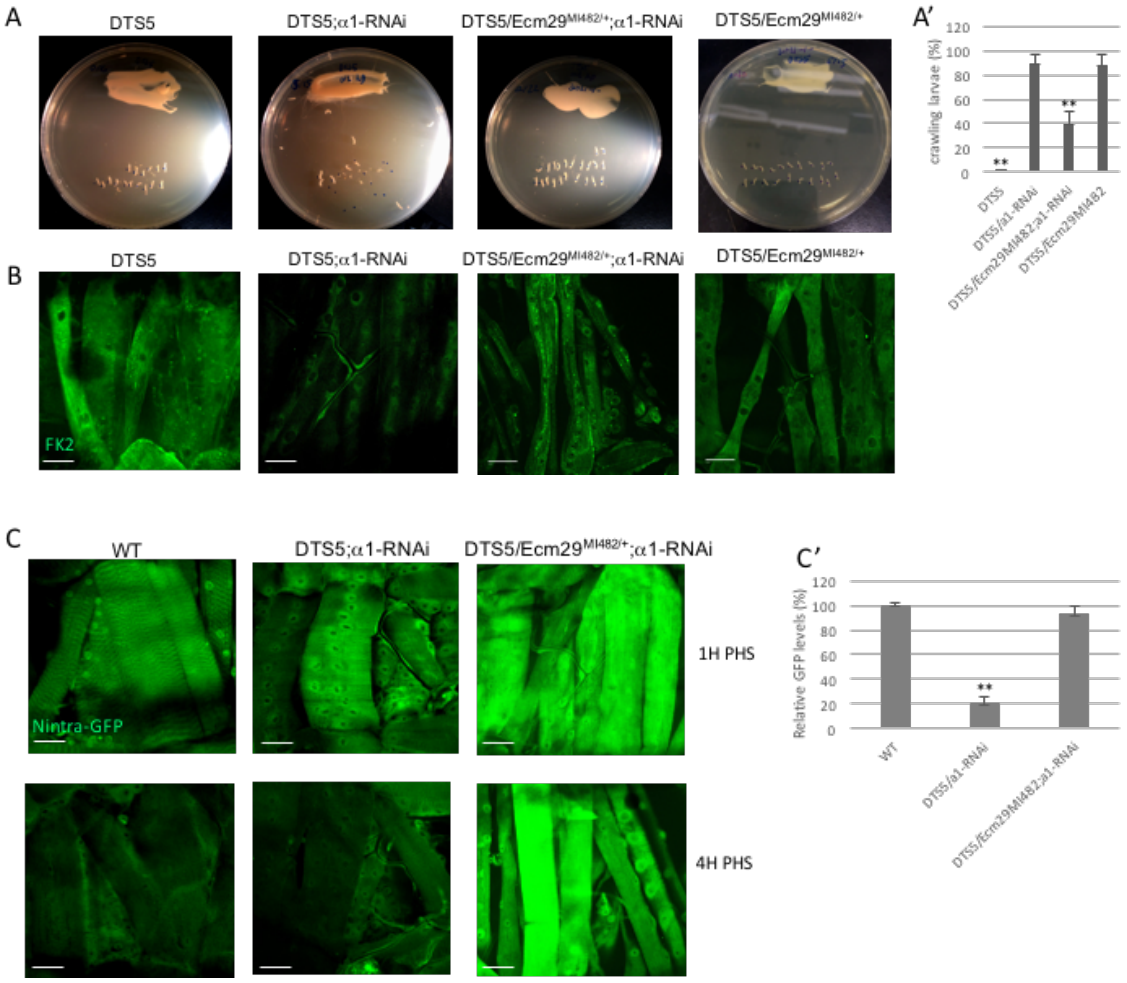
A
DTS5
DTS5;α1-RNAi
DTS5/Ecm29MI482/+;α1-RNAi
DTS5/Ecm29MI482/+
A′
crawling larvae (%)
120
100
80
60
40
20
0
**
**
DTS5
DTS5/α1-RNAi
DTS5/Ecm29MI482;α1-RNAi
DTS5/Ecm29MI482
B
DTS5
DTS5;α1-RNAi
DTS5/Ecm29MI482/+;α1-RNAi
DTS5/Ecm29MI482/+
FK2
C
WT
DTS5;α1-RNAi
DTS5/Ecm29MI482/+;α1-RNAi
Nintra-GFP
1H PHS
4H PHS
C′
Relative GFP levels (%)
120
100
80
60
40
20
0
**
WT
DTS5/α1-RNAi
DTS5/Ecm29MI482;α1-RNAi

3.3.7 α1-RNAi induces recruitment of Ecm29 to promote RP-CP association

The mobility shift I observed in Figure 3.6 pointed to a major structural difference between wild-type and proteasomes assembled in in the presence of α1-RNAi, which can be indicative of Ecm29 binding to proteasomes. To test whether Ecm29 binding produced a reduction in electrophoretic mobility of proteasomes, I introduced Ecm29^{MI482} to the DTS5;α1-RNAi strain. Resolving muscle protein extracts of this strain on native gels, revealed dependence of the mobility shift on Ecm29 levels compared to wild-type proteasomes (Figure 3.9A,C). Ecm9 mutant strongly reduced the level of RP-CP species in DTS5;α1-RNAi and the level of free CP was correspondingly increased (Figure 3.9A). Reduced ratio of 26S to 20S is the hallmark of holoenzyme assembly defects and clear indication that Ecm29 was needed to maintain RP-CP association. Proteasomes resolved from Ecm29^{MI482}/DTS5;α1-RNAi strain, which preserved their holo-complex likely represent residual binding of Ecm29 protein and therefore also displayed reduced mobility. It is possible that this strain still had some Ecm-29 free holo-complexes but their levels were too low for this assay to detect. In conclusion DTS5;α1-RNAi strain carrying a mutant Ecm29 could not initiate an adaptive response to proteotoxic stress, despite experiencing one due to DTS5 and a1-RNAi presence, because of depleted Ecm29 levels.

To confirm Ecm29 recruitment by aberrant proteasomes (formed in strains carrying α1-RNAi) I immunoblotted native gels for Ecm29 (Figure 3.9B). Wild-type Ecm29 presence on aberrant proteasomes was significantly higher. In Ecm29^{MI482}, Ecm29 binding was reduced most likely due to reduced total levels of Ecm29 and not due to decreased affinity. I repeated my analysis with purified proteasomes to test physical association of

Ecm29 (Figure 3.9C). The proteasome CP subunit β5, carrying a protein GFP tag, was chosen to selectively isolate proteasome holoenzymes. Using this tag I also isolated free CP, but previous reports and my observations showed this complex does not bind Ecm29 and Ecm29 preferentially binds to RP-CP species (Lehmann et al., 2010; Park et al., 2011). Ecm29 was enriched on proteasomes purified from DTS5;α1-RNAi strain compared to wild-type proteasomes.

Proteasomes were also tested for a possible effect of Ecm29 on the proteasome gate (Figure 3.9D). Gate opening was assessed using in-gel peptidase assay, in which native gels are exposed to the fluorogenic peptide LLVY-AMC. Band intensity in this assay correlates to peptide hydrolysis rate, serving as an indicator of gate state and proteasome levels. SDS is applied to open latent species, such as the CP and possible holoenzymes with closed gate. If a proteasome species has an open channel, the intensity of the corresponding band is comparable in the presence and absence of SDS. If the intensity of the band is elevated with SDS, it indicates a closed or partially closed gate (Groll et al., 2000; Smith et al., 2007). Some fraction is always found in a closed form so it is natural for the bands depicting the holoenzyme forms to increase to a certain extent in the presence of SDS. The results indicated that aberrant proteasomes found with bound Ecm29 had comparable activity to wild-type proteasomes. Holoenzyme activity was barely detectable with mutant Ecm29 whether SDS was present or not (Figure 3.9D); this result was probably a measure of significantly lower levels of proteasomes (Figure 3.9A) as opposed to gate opening state.

Of special interest is the discrepancy in CP activity of DTS;α1-RNAi strain carrying normal versus mutant Ecm29. When Ecm29 is depleted CP levels rise due to RP-

CP dissociation (Figure 3.9A), however in-gel peptidase assay revealed higher activity for CP derived of strain expressing wild-type Ecm29 (Figure 3.9D). One possible explanation for this observation is alterations in rate of CP maturation. Several studies suggested a role for Ecm29 in facilitating CP maturation (Lee et al., 2011; Lehmann et al., 2010; Park et al., 2011). Ecm29 recognized RP-CP species in which CP maturation was stalled and functioned as a scaffold protein during the remodeling of incompletely matured RP-CP assemblies into active holoenzymes. One hypothesis is that limited amounts of α ring subunits could create a maturation defect that would enlist Ecm29 to act as a proteasome quality control chaperone, further investigations regarding this mechanism are underway.

Figure 3.9 Ecm29 is enriched on aberrant proteasomes to promote RP-CP association. A. Protein extracts (90μg) of muscle were resolved on native gel as described before in section 3.3.4. Membranes were blotted for Rpt3 and α7 to analyze prevalence of the different proteasome species. RP-CP association was weakened in DTS5;α1-RNAi in a manner dependent on Ecm29 presence. **B.** Same membrane from panel A was stripped and re-blotted for Ecm29. Ecm29 was enriched on proteasomes resolved from strains depleted of α1 protein in an Ecm29-dependent manner. * denotes un-specific bands. **C.** Proteasomes were purified from muscles extracts (0.4 mg) expressing β5-GFP tagged subunits. Proteasomes were analyzed by SDS-PAGE and immunoblotted with either Ecm29 (upper panel) or Rpt3 (lower panel) as loading control and measure for proteasome selectivity. Lower amounts of proteasomes were purified from an α1-RNAi strain (likely a technical aberration in the purification process) but Ecm29 levels were still comparable to wild-type, depicting Ecm29 enrichment. **D.** 90 μg of protein extracts (same extracts used in panel A) from indicated strains were resolved on 5% native gels and subjected to in-gel peptidase assay with fluorogenic substrate LLVY-AMC. The addition of SDS activates latent particles.

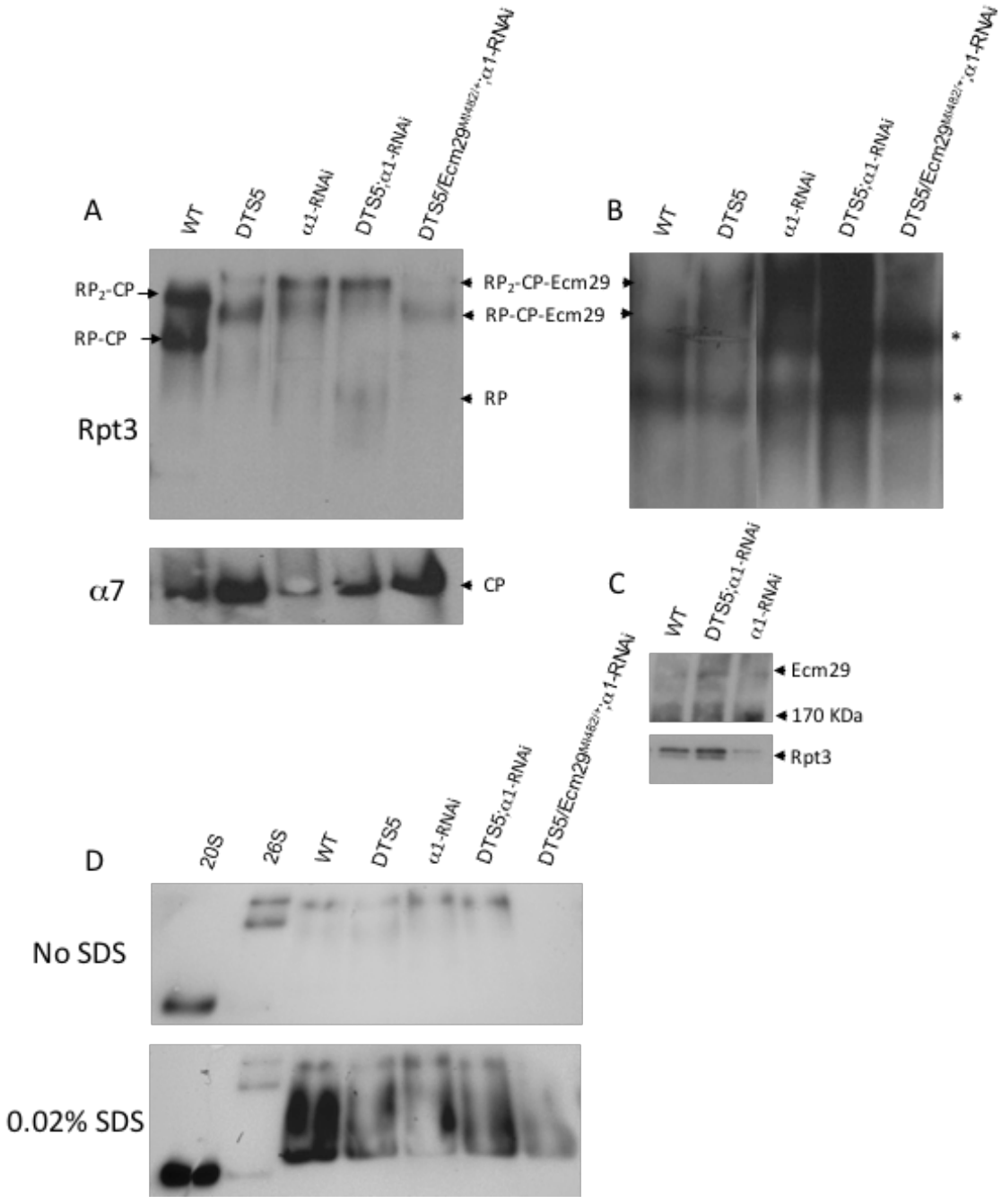
A
WT
DTS5
α1-RNAi
DTS5;α1-RNAi
DTS5/Ecm29Δ682-1;α1-RNAi
RP2-CP
RP-CP
RP2-CP-Ecm29
RP-CP-Ecm29
RP
Rpt3
α7
CP
B
WT
DTS5
α1-RNAi
DTS5;α1-RNAi
DTS5/Ecm29Δ682-1;α1-RNAi
*
*
C
WT
DTS5;α1-RNAi
α1-RNAi
Ecm29
170 KDa
Rpt3
D
20S
26S
WT
DTS5
α1-RNAi
DTS5;α1-RNAi
DTS5/Ecm29Δ682-1;α1-RNAi
No SDS
0.02% SDS

3.3.9 Suggested alternative subunit composition of aberrant proteasome

Proteasome assembly is a multi-step process coordinated by a specific set of conserved chaperones (Hirano et al., 2005; Kunjappu and Hochstrasser, 2014; Kusmierczyk et al., 2008; 2011). In recombinant systems, in the absence of chaperones, α subunits retained the ability to self-assemble into homo-multimeric rings but could not form functional proteasomes (Gerards et al., 1997; Zwickl et al., 1994). Several hypotheses could explain how cells compensate for depleted α subunits and preserve high proteasome function. The remaining α subunits might arrange themselves into a six-membered ring analogous to the homo-hexamer formed by the bacterial proteasome-related protease (Baumeister et al., 1998). Alternatively, a gap could exist in the α ring lacking α1, which might be stabilized by contacts among the remaining subunits. Finally, the position normally occupied by α1 might be taken by another protein, such as another proteasome subunit. In yeast loss of α3 subunit or the 20S chaperones Pba3-Pba4 produced remodeling of proteasomes with the appearance of alternative species containing a double copy of α4 subunits (Kusmierczyk et al., 2008; Velichutina et al., 2004). These alternative proteasomes can be formed naturally albeit at a slower pace than the canonical proteasomes, and they have an advantage under specific stresses such as high metal and oxidative stress (Kusmierczyk et al., 2008).

To assess subunit composition in the different proteasome populations I purified proteasomes as described before with β5-GFP tagged subunits. Proteasomes were purified from protein extracts of dissected muscle tissue and were resolved on SDS-PAGE gel for

further analysis with silver stain. Amongst the α subunits bands one band was absent in genotypes expressing α1-RNAi compared to wild-type, it stands reason that this band might depict α1 protein (Figure 3.10*). Interestingly there was one band amongst the α subunits which was especially enriched in proteasomes derived of DTS5;α1-RNAi strain. This intriguing band may depict an alternative α subunit, which took over α1 position and explain how alternative proteasomes are formed. This hypothesis is still at its preliminary stages and requires more rigorous investigation. For instance, specific bands can be excised and be sent for mass-spectometry for further identification.

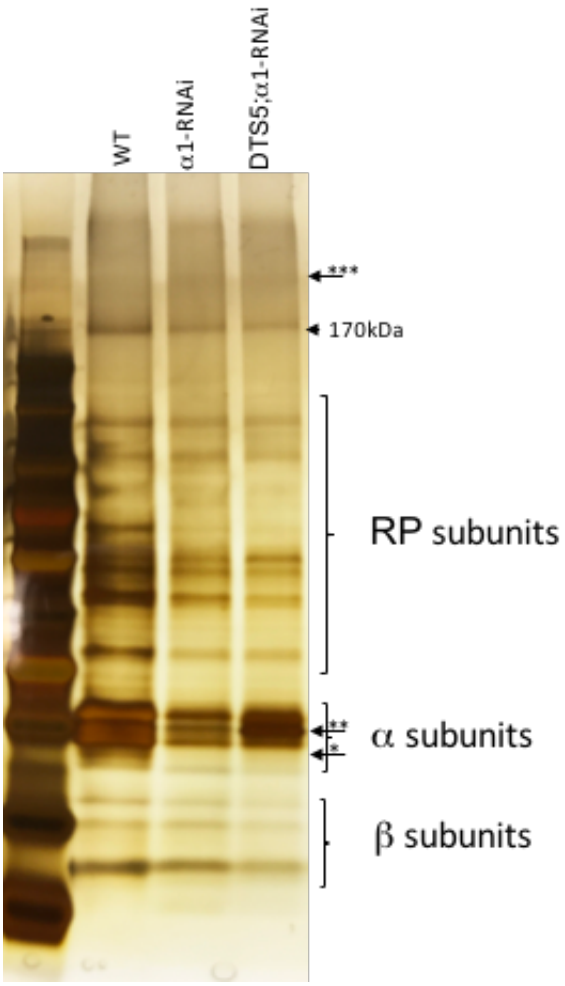

Figure 3.10 α1 RNAi produce proteasomes with an alternative composition of α subunits. Proteasomes were purified from protein muscle extracts (0.4mg) of indicated genotype using a β5-GFP tagged subunit and were resolved on SDS-PAGE gel for Silver stain. There are less bands than total subunits of the proteasome since some bands contain more than one subunit. *disappearance of band in α1 RNAi-expressing strain comparable to wild-type is likely depicting depletion of α1 subunit. **Band was intensified in α1 RNAi-expressing strain compared to wild-type, could indicate doubled amount of a specific subunit instead of α1. ***by size this band could possibly be of Ecm29 and depict its enrichment on proteasomes of α1-RNAi strains compared to wild-type

3.4 Materials and Methods

Fly stocks

John Belote generously provided us with transgenic proteasome reporters α2-GFP and β5-GFP (Ma et al., 2002). RNAi fly stocks was procured from Bloomington stock center and Vienna *Drosophila* research center. Ecm29 mutant Mi{MIC}CG8858^{MI00482} was obtained from Blomington stock center and used following P-element excision. All stocks were in a yw or w1118 background and were cultured on cornmeal–molasses medium supplemented with 3% active yeast at indicated temperature or room temperature.

Immunohistochemistry

Muscles or heads were dissected and prepared for immunohistochemistry as described in chapter 2 methods. ELAV, 24B10, Rpt3, GFP antibodies were used as described before. Rpt-2 was stained with rabbit polyclonal antibody at 1:100 dilution (Enzo). For Ecm29 detection rabbit polyclonal antibody was used at 1:200 dilution (Abcam). 20S rabbit polyclonal antibody was kindly provided from Dr. Udvardy and used at 1:100 dilution.

Western blot

Protein lysates were prepared for Western blot as described in chapter 2. For Rpt3 detection rabbit polyclonal antibody was used at 1:1000 dilution (Enzo). For α7 detection mouse monoclonal antibody was used at 1:1000 dilution (Enzo). For Ecm29 detection rabbit polyclonal antibody was used at 1:1000 dilution (Abcam).

FLP/FRT Induction of Mitotic Recombination

The FLP/FRT system is a site-directed recombination technology based on the targeting of a recombination enzyme (flipase - FLP) to specific DNA regions designated as flipase recognition target (FRT) sites (Golic and Lindquist, 1989). To generate mosaic clones hs*flp*;*sp/cyo;*DsRed,tub<y^{+}*GFP*>GAL4 females were crossed with DTS5;α1-RNAi (TRiP27557) males. Crosses were carried in fly cages at 25°C for a duration of 6 hours, egg laying on apple-juice/agar plates. In order to induce the flipase enzyme for mitotic recombination, after 24-hours apple plates were subjected to a 30-minutes heat shock at a 37°C water bath in order to induce mitotic recombination. Early third instar larvae were seeded on food vials and left for 24-hours incubation in 28.3°C. Muscles were dissected and prepared for immunohistochemistry.

In vitro and in vivo proteasome activity

Detailed description is provided in Chapter 2 materials and methods

Native gel analysis

30 muscles of each genotype were dissected and lysed in native lysis buffer (50 mM Tris-HCl (pH 8.0), 5 mM MgCl2, 0.5 mM EDTA, 2 mM ATP (added fresh), 0.2% NP40 (added fresh), Protease and Phosphatase inhibitors (added fresh)) and homogenized using pellet pestle motor (Kontes) on ice. Samples were left on ice for 30 minutes with homogenization taking place every 10 min. Protein extracts were spun at 14,000 rpm for 15 minutes at 4°C, supernatant was moved to a fresh tube. Protein concentration was determined with a BSA

titration column, measured with SpectraMax M-2 micro-plate reader (Molecular Devices). Native running buffer (5X, diluted 1:5 for use) was prepared as follows: 0 .45M Tris, 0.45M Boric Acid, 5mM EDTA, 12.5 mM MgCl2. Running buffer was chilled at 4°C while 0.5mM ATP and 0.5 mM DTT were added fresh prior to use. 25 μg of total protein was dissolved in native loading buffer at 1:1 ratio and resolved on 3–8% Criterion™ XT Tris-Acetate Gel. Along samples purified bovine proteasome 19S, 20S and 26S particles were loaded for control (UBPBio). Electrophoresis was carried for 1 hour at room temperature at 60V voltage and continued for additional 4 hours in 4°C at 120V. Protein transfer to immobilon-P membrane (Milipore) was carried at 12V for 3 hours at room temperature with Tris-Glycine transfer buffer devoid of methanol. Membranes were blocked with 5% milk in PBST (0.5% Tween20 in PBS) over night at 4°C. Afterwards, membranes were washed three times for 10 min in PBST and incubated with primary antibody for 2 hours at room temperature. Primary antibodies were diluted and kept in PBST supplemented with 0.02% Azide and 3% BSA. Following additional wash steps, membranes were incubated in HRP-conjugated secondary antibody (1:5000 dilution) for 1 hour and washed three more times with PBST before developing them with Western Lighting ECL blotting detection reagent (Perkin Elmer) on a Kodak Biomax MR film. Rpt3, α7 and Ecm29 antibodies were used as described for Western blot application.

In gel peptidase assay

Protein extracts preparation and electrophoresis was carried out as described for native gel with a few differences. Lysis buffer was prepared without protease and phosphatase inhibitors. For this assay 90 μg protein was resolved on gels. Gels were placed in a clean

tray containing 20 mL of buffer A (50 mM Tris-HCL pH 7.5, 150 mM NaCl, 5mM $MgCl_2$, 10% glycerol). Following a short rinse, buffer A was decanted and replaced with 20mL of developing buffer (50 mM Tris-HCL pH 7.5, 150 mM NaCl, 5mM $MgCl_2$, 5mM ATP added fresh, 200 μM Suc-LLVY-AMC added fresh). For the preparation of 10mM Suv-LLVY-AMC (Becham) 10 mg of the compound were dissolved in 1.3 mL DMSO and stored at -20°C. Gels were incubated for 45 min in 37°C incubator with slow agitation (~30 RPM). For imaging gels was were placed on a UV illuminator and pictures were taken with an iPhone7. For 20S visualization gels were placed back in the tray containing developing buffer supplemented with 0.02% SDS and incubated at 37°C as before. Following incubation, gels were visualized as before on a UV illuminator.

Immunoprecipitation

Dissected muscle tissue from 30 larvae of each genotypes were lysed in native lysis buffer (Hepes 20mM (pH 7.4), 5 mM $MgCl_2$, 150 mM NaCl, 0.2% NP40, 10% glycerol, 2 mM ATP (added fresh), protease and phosphatase inhibitors (added fresh)) and homogenized using a pellet pestle motor (Kontes) on ice. Samples were left on ice for 30 minutes with homogenization taking place every 10 min. Protein extracts were spun at 14,000 rpm for 15 minutes at 4°C and the supernatant was moved to a fresh tube. GFP-TrapA beads (ChromoTek) were washed with 500 μl of wash buffer (10mM Tris-HCL pH7.5, 150 mM NaCl, 0.5 mM EDTA) and spun down for 2 min at 2500 g, wash and spin steps were repeated three times. Equal amounts of protein extracts were mixed with 20 μl washed beads per reaction. Of each reaction 20 μl was left aside for total protein control. For immunoprecipitation samples were rotated for 2 hours in 4°C. Afterwards samples were

washed with 200 µl lysis buffer and spun down for 2 min at 2500g, wash and spin steps were repeated three times. Elution was carried with 50 µl of 0.2M glycine pH 2.5 and neutralized after 30 seconds of vortex with 5 µl 1M Tris pH 10.4.

Silver stain

Purified proteasomes obtained by immunoprecipitations were mixed with SDS loading buffer and resolved on 4-20% Mini-PROTEAN TGX precast protein gel. Electrophoresis was carried for 2.5 hours at 100V voltage. Gel was placed in a clean tray and assay was carried as specified by the protocol of Thermo Scientific™ Pierce™ Silver Stain kit.

4. α1 role as general proteasome regulator: function in physiologic stress

4.1 Summary

This chapter summarizes supplementary information regarding the contribution of α1 knockdown in coping with two models of physiologic stress. First I used an *in vivo* assay of oxidative stress to show that α1 knockdown can attenuate oxidative stress, furthermore this attenuation was dependent on Ecm29. A second model that I used was of dietary restriction (DR). Muscle wasting plays a beneficial role in response to nutrient deprivation by funneling amino acids to sustain vital organs of the organism. At chronic DR stress, wild-type larvae experienced severe growth retardation which was suppressed by α1 knockdown. The data suggested that despite some moderate disassembly, suppression of stress is more likely to originate from a general response to nutrient deprivation such as autophagy. The last section describes a brief analysis of the PI31-tankyrase network in muscle function.

4.2 Results

4.2.1 Muscle atrophy progress with oxidative stress

In previous chapters I described how α1 knockdown relieved DTS5 dependent proteotoxic stress. Whereas DTS5 is a useful system to study proteasome regulation it is still a mutant that does not occur in nature. To investigate α1 role in proteasome regulation at physiological stress models, I studied oxidative stress and caloric starvation, both described previously to promote muscle atrophy.

Oxidative stress has been implicated in aging and many human diseases, notably in neurodegenerative disorders (Aiken et al., 2011; Finkel and Holbrook, 2000; Page et al., 2010; Smith et al., 1991). The reactive oxygen species that are generated by aerobic metabolism and environmental stressors can chemically modify proteins and alter their biological functions (Boveris, 1984; Chou et al., 2010; Leach et al., 2001; Turrens and Boveris, 1980; Watanabe et al., 2003). Cells have developed various mechanisms to remove oxidized proteins or restore their functions. If oxidized proteins are allowed to accumulate they may become cytotoxic to cells. Cell homeostasis and viability are therefore dependent on the removal of oxidized damaged proteins. Although there is evidence to suggest that chaperone-mediated autophagy is activated during oxidative stress response (Kiffin et al., 2004); numerous studies have demonstrated that the proteasome plays a pivotal role in the selective recognition and degradation of oxidized proteins (Breusing and Grune, 2008; Davies, 2001; Goldberg, 2003; Jung and Grune, 2008).

Several reports signify reactive oxygen species (ROS) production role in muscle atrophy, both in insects and in mammals (Davis et al., 1993; Dodd et al., 2010; Jang and Van Remmen, 2011; Muller et al., 2006). Since there is no way to control for larvae feeding behavior I developed my own protocol to study oxidative stress in muscles *in vivo*. Muscle tissue is still viable *in situ* and can be manipulated for *in vivo* assays. Muscles were incubated with hydrogen peroxide (H_2O_2) followed by wash and incubation steps to allow for ROS accumulation. ROS production was measured with a commercial kit based on a fluoregenic dye, flouresence intensity correlates with ROS prevalence. As seen in figure 4.1A level of ROS production was dose-dependent with H_2O_2. As before Phalloidin (actin marker) was used to assess damage to sarcomeric pattern in order to observe muscle atrophy. Loss of sarcomeric pattern worsened progressively with increase in oxidative stress. At 50 μM H_2O_2 muscles still presented normal architecture but by 100 μM H_2O_2 muscle width was reduced by 3.3, fold on average (n=12). 150 μM was too damaging for muscles and tissues were completely disintegrated and could not be used for analysis, hence all future assays were carried with 100 μm H_2O_2. To confirm oxidative stress, I also stained muscles with a red-mitotracker. Mitochondrial fission is a common consequence of oxidative stress (Lee et al., 2012a) and therefore can serve to measure it. Tracking mitochondrial fission confirmed these observations. Fission worsened progressively with increase in H_2O_2 concentration, 100 μm was sufficient to produce significant fission.

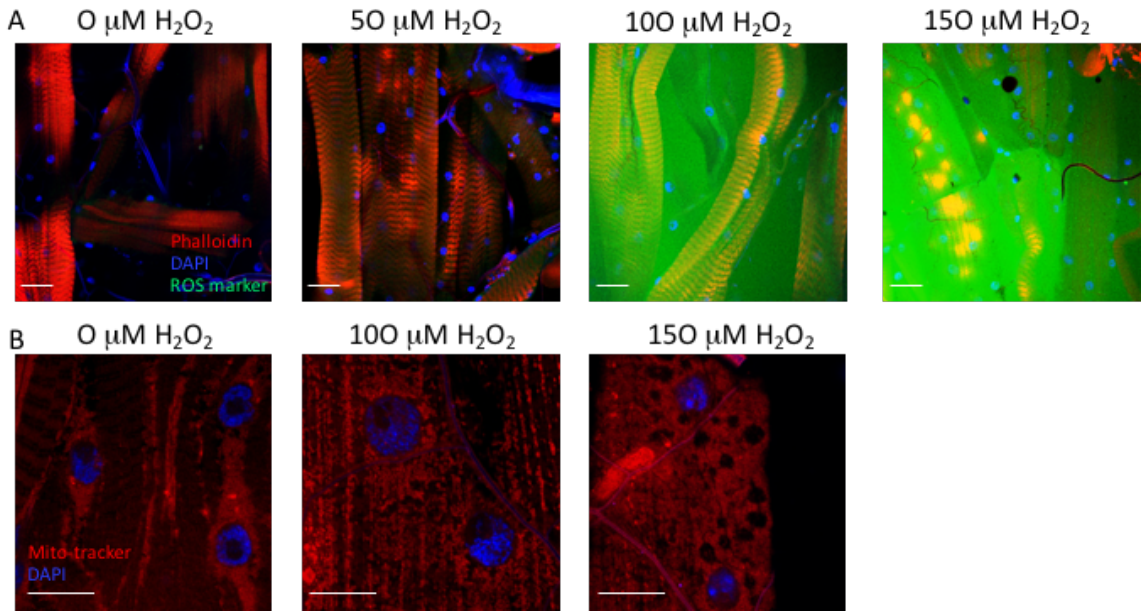

Figure 4.1 Atrophy progressed with increased oxidative stress. A. Muscles of early third wild-type larvae with no pretreatment were incubated *in situ* with increasing dosage of hydrogen peroxide (H_2O_2). The green channel shows the fluorogenic dye reactive with ROS, signal intensity depends on ROS prevalence. Phalloidin (red) depicts sarcomeric pattern (actin fibers)..**B.** Muscles treated as in panel A were stained with red mitochondrial tracker. Mitochondrial fission progressed with severity of oxidative stress.

4.2.2 Muscles expressing α1 RNAi are more resistant to oxidative stress

α1 role in muscle atrophy was further investigated and generalized using the oxidative stress model. I first asked how does α1 reduction effect ROS production when muscles are exposed to acute H_2O_2 stress. For this purpose, I used the same method describe in the previous section. As α1 reduction helped in salvaging muscles expressing DTS5, so it also helped in recovery of muscles from oxidative stress. Untreated muscles displayed very base levels of ROS, as depicted by ROS marker, whether they had normal or reduced levels of α1 protein. However, when treated with 100 μM H_2O_2 wild-type muscles displayed enhanced accumulation of ROS, 3.7-fold, whereas muscles derived from α1-RNAi no significant accumulation was detected (Figure 4.2A). It is possible that α1 RNAi completely halted production or it expedited their removal once formed. Plotting time course of ROS production over different time points may address this open question.

I next investigated proteasome action in response to oxidative stress by observing accumulation of poly-ubiquitinated proteins (Figure 4.2B). Unsurprisingly α1-RNAi muscles had higher levels of FK2 staining when no oxidative stress was applied. α1 RNAi function in base levels of proteotoxic stress was already discussed in Chapter 3. On the other hand, under acute oxidative stress, poly-ubiquitinated proteins were significantly accumulated in wild-type muscles whereas in muscles of α1-RNAi background levels remained at levels comparable to un-treated muscles. This observation implies that proteasome activity was disrupted in response to oxidative stress

Figure 4.2 Reduced α1 levels facilitate oxidative stress response. A. *In situ* muscles from indicated genotype were treated with H_2O_2 and analyzed for ROS production with DCFDA marker (green) as described in section 4.3.1. Phalloidin (red) and DAPI (blue) were used to delineate muscles. **A'.** Quantification of ROS marker signals normalized to counterstained DAPI signals. Bars represent mean values (relative to the ROS signal in non-treated wild-type tissue) from 2 independent experiments, 8 larvae in total. **B.** Muscles prepared as in A were immunostained with FK2 (green) to observe accumulation of poly-ubiquitinated proteins. Phalloidin (magenta) and DAPI (blue) were used to delineate muscles. Scale bar 50 μm.

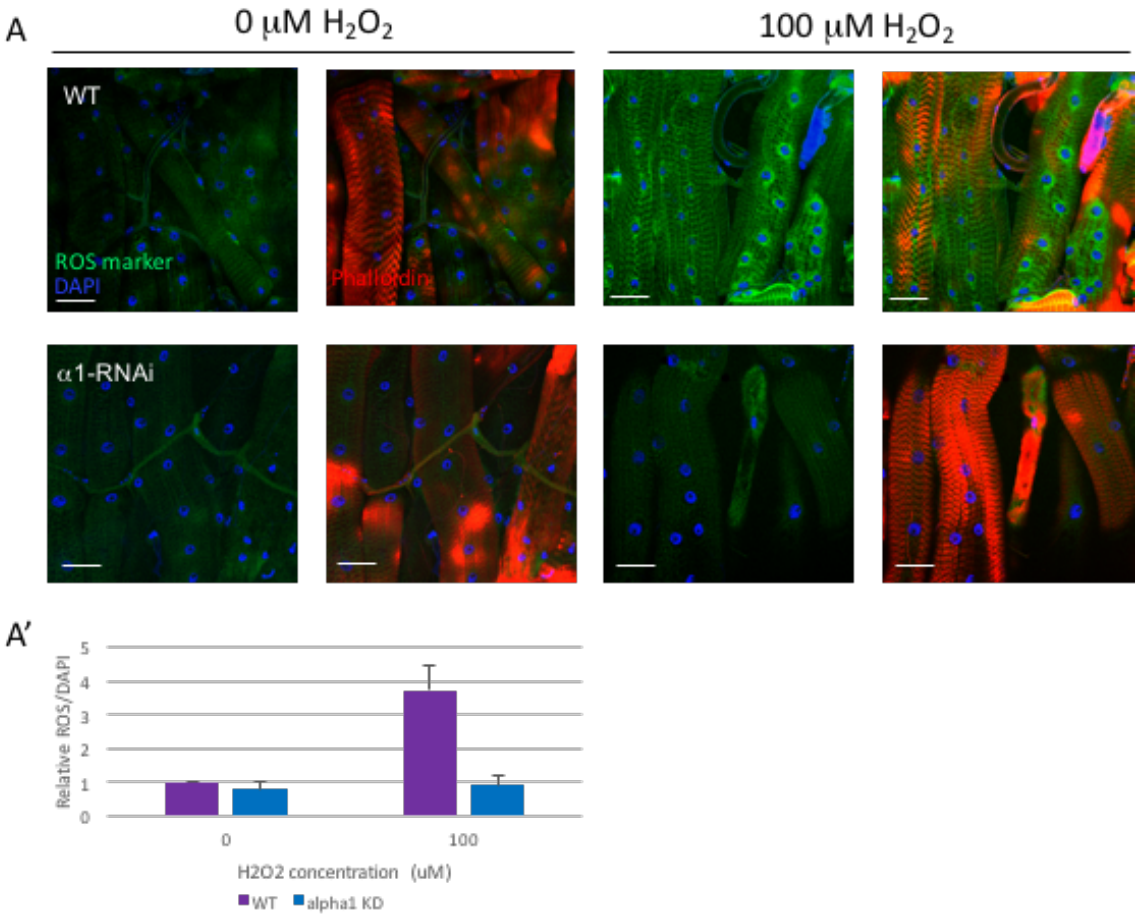
A
0 μM H_2O_2
100 μM H_2O_2
WT
ROS marker
DAPI
Phalloidin
α1-RNAi
A'
Relative ROS/DAPI
0
1
2
3
4
5
0
100
H2O2 concentration (uM)
WT
alpha1 KD
B
0 μM H_2O_2
100 μM H_2O_2
WT
FK2
DAPI
Phalloidin
α1-RNAi

4.2.3 α1 knockdown relief of oxidative stress is Ecm29 dependent

Ecm29 is thought to strengthen the tethering between 20S CP and 19S RP. However, Wang and colleagues showed that acute H_2O_2 stress promoted RP-CP dissociation because of Ecm29-dependent disassembly of the 26S proteasome complex (Wang et al., 2010b). Ecm29-dependent proteasome dissociation was important for recovery following oxidative stress, suggesting that Ecm29 may have multiple functions in controlling 26S proteasome structure. Haratake and colleagues studied KIAA0368, Ecm29 mammalian orthologue, role in oxidative stress - to date the only physiological study of Ecm29 in mammals (Haratake et al., 2016). KIAA0368-deficient mice were more resistant to oxidative stress as opposed to ΔEcm29 yeast. Unexpectedly, resistance was accounted to by increased stability of 26S and efficient degradation of damaged proteins. They suggested that Ecm29 absence might have been compensated by Psme4, the mammalian orthologue of PA200. Both studies highlight Ecm29 as a key regulator of 26S proteasome structure in response to H_2O_2 stress, though they disagree on its functional mechanism.

As opposed to knockdown in a wild-type strain (Figure 4.2A) when α1 RNAi was introduced into $Ecm29^{MI0482}$, Ecm29 hypomorphic mutant strain, ROS prevalence was enhanced following acute oxidative stress by 2.9-fold (Figure 4.3A lower panel). Likewise, high levels of Ecm29 were needed for α1 knockdown to prevent subsequent accumulation of poly-ubiquitinated proteins, indicative of impaired proteasome activity (Figure 4.3B lower panel). Diminished Ecm29 levels did not alter oxidative strain response compared to wild-type muscles, and displayed enhanced accumulation of both ROS and poly-

ubiquitinated proteins under acute oxidative stress (Figure 4.3A-B upper panel). In conclusion α1 knockdown was dependent on Ecm29 to alleviate acute oxidative stress. Though Ecm29 was critical to mitigate acute oxidative stress as shown for DTS5-dependent proteotoxic stress, it still remains to be determined whether it does so through promoting RP-CP association as described in Chapter 3 or through other mechanisms of action.

Figure 4.3 Ecm29 role in α1 knockdown mediated oxidative stress response. A. *In situ* muscles from indicated genotype were treated with H_2O_2 and analyzed for ROS production with DCFDA marker (green) as described in section 4.3.1. Phalloidin (red) and DAPI (blue) were used to delineate muscles. **A'.** Quantification of ROS marker signals normalized to counterstained DAPI signals. Bars represent mean values (relative to the ROS signal in non-treated wild-type tissue) from 2 independent experiments, 8 larvae in total. **B.** Muscles as in A were immunostained with FK2 (green) to observe accumulation of poly-ubiquitinated proteins. Phalloidin (magenta) and DAPI (blue) were used to delineate muscles. Scale bar 50 μm.

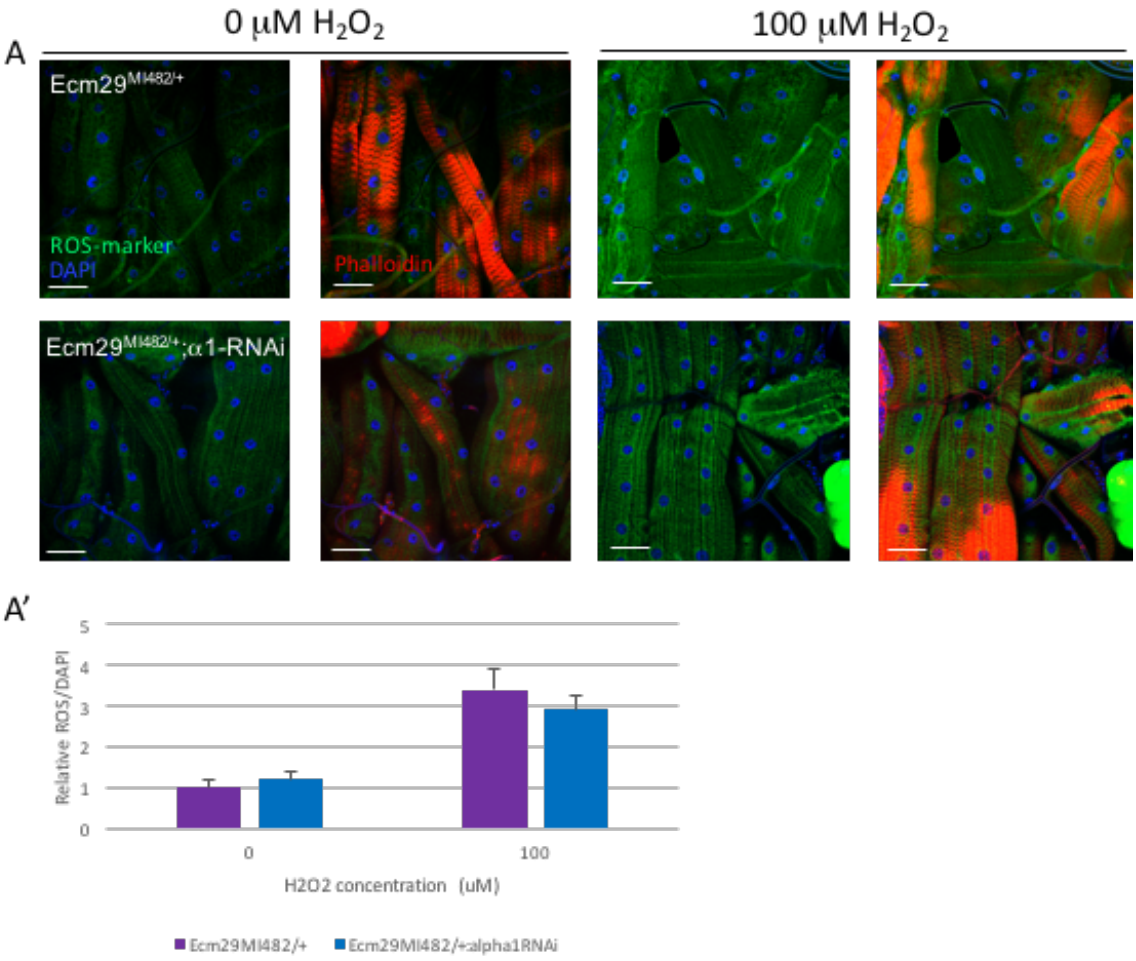
A
0 μM H_2O_2
100 μM H_2O_2
Ecm29$^{MI482/+}$
ROS marker
DAPI
Phalloidin
Ecm29$^{MI482/+}$;α1-RNAi
A'
Relative ROS/DAPI
0
1
2
3
4
5
0
100
H2O2 concentration (uM)
Ecm29MI482/+
Ecm29MI482/+alpha1RNAi

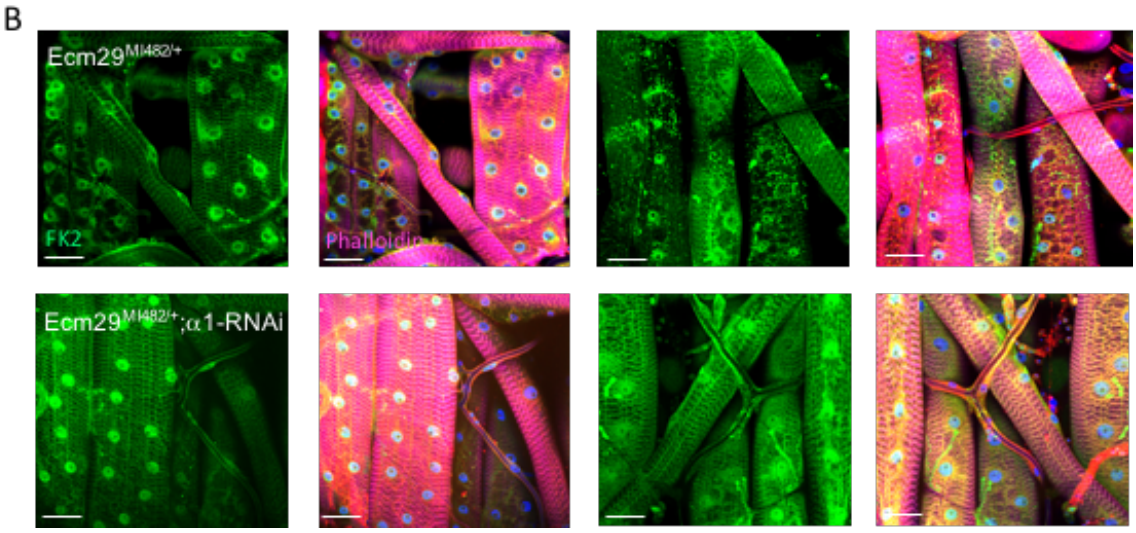
B
Ecm29$^{MI482/+}$
FK2
Phalloidin
Ecm29$^{MI482/+}$;α1-RNAi

4.2.4 Dietary restriction reduced size is suppressed by α1 knockdown

Skeletal muscle serves two essential functions, a contractile function for locomotion/maintenance of posture and a metabolic function as the protein reservoir of the body. Upon fasting, body homeostasis is maintained through muscle protein degradation though it comes at a cost of loss of muscle mass. Muscle atrophy provides amino acids as building blocks for new protein synthesis in the body vital organs (Bilodeau et al., 2016). The UPS is the main driving force of muscle atrophy upon fasting and caloric restriction (Medina et al., 1991; 1995; Wing and Goldberg, 1993).

Food can be a scarce resource; therefore, organisms have developed various strategies to cope with acute periods of absent or limited food supply. Dietary restriction (DR) in Drosophila usually involves reduction of the yeast and sugar components of the diet (Partridge et al., 2005), and yeast appeared to account for the majority of the DR effect on life span (Chippindale et al., 2011; Mair et al., 2005). Dietary restriction conditions were achieved by limiting yeast, the protein resource , food was prepared with 0.25% compared to 3% yeast in control food (CF) yeast (Bass et al., 2007). Initial experiments were also compared to dietary restriction food devoid of sugar source however these conditions were found to be too stringent. Additionally, each intervention could operate through different molecular pathways thus complicating interpretations. In previous chapters, egg laying was carried on apple plates, yet transfer from apple plates to DR or CF constitutes nutritional downshift which might obscure results, thus plates with control yeast food were prepared for this assay. Larvae were raised on yeast plates for 72 hours; early third instar larvae were subsequently seeded in DR versus CF vials, that were supplemented with RU-486. Ensuing

growth was carried out in 25°C till eclosion. Changes in growth were observed only after 48 hours of feeding on DR food, whereas at 24 hours there was still no comparable difference in larvae size (Figure 4.4 A-B). Organisms developed a multi stress response to nutritional deprivation, differing from acute to chronic deprivation. Distinction between these time points is in line with previous analysis of rodents response to starvation (Kee et al., 2003; Mizushima et al., 2004). Most striking was that after 48 hours of DR wild-type larvae were reduced in size compared to α1 RNAi transgenic larvae. Both genotypes showed loss in mass after 48 hours of DR, however there was no significant disparity in their average weight in comparison to each other (Figure 4.4 C). Larvae of α1 RNAi genotype displayed slightly higher eclosion levels, which could suggest better adaptation to DR conditions, however it was not statistically significant (Figure 4.4D). Loss in size could be from reduced intake of food. To monitor food intake, I supplemented food with bromophenol blue dye so it can be observed in the larvae gut. Wild-type larvae were still consuming food by the appearance of dyed food in their gut but at lower levels, therefore reduced intake cannot be completely excluded. It is possible that food intake was diminished due to reduced contractile force of muscles effecting also muscles involved in digestion. Adult flies commonly do grow on DR food, but it stands reason that interfering with protein balance during the early stage of development would be more detrimental to larval growth.

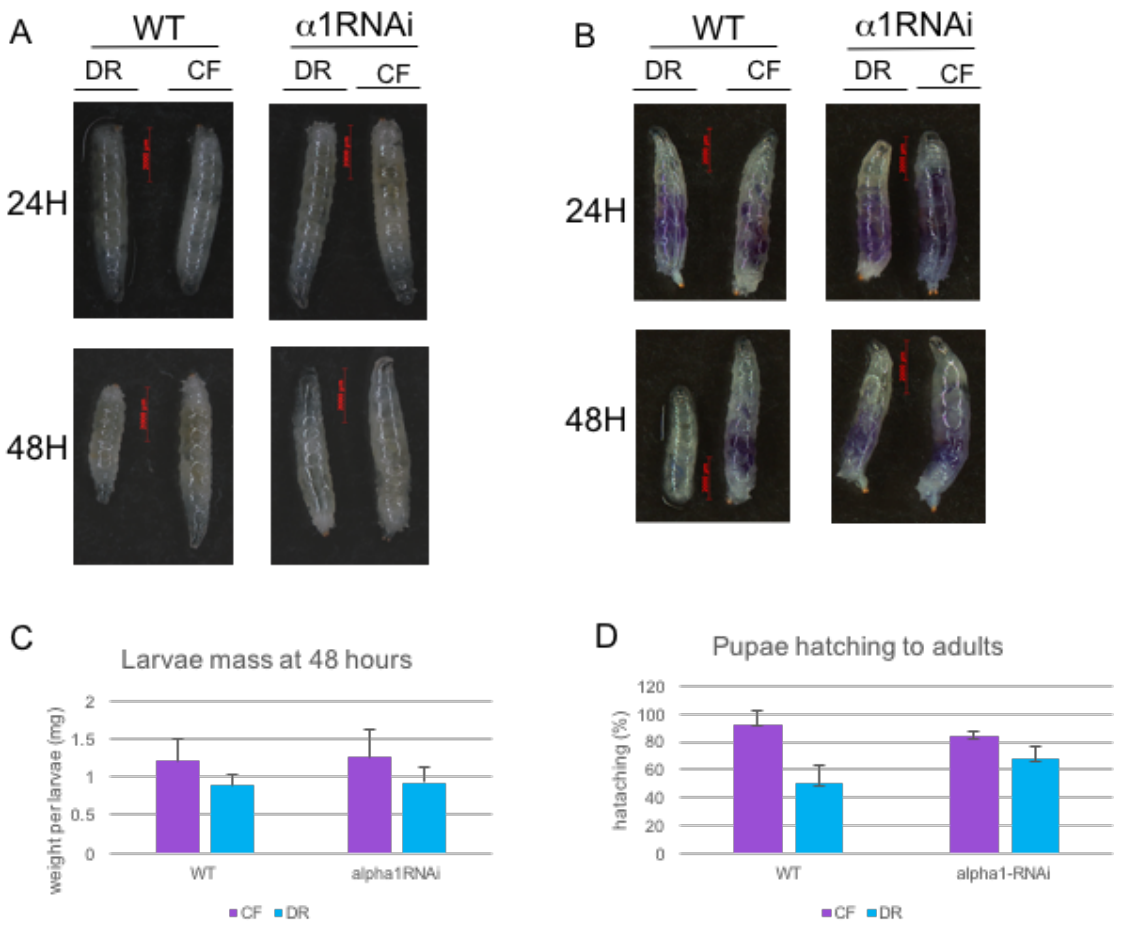

Figure 4.4 α1 knockdown suppressed size loss due to DR. A-B. Larvae were age-matched and grown on yeast plates for 72 hours, then seeded on vials containing DR and CF supplemented with RU-486 and were left to propagate at 25°C. At 48 hours of DR wild-type larvae shrunk in size compared to α1-RNAi expressing larvae. **B.** Food was supplemented with bromophenol dye to track feeding behavior. At 48 hours of DR wild-type larvae showed reduced intake of food. **C.** Average weight per one larvae, measured over three independent repeats, for each measurement 20 larvae were taken and measured on analytical measurements. **D.** Percentage of larvae reaching adulthood out of total larvae seed on DR and CF vials, measured over three independent repeats, they showed no significant changes.

4.2.5 Dietary restriction effects on the proteasome

In the aim of characterizing proteasome role in response to DR I examined proteasome activity and distribution. For activity measurements, I used the *in vivo* activity assay supplemented with *in vitro* activity assay as described before. Both assays depicted disruption in proteasome activity in wild-type musculature after 48 hours of DR. This disruption was not observed after 24 hours only, neither in CF environment, suggesting it was dependent on chronic stress of nutrient deprivation (Figure 4.5 A-B,E). In comparison, α1 knockdown suppressed this disruption and presented suitable activity like in control food, independent of food content or incubation time. Both genotypes displayed proper *in vivo* activity in control food independent of incubation time (data not shown). Moreover, significant accumulation of poly-ubiquitinated proteins was observed only in wild-type muscles after chronic DR stress, in line with concomitant disruption in proteasome activity. Phalloidin staining revealed no damage to cyto-architecture of the muscle in either genotypes or conditions, sarcomeric pattern was intact in all analyzed muscles (Figure 4.5 C and data not shown). If indeed organismal protein balance was maintained by redistribution of amino acids from the muscle, it did not elicit destruction of sarcomeric proteins and overhaul atrophy of complete muscle. Interestingly, like in the DTS5-dependent stress (Figure 3.2) changes in distribution of Rpt3 were observed when α1 was knocked down (Figure 4.5 D). Localization changes correlated with stress, as Rpt3 distribution remained primarily nuclear after 24 hours of growth in either DR or CF. Clonal analysis of α1 RNAi depicted distinguished Rpt3 staining in cytoplasm compared to wild-type clones, however it was still primarily nuclear (data not shown).

Figure 4.5 DR stress effects correlate with loss in proteasome activity. A-B. *In vivo* proteasome activity of indicated genotypes after acute and chronic stress (24-hours versus 48-hours incubation respectively) reveal apparent proteasome inhibition in wild-type flies following DR chronic stress, whereas α1 RNAi genotype maintained intact activity. Analysis was carried out as described in Figure 2.9, GFP signal persistence at 4-hours post heat shock depicts inhibition of *in vivo* proteasome activity. **C.** Muscles were dissected and stained for phalloidin (actin), DAPI and poly-ubiquitinated proteins (FK-2) following 48-hours incubation in DR food. Significant accumulation of Poly-ubiquitinated proteins correlated with loss in proteasome activity. **D.** Rpt3 distribution in dissected muscles of indicated genotype following 48-hours incubation in DR food. **E.** *In vitro* analysis of proteasome activity as described in Figure 2.8. Measurements were normalized to wild-type after 48-hours incubation in CF and plotted as relative luminescence units. Standard deviation measured from three independent repeats. Scale bar 50 μm.

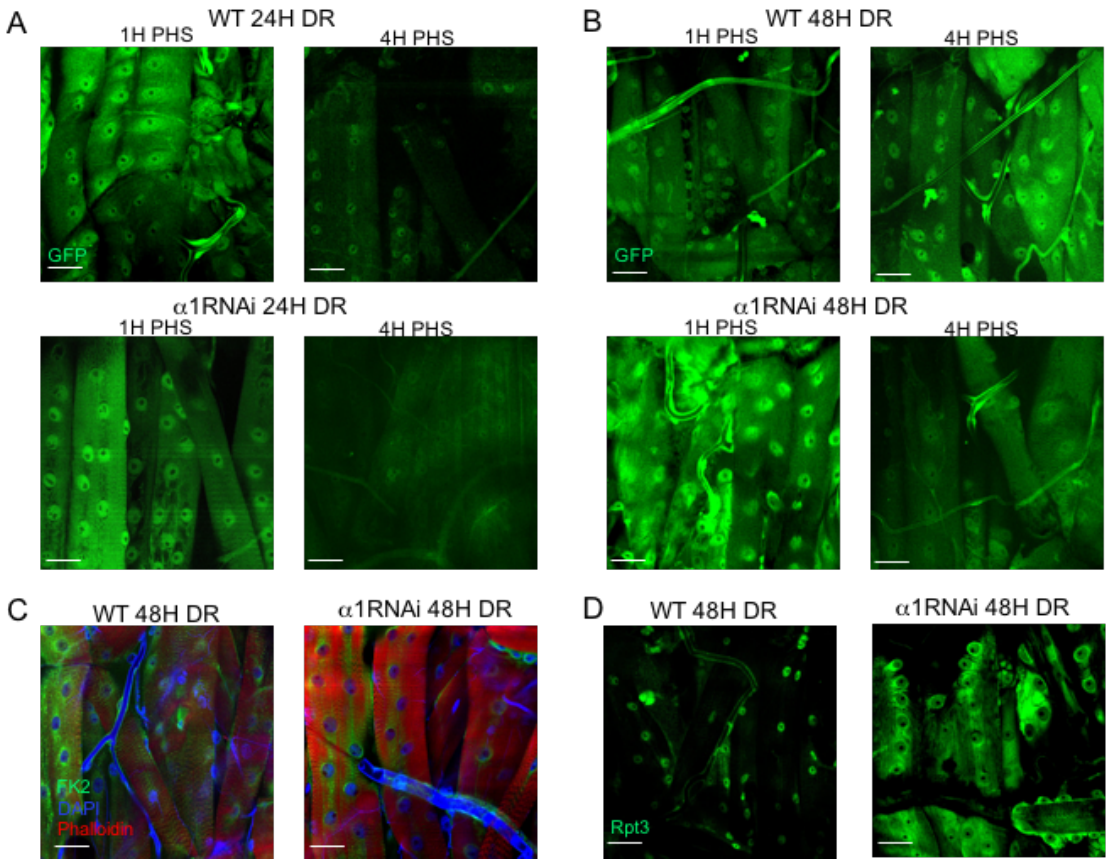
A
WT 24H DR
1H PHS
4H PHS
GFP
B
WT 48H DR
1H PHS
4H PHS
GFP
α1RNAi 24H DR
1H PHS
4H PHS
α1RNAi 48H DR
1H PHS
4H PHS
C
WT 48H DR
α1RNAi 48H DR
FK2
DAPI
Phalloidin
D
WT 48H DR
α1RNAi 48H DR
Rpt3

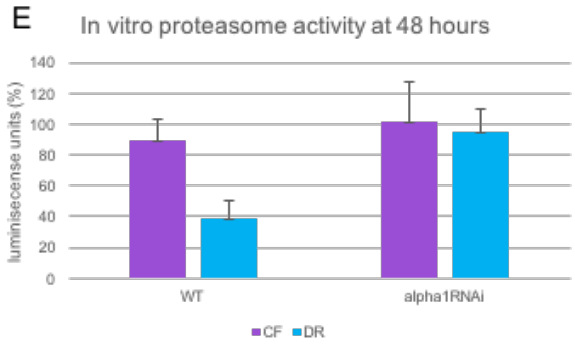
E
In vitro proteasome activity at 48 hours
luminisecense units (%)
140
120
100
80
60
40
20
0
WT
alpha1RNAi
CF
DR

To distinguish effects on proteasome biogenesis I examined dissected muscles using native gel analysis. DR chronic stress of wild-type levels reduced the 26S/20S ratio. This observation indicates disassembly of holoenzymes and increase in the free pool of CP. While this ratio remained relatively steady in transgenic larvae of α1 RNAi, still 26S levels were not significantly different in wild-type musculature; which makes dis-assembly an un-likely basis to reduced proteasome activity. It is more likely to speculate that intact proteasomes were inhibited directly, perhaps by an upstream signal. Of special note was the mobility shift observed for α1 RNAi genotype. Though not further characterized in this model it goes in line with Ecm29 presence as discussed in chapter three.

One possible mechanism to increase proteasome activity is through induction of subunits expression. Western blot analysis specified a puzzling observation in regard to this hypothesis. Rpt3 levels remained constant and comparable to CF in both genotypes, while α7 was induced in an α1 RNAi genotype. Though the prevalent theory is that proteasome subunits are expressed in a stoichiometric fashion, perhaps α7 mediates a tightly regulated step in proteasome biogenesis and its induction is enough to drive the whole process forward. For example β7 overexpression stimulates 20S assembly by overcoming a Ump1 dependent checkpoint (Li et al., 2007). Alternatively, increased levels of 20S were enough to confer an advantage under DR conditions. Though 20S is considered a latent particle it is still capable of degrading small, partially unfolded substrates. For example 20S activity is thought to be advantageous in resolving oxidative stress (Wang et al., 2010b).

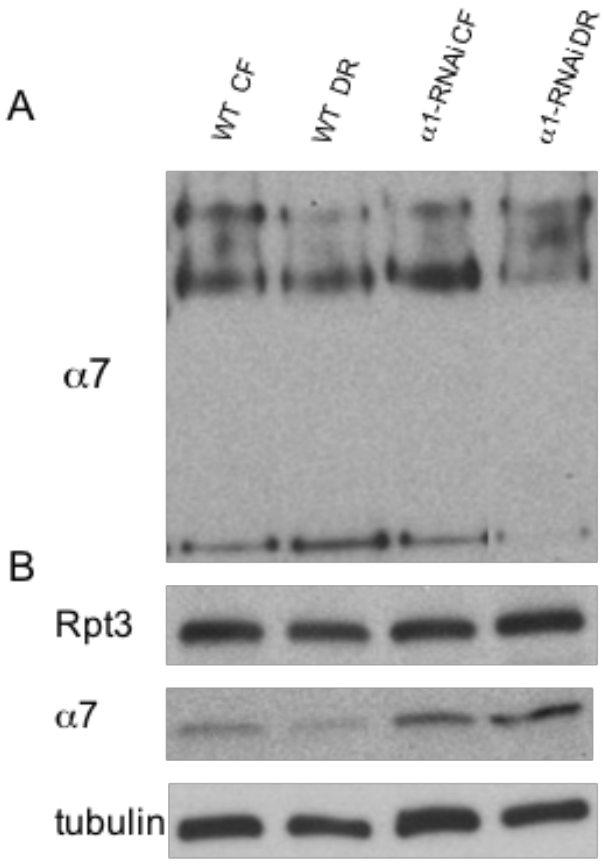

Figure 4.6 DR stress promotes moderate disassembly of 26S holoenzyme. A. To differentiate 26S/20S ratio, protein extracts (25 μg) of muscle tissue from indicated strains, following 48-hours incubation, were resolved on native gels and subjected for α7 immunoblot. **B.** To differentiate subunits induction protein extracts (10 μg) of specified muscles were resolved on SDS-PAGE gels and immunoblotted for Rpt3, α7 and tubulin.

It is possible that α1 knockdown in the muscle was beneficial to whole body homeostasis under DR by expediting proteasome-dependent degradation of muscle proteins. Alternatively, α1 knockdown may have activated a response of compensatory autophagy. Nutrient deprivation is a potent inducer of autophagy. Deprivation of only essential amino acids has been shown to activate autophagy through the mTOR pathway (Sancak et al., 2010). In atrophying muscles, both the UPS and autophagy catalyzed the degradation of different cellular components. While proteasomes degrade myofibrillar and soluble proteins (Goldberg, 1996); organelles (especially mitochondria) are degraded primarily in lysosomes (Scott and Klionsky, 1998). Still in both studies muscles were found with relatively normal composition, but displayed reduced strength and endurance. It is commonly accepted that autophagy is activated as a compensatory mechanism when proteasome function is inhibited (Kageyama et al., 2014; Pandey et al., 2007). In addition to compensatory mechanisms, nutrient deprivation is a unique catabolic condition that simultaneously activates both pathways by a common FoxO3 and mTOR regulation; both are negatively regulated by rich food signals (IGF1/Insulin) (Mammucari et al., 2007; Zhao et al., 2007). I hypothesize that beneficial adaptation to DR stress was afforded by coordinated activation of the UPS and autophagy through common signaling pathways and activation of compensatory mechanisms. A compromised 20S complex due to α1 depletion may have triggered those pathways and signaling cascades. For in depth analysis of this hypothesis, examination of autophagy function is needed, however I did not follow up with this line of investigation.

4.2.6 Analysis of the PI31-Tankyrase regulatory pathway in muscle atrophy

PI31 is physiologically required for optimal 26S proteasome activity *in vivo*, and inactivation of the corresponding gene in *Drosophila* causes reduced protein breakdown and organismal lethality (Bader et al., 2011). PI31 is regulated by Tankyrase-mediated ADP-ribosylation, altering the affinity of PI31 for 20S proteasome α subunits and 19S assembly chaperones, thereby stimulating 26S proteasome assembly (Cho-Park and Steller, 2013).

In chapter 2 I carried an RNAi screen of DTS5 induced proteasome inhibition and larval paralysis to identify proteasome activators. Overexpression of PI31 was previously shown to suppress DTS5 dependent retinal degeneration. I used my muscle atrophy model to assay for PI31 function. As expected for a positive regulator of the proteasome, PI31 overexpression attenuated larval paralysis and suppressed proteasome inhibition (Figure 4.7 A,C), while muscle wasting and proteasome inhibition persisted when PI31 was knocked down. PI31 knockdown was validated with Western blot (Figure 4.7 D). Yet, PI31 RNAi alone was not enough to elicit muscle atrophy (data not shown). Either minimum levels of PI31 are enough to sustain proteasome activity or more likely at physiological conditions multiple mechanisms cooperate to sustain proteasome activity. This assay also served as positive control to my screen, validating its ability to identify proteasome regulators.

Likewise, Tankyrase knockdown did not promote muscle wasting, but I did not observe reduced Tankyrase protein either (figure 4.8 A-B). I next investigated Tankyrase significance using a pharmacological approach. For this purpose, I took advantage of

XAV939, a small-molecule inhibitor of human Tankyrase (Huang et al., 2009). XAV939 is a highly specific inhibitor of hTNKS1/2 but is also able to inhibit the auto-ADP-ribosylation activity of dTNKS, making him a highly specific and effective inhibitor of Tankyrase in *Drosophila* as well (Cho-Park and Steller, 2013; Smith et al., 1998). Together with XAV939 I tested IWR1. IWR1 is a potent inhibitor of hTNK which works through a disparate mechanism to XAV939. TNK functions by consuming NAD^+, IWR1 interferes with TNK's nicotinamide binding site (Narwal et al., 2012). Feeding larvae with XAV939 resulted in a severe growth impairment, likely from a systemic effect. At the time DMSO treated larvae reached pupation, XAV939 fed larvae were still estimated to be the size of a third instar larvae and ultimately never reached adulthood (Figure 4.8 C). Their delayed growth is likely not due to impaired feeding behavior (figure 4.8D). IWR1 fed larvae were comparable to control. However, discrepancies between XAV939 and IWR1 could stem from their pharmacological suitability and indicate differences in digestion and absorption rather than a true result.

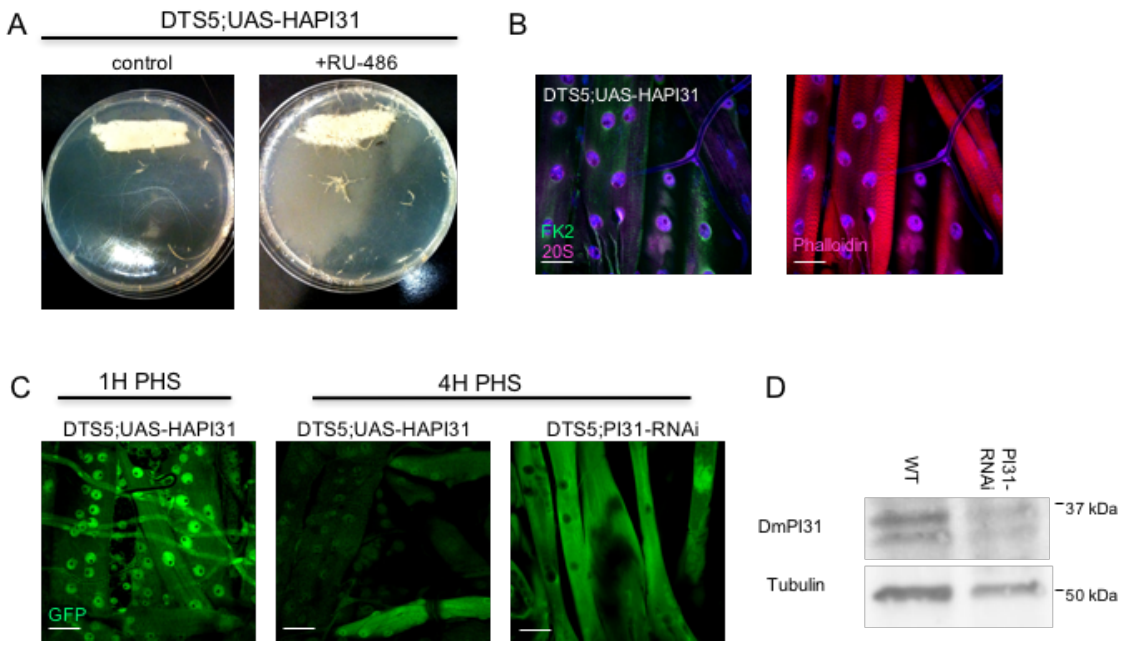

Figure 4.7 PI31 suppressed muscle atrophy. A. MHC-GS driving expression of indicated genotype at permissive temperature. Induction of DTS5 together with PI31 overexpression was comparable to control with intact muscle function and motility. **B.** PI31 overexpression suppressed accumulation of poly-ubiqitinated proteins and protected muscle architecture. Muscles were dissected and stained for FK2 (green) and 20S (magenta) on the left, merged with phalloidin (red) on the right. **C.** *In vivo* proteasome activity is shown for indicated genotypes. 4 hours after GFP-Nintra induction signal was lost when PI31 was overexpressed but persisted when PI31 was knocked down. Muscles of DTS5;PI31-RNAi transgenic larvae displayed a wasted architecture (right panel). **D.** Western blot analysis of PI31 antibody confirmed knockdown by RNAi.

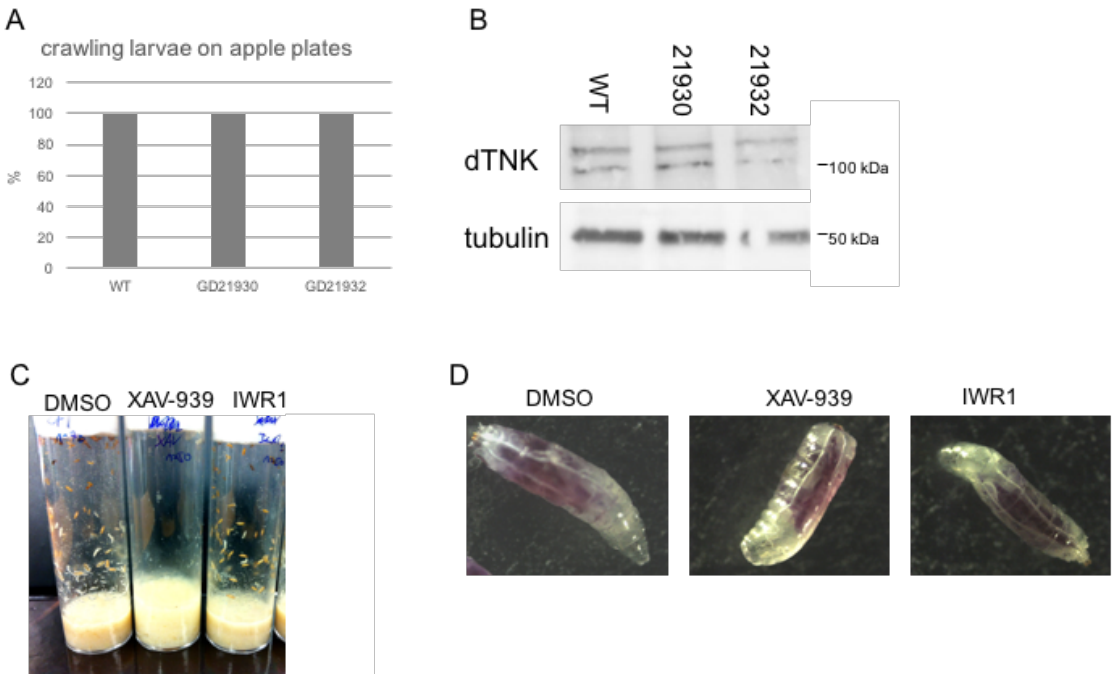

Figure 4.8 Analysis of Tankyrase inhibition. A. transgenic expression of Tankyrase RNAi displayed comparable motility to wild-type. **B.** Western blot analysis of Tankyrase exhibited no knockdown by RNAi. **C.** Equal amounts (50) of wild-type second instar larvae were seeded on yeast dry food supplemented with Tankyrase inhibitors, XAV939 and IWR1 (4 μm) or DMSO as control. Growth was monitored at 25°C. **D.** Food was supplemented with blue bromophenol dye to track feeding behavior. No discernable disturbance in feeding was observed at 48-hours post exposure to drugs.

4.3 Materials and Methods

Fly stocks

Overexpression line was procured from Dr. Maya Bader (Bader et al., 2011). RNAi lines of PI31 and Tankyrase were obtained from the Vienna *Drosophila* research center.

In vivo oxidative stress assay

Muscles were dissected in PBS (130 mM NaCl, 7 mm Na_2HPO_4, 3 mm NaH_2PO_4, pH 7.0) along their dorsal mid line, taking out body fat and secured flat with insect pins (Fine Science Tools) on silgard plates. Dissected muscles were incubated with hydrogen peroxide (H_2O_2) for 1 hour at concentration ranging from 50-150 μM, followed by 3 wash steps with PBS 10 min each. Muscles were incubated for 45 min with freshly prepared CM-H_2DCFDA kit (life technologies) for detection of ROS. Muscles were then transferred to Eppendorf tubes, washed three times with PBS. Following steps of fixation, permeabilization and staining were carried out immediately as described for immunohistochemistry in chapter 2.

Dietary restriction

For dietary restriction assays food was prepared with 0.25% (3 g/L) versus 3% (36 g/L) of active dry yeast (Red Star). Food was prepared with: 1.2L H_2O, 87.5 g/L cornmeal, 10 g/L agar, 83 mL molasses, 8.3 mL 30% tegosept and 0.89 mL propionic acid. Bromphenol dye was obtained from Sigma. Instant dry yeast food was procured from Carolina.

Immunohistochemistry, Western blot and *in vivo* proteasome activity assay

For detailed description refer to chapter 2.

Native gel

For detailed description refer to chapter 3.

5 Discussion

5.2 A screen for proteasome modifiers in muscle atrophy model

The work described in this thesis originated in a screen for genes that can suppress proteasome inhibition induced by DTS5. DTS5 is a β subunit of the 26S proteasome previously shown to dominantly block proteasome function dependent on permissive temperature. I employed an inducible transgenic approach with the benefits of *in vivo* analyses, specifically targeting proteasome inhibition only within muscle cells and tight temporal control of the period of proteasome inhibition via induction with the transcriptional activator RU486. The screen was based on the primary observation that DTS5 induction in muscles resulted in a rapid muscle atrophy, signs of atrophy appeared as early as 12 hours but severely progressed by 24 hours (Figure 2.3). Muscle wasting was evident by a loss of the sarcomeric cyto-architecture, irregular nuclei pattern, aggregates of poly-ubiquitinated proteins and autophagic vesicles. Loss of contractile activity was scored on apple plates (Figure 2.2).

5.1.1 Apoptosis involvement in muscle atrophy

Some studies reported induction of active caspase-3 and apoptotic cell death of muscle cultures upon proteasome inhibition (Goldbaum et al., 2006; Lang-Rollin et al., 2004). In contrast to these studies muscles in my study showed no indication of apoptotic cell death. There was no increase in active capase-3 staining or ultrastructural changes in nuclear architecture (Figure 2.4). Likewise, there was no decline in nuclei number, only

loss in muscle width. This discrepancy is first primarily due to the employment of different systems. Past studies that did look for apoptotic observations employed *in vitro* analysis in mammalian cultures, whereas my system is an *in vivo* one in *Drosophila* muscles. Greene et al. saw that *in vivo* UPS obstruction in Parkin mutant flies led to apoptotic muscle degeneration (Greene et al., 2003). However, Parkin is an E3 ligase therefore its inactivity translates first to a ubiquitin stress and not a direct inhibition of the proteasome. Protein ubiquitination plays a role in the apoptotic cascade and can explain dissimilar responses. As a general rule atrophy does not depict cellular degeneration but rather elimination of mass from cell bodies, therefore accordingly should not involve apoptotic response. However more detailed analysis is needed, as up to date the vast majority of studies that investigated proteasome inhibition *in vivo* in muscles did not assay for apoptosis role.

5.1.2 Autophagy involvement in muscle atrophy

Increased autophagy has been previously reported in other models of proteasome inhibition (Pan et al., 2008; Pandey et al., 2007) (Ding et al., 2007; Kitajima et al., 2014). This is commonly considered to be a compensatory mechanism, allowing cells to resolve protein accumulation left by absence of UPS dependent degradation. Indeed, treatment with rapamycin to upregulate autophagy both in mice and in mammalian cell culture, was demonstrated to protect against cell death caused by proteasome inhibition (Pan et al., 2008). In *Drosophila* as well upregulation of autophagy alleviated retinal degeneration. Retinal degeneration was induced by loss of proteasome function due to DTS7 expression (Pandey et al., 2007). In accordance with previous observations I also noted mild upregulation of autophagosome formation, evident by ATG8 puncta (Figure 2.4).

However, that response was not enough to prevent muscle atrophy. Interestingly, recently it was reported that chronic induction of DTS5 attenuates ATG8 puncta formation in larval muscles (Zirin et al., 2015). Autophagy is a double edge sword for the system studied in this thesis. On the one end, it can help mitigate proteotoxic stress by filling the gap in protein degradation left by UPS inhibition. On the other hand autophagy itself plays an active role in propagating muscle wasting (Dobrowolny et al., 2008; Mammucari et al., 2007; Wang et al., 2005; Zhao et al., 2007). Indeed, when autophagy was incapacitated by RNA interference of ATG genes, DTS5 induced muscle atrophy was moderately alleviated (Figure 3.5B).

Impaired autophagy is known to induce skeletal myofiber degeneration and muscle weakness (Masiero et al., 2009; Raben et al., 2010). Similar alterations in muscle architecture were found in an $Rpt3^{-/-}$ mice as in an $Atg7^{-/-}$ mice, but the extent of muscle wasting or failure in muscle development was apparently more severe in the $Rpt3^{-/-}$ mice (Kitajima et al., 2014; Masiero et al., 2009). Moreover, shortened life expectancy was observed only for $Rpt3^{-/-}$ mice. This data suggest that the UPS pathway is far more important in maintaining muscle homeostasis and function, alternatively ATG7 loss is compensated by other redundant factors.

5.1.3 Etiology of muscle wasting due to proteasome inhibition

My primary finding that proteasome inhibition promoted muscle wasting stands in contrast to the notion that muscle degeneration proceeds through proteasome dependent degradation. In agreement, Haas et al. also reported that proteasome function was vital for

muscle integrity and function, using DTS5 induction in a similar manner (Haas et al., 2007). Additionally, supporting my finding is the observation that conditional knockout of Rpt3 in muscles of mice resulted in loss of contractile function and muscle wasting. Muscle wasting correlated with similar morphological and molecular alterations like the ones I observed (Kitajima et al., 2014).

Studies which reported that pharmacologic inhibition of the proteasome improved muscle wasting mostly used MG-132 (Bailey et al., 1996; Carmignac et al., 2011; Tawa et al., 1997). Yet, MG-132 administration might have systemic effects independent of muscular inhibition of the UPS system. Same goes to every drug, however MG-132 specifically is known to salvage IκB which inhibits NFκb in inflammatory cells (Lee and Goldberg, 1998). It is possible that an attenuated inflammatory response is what protected muscles from atrophy in these models. However, this does not explain the apparent contradiction as a whole.

In living cells, polypeptide chains emerging from ribosomes and preexisting polypeptide chains face constant threat of mis-folding and aggregation, this threat is especially magnified in muscle tissue. Muscles are especially susceptible to such damage in comparison to other tissues, due to mechanical and thermal stressors and continuous oxidative insults during muscle contraction (Arndt et al., 2010). Mounting evidence suggests that protein aggregation is often part of the cellular response to an imbalanced protein homeostasis. Abnormal protein accumulation and/or mis-folded protein aggregation generates multifactorial toxic effects in cells (Chhangani et al., 2012; Olzscha et al., 2011; Taylor et al., 2002). Protein aggregates are often associated with the perturbation of protein degradation in many physiological processes and various human

pathologies, especially neurodegeneration diseases (Chai et al., 2002; Dobson, 1999; Martin, 1999; Nucifora, 2001; Steffan et al., 2000). Preventing the accumulation of aggregation-prone proteins is the first and most effective intervention point to control protein aggregation. Cells of all kingdoms of life have evolved an elaborate protein quality-control system to prevent such toxic aggregates. This cellular response is termed unfolding protein response (UPR) and it involves various strategies. The UPR involves foremost chaperones to facilitate correct protein folding or target them for proteolytic degradation by either the UPS or autophagy, thereby preventing protein aggregation (Ellgaard and Helenius, 2003; Goldberg, 2003; Hartl and Hayer-Hartl, 2009; Rubinsztein, 2006). Many intracellular cytosolic misfolded and aggregated proteins are targeted and degraded by UPS (Reinstein and Ciechanover, 2006). Decreased proteasome activity seems to be a feature of many cellular models and proteinopathic diseases in which intracellular aggregates are formed (Bedford et al., 2008; McNaught et al., 2003; Seo et al., 2004). The progressive appearance of autophagocytic vacuoles, and more decisively the progressive accumulation of poly-ubiquitinated proteins in punctate aggregates, suggest that proteasome inhibition in the musculature triggered a UPR that may stand as the mechanistic cause for the rapid muscle wasting. Such mechanism might also explain age-related decline in muscle strength. Demontis and Perrimon found that increasing FOXO signaling in muscles can prevent muscle wasting in aged flies and increase life span (Demontis and Perrimon, 2010). Accumulation of poly-ubiquitinated proteins in aggregates is a hallmark feature of aging muscles. FOXO signaling reduced protein aggregation and preserved muscle function, through elevated activation of the autophagy system. These results present a similar contradiction as autophagy like the UPS has been identified in propagating muscle atrophy.

The observation that muscle aging is characterized by loss of proteostasis further suggests some similarity between muscle aging and neurodegenerative diseases.

In addition to toxicity of protein aggregates, proteasome inhibition may cause deficiency in metabolic resources. Protein degradation by the ubiquitin proteasome systems might provide resources, such as oligopeptides and amino acids, for maintaining cellular integrity in skeletal muscle tissue (Bonaldo and Sandri, 2013). Therefore, proteasome inhibition might have resulted in deprivation of resources needed for cellular maintenance. However, I would assume muscles have enough resources to sustain them in the time frame of my experiments. In conclusion, chronic inhibition of the UPS may have resulted in atrophy and impaired muscle function, since this pathway plays a critical role in cell homeostasis through the removal of protein aggregates. Therefore, the key is in balanced protein homeostasis, with both excessive catabolism and insufficient proteasome activity leading to muscle atrophy.

5.3 α1 knockdown aids proteasome stability through Ecm29 chaperone recruitment

The screen I carried resulted in the identification of various possible modifiers of proteasome activity, amongst them most surprising was the identification of proteasome subunit α1 in this process. This subunit is a core subunit of the 20S catalytic particle, and therefore one would expect for its depletion to exacerbate proteasome inhibition rather that alleviate it. Further characterization demonstrated a functional significance to the recruitment of CG8588, the *Drosophila* orthologue of Ecm29, in relieving proteasome inhibition and preventing muscle wasting. These findings highlight a quality control

response to compromised proteasome assembly through the enlistment of alternative proteasome interacting protein. This study demonstrates the significance of controlled proteasome assembly for muscle function and adaptation to proteotoxic stress.

5.3.1 DTS5 disrupts proteasome stability

DTS5 and DTS7 are widely used to study the UPS due to their dominant temperature-sensitive nature making them useful for manipulating proteasome function *in vivo*. These mutants encode abnormal β6 and β2 subunits that incorporate into proteasome particles and interfere with their function (Saville and Belote, 1993; Schweisguth, 1999; Smyth and Belote, 1999). Due to their excessive expression and the structure of the 20S proteasome these mutants act as 'poison subunits' in a dominant manner (Herskowitz, 1987). According to this model when an abnormal protein is part of a multimeric complex, as the 20S is, its integration can poison and disrupt the function of the entire structure. This hypothesis explains how DTS mutants work in a dominant fashion to disrupt proteasome function. However, the exact mechanism by which these abnormal subunits are interfering with proteasome activity is not known. In DTS7 a highly-conserved glycine is replaced by an arginine and in DTS5 there is a threonine to isoleucine substitution. High resolution structural analysis of both bovine and yeast 26S proteasomes showed extensive interactions between β2 and β6 (Groll et al., 1997; Huber and Groll, 2016). The β2 mutation might have a direct effect on its catalytic function, since the amino acid substitution is only 3.0 Å from the amino group of its active site threonine (Smyth and Belote, 1999). Though β6 is not a catalytic subunit, the location of its substitution might sterically interfere with β2 catalytic activity. Alternatively, each mutant is altered near the β2-β6 interfacing regions, in areas

critical for stabilizing the interaction between the β2 and β6 subunits on opposing rings. This hindrance might result in a conformational shift destabilizing the 26S structure. I expect this shift to occur more readily at elevated temperatures, thus explaining the temperature sensitivity of these mutants. Examining proteasome activity is not enough to differentiate between these two hypotheses. For this goal, I performed native gel analysis which can differentiate distribution of the different particles that make up the holocomplex. DTS5 led to a reduction in 26S to 20S ratio and increased presence of free RP (Figure 3.6). This observation signifies DTS5 role in proteasome assembly, providing a mechanistic functional explanation for the first time as to how DTS mutants disturb proteasome function. Still the question remains whether this mechanism favors disassembly or prevents assembly. I have begun a more in depth analysis, which could shed light on this missing link. For this purpose, I am using a gel filtration system (fast protein liquid chromatography [FPLC]) to purify specific particles in combination with native gels. Purified 26S will be incubated for different times at permissive temperature and analyzed for their dynamic disassembly.

5.3.2 Compromised 20S proteasome assembly mitigates proteotoxic stress

Knocking down α1 reversed the diminution in 20S/26S ratio caused by DTS5 expression, in favor of 26S over 20S (Figure 3.6). Suggesting that relief of larval paralysis and proteasome inhibition was a derivative of an increase in protein assembly and stability. Though the identification of α1 involvement in this system was unexpected, it does have a precedent (Gerlinger et al., 1997). *crl3-2* (cyclohexamide resistance) is an

Rpt6 mutant exhibiting growth defects and accumulation of poly-ubiquitinated proteins, indicating reduced proteasome activity. Double mutant of *crl3-2* and *SCL1-1*, α1 mutant, displayed reduced accumulation of poly-ubiquitinated proteins at 30°C and was viable at 37°C, compared to *crl3-2* mutant alone. Cloning of the *SCL1–1* mutant allele showed that the suppressor mutation is due to an exchange of tyrosine 30 against cysteine. Tyr 30 is located at an N-terminal H0-helix domain and is entirely conserved in all 20S proteasome α-type subunits known so far. In addition, all cloned crl mutations reside in different types of 19S cap as well as 20S core subunits. Leading to the assumption that these mutations do not impair a specific function of the proteasome but cause a general defect in proteasomal protein degradation.

An earlier study showed that compromising 19S proteasome complex can protect cells against proteotoxic stress incurred by the proteasome inhibitors MG-132 or Bortezomib (Tsvetkov et al., 2015). Under toxic levels of inhibition, most intriguingly suppressing individual components of the 19S regulatory complex increased cell survival. In light of these observations I also found that all α ring subunits except α6 were successful at rescuing larval paralysis (Figure 3.4). Supporting the notion that α1 role might not be exclusive but rather part of a general stress adaptation mechanism enlisted when compromising the 20S complex. Additional mechanisms that may contribute include the induction of autophagy, induction of alternative proteasome regulatory components, or the disruption of normal gating. Preliminary observations hint that compensatory autophagy or subunits up regulation can be excluded (Figure 3.5).

Depiction of other α subunits capability to rescue paralysis suggests some general adaptation, nonetheless it still cannot be assumed that all subunits compensate for

proteasome inhibition in a similar manner. In fact, despite attenuation of larval paralysis, knockdown of all the remaining subunits did not restore *in vivo* proteasome activity or presented localization changes, with the exception of α2 knockdown (Supplementary figure 5.1). Although, general features of the structure and function of the proteasome are known, the exact roles of each of the individual subunits are less well understood. From structure analysis we do know they likely play different roles in gate closing as they do not contribute equally to this mechanism, with N-terminal tails of α2, α3, and α4 and an internal loop of α5 sealing the 20S chamber (Groll et al., 2000; Unno et al., 2002). It is possible they have specific functions in facilitating 19S assembly and binding of different activators. Previous studies have suggested that Rpt ring assembly in yeast is guided, in part, by pre-existing α-rings (Kusmierczyk et al., 2008; Park et al., 2009; 2010; Roelofs et al., 2009). To date, only core particle α3 has been implicated in Rpt ring assembly (Kusmierczyk et al., 2008), but a thorough analysis of all subunits is still missing.

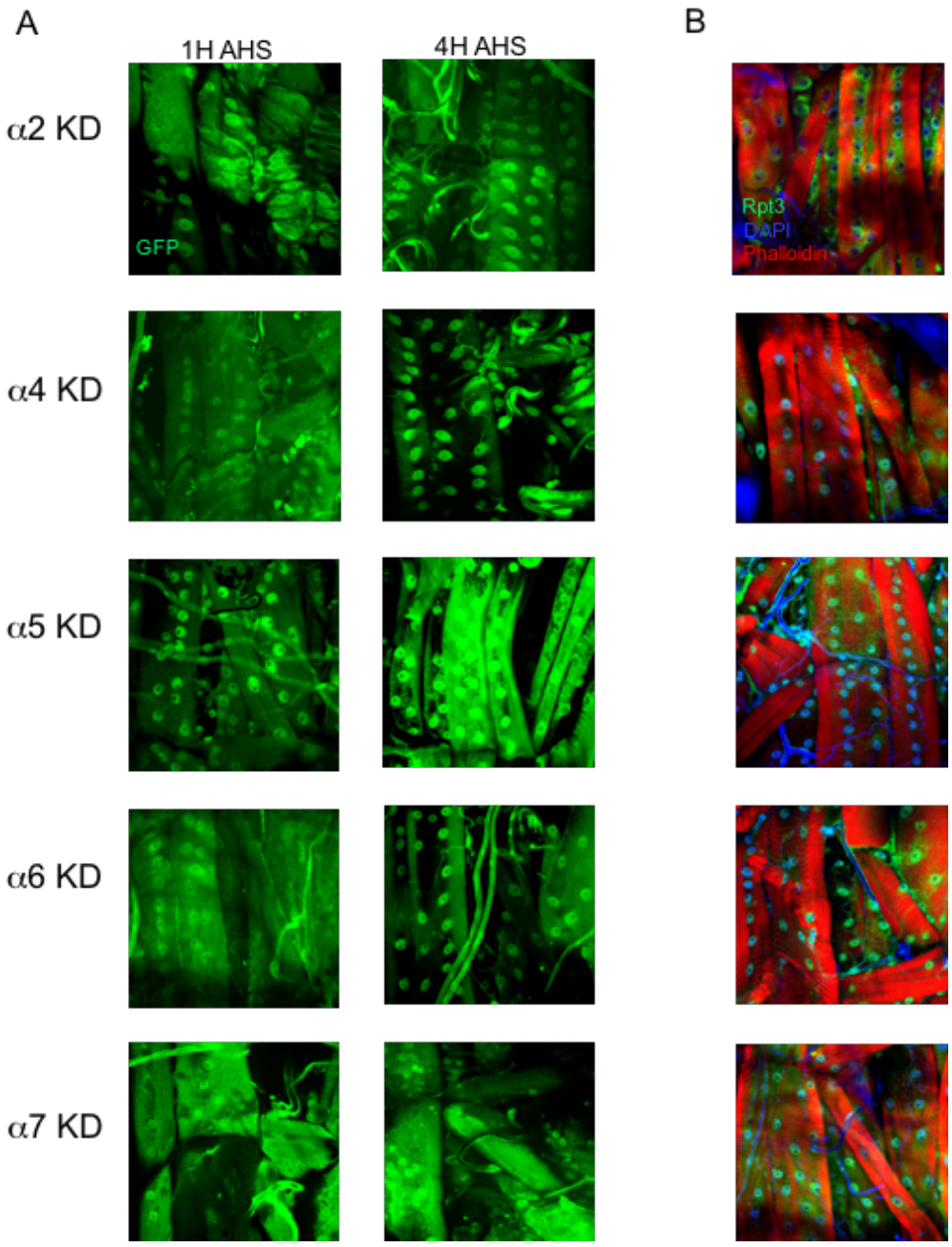

Figure 5.1 α subunits role in proteasome activity and localization. A. Transgenic larvae expressing DTS5 and indicated RNAi were analyzed for *in vivo* proteasome activity. GFP signal persisted past 4 hours indicating proteasome inhibition. **B.** Muscles were dissected, fixed and stained for Phalloidin, DAPI and Rpt3. All but α2 were found in normal nuclear localization, α2 displayed differential localization similarly to α1 knockdown.

The question that still remains is if and how proteasomes lacking α1 are formed. From the native gels analysis, it can be deduced that novel alternative forms of holocomplexes are formed when α1levels are minimal (Figure 3.6). Velichutina and colleagues showed in yeasts that in the absence of the chaperone dimer pba-3-pba4 or α3 subunit, alternative proteasomes can be created with α4 as a substituting for α3 (Velichutina et al., 2004). These proteasomes had an advantage under specific stresses such as high metal and oxidative stress (Kusmierczyk et al., 2008), hence I suggest these novel forms act as a safety net under stress. Though assembly of these proteasomes might be slower and less efficient, if proteotoxic stress is already present an increase in net assembly of proteasomes will be advantageous. Preliminary examination of proteasome composition using silver stain suggests altered subunit composition (Figure 3.10), nevertheless additional investigation of these bands using mass-spectrometric analysis is necessary.

5.2.3 α1-RNAi induces recruitment of Ecm29 to promote RP-CP association

Interestingly, proteasomes from α1-RNAi flies also exhibited reduced electrophoretic mobility in native gels, observed in both RP-CP and RP_2-CP forms (Figure 3.6). Simple substitution of subunits cannot account for the magnitude of this shift as they are roughly the same size. I suggest this shift is due to a major structural difference, conferred by the binding of an exterior proteasome regulator. I focused my attention first on Ecm29, because Ecm29 is a large protein described to interact with both RP and CP

and to contribute to proteasome stability. In agreement with its function as a quality control chaperone of proteasomes, both yeast and mice (KIAA00368) can grow normal in its absence, but are sensitized to proteotoxic stress (Haratake et al., 2016; Lee et al., 2011; Lehmann et al., 2010; Park et al., 2011). Genetic analysis determined that larval paralysis and accumulation of poly-ubiquitinated proteins in the Ecm29 mutant correlates with modifications of the proteasome in biochemical assays. Moreover, suppression of proteasome inhibition by α1 RNAi was dependent on Ecm29 (Figure 3.8-3.9). Transgenic flies of α1 RNAi did not suffer from gross phenotypical stress nor were they more sensitive to proteotoxic stress, on the contrary they were more resistant, advocating the enlistment of a quality control pathway.

The relevant question is obviously how Ecm29 may contribute to the functional assembly of the proteasome. Since Ecm29 was important for the stability of aberrant proteasomes in comparison to wild-type, these findings suggest that Ecm29 is a proteasome chaperone when proteasome assembly is at risk. Interactions between Ecm29 and proteasome intermediates might contribute to dynamic alterations of proteasome composition or assembly. Upon α1 knockdown CP fell below the detection limit, and the predominant holoenzymes were the RP_2-CP species. Remarkably, there were also more RP assembly intermediates (Figure 3.6B). Together these observations suggest that a CP assembly defect do follow α1 exhaustion. Accumulation of RP intermediates fit with the model that RP assembly is dependent on the CP as template. I propose that Ecm29 compensate for deficiencies in CP assembly and acts at the juncture of CP maturation and RP-CP assembly (Figure 5.2).

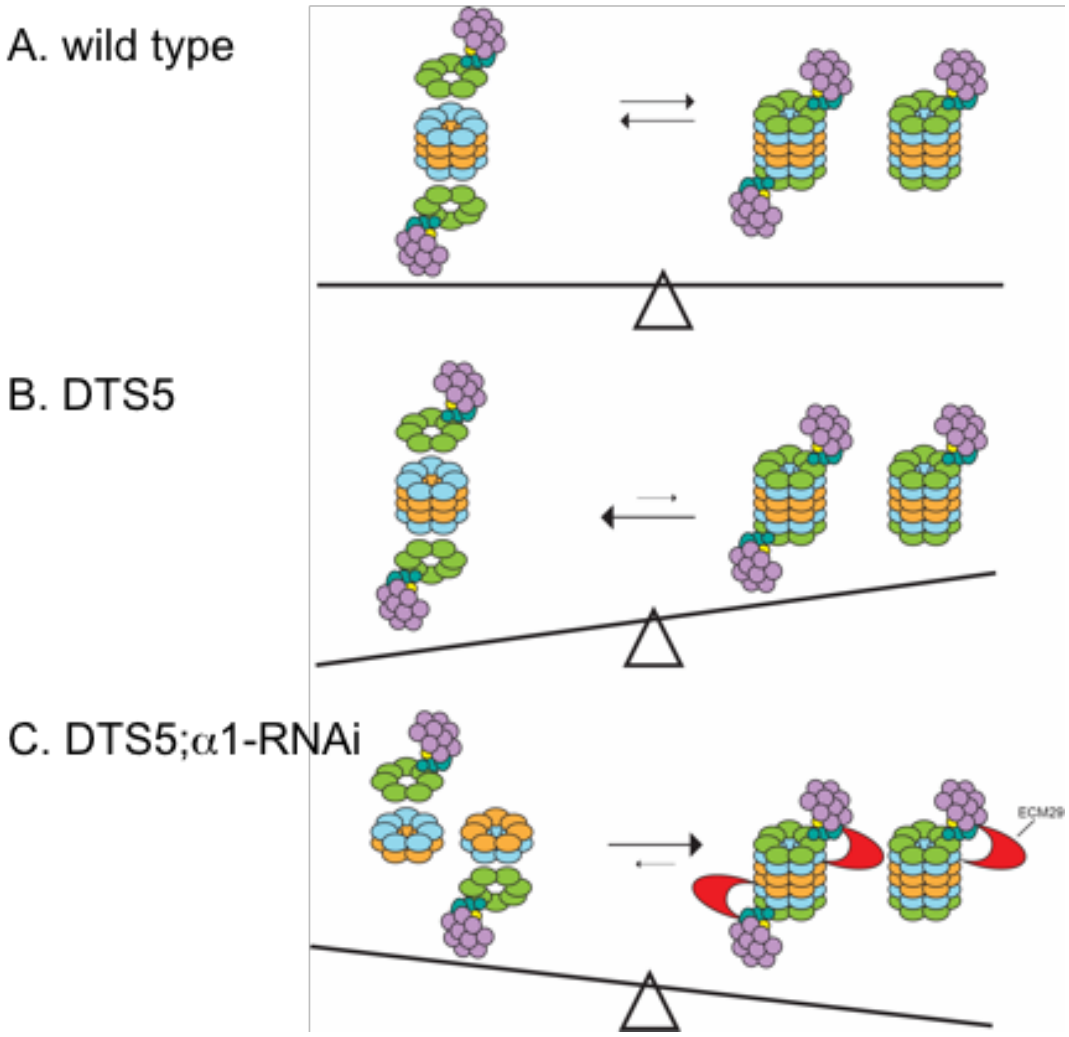

Figure 5.2 A model for balanced proteasome assembly. A. Homeostatic balance between holocomplexes and free 19S and 20S pools. Balance is dynamic based on cell needs at a given environment and developmental stage. **B.** Balance in favor of free RP and CP: DTS5 complexes are less stable and in the restrictive temperature disassembly over comes assembly. **C.** α1 knockdown presents an affinity switch, which recruits Ecm29, so that assembly defects are counteracted by increased stability of the holocomplex. The cost to increased assembly could be in reduced dynamic flexibility of the holocomplex. Loss in dynamic assembly-disassembly could sensitize this strain to various proteasome mutants and stress conditions but has the advantage when disassembly is favored.

Currently there is no molecular insight into how Ecm29 is regulated and how it recognizes defective proteasomes, yet mounting evidence suggest that it does show preference to such proteasomes. The prevailing model suggests that Ecm29 is selectively enriched on structurally aberrant holoenzymes due to increased affinity. Other proposed models are first Rpn4 dependent induction of Ecm29. Though Ecm29 does have a PACE element, when its promoter was replaced with a synthetic one it was still enriched on aberrant proteasomes (Lee et al., 2011). A second alternative model suggests that Ecm29 is a proteasome substrate, and as such would be stabilized when proteasome is inhibited, however Ecm29 was found to be a stable protein (Park et al., 2011).

Though minor induction in Ecm29 levels was apparent (Figure 3.7), it is highly unlikely to be enough to account for the massive recruitment observed in Figure 3.9. I envision two ways by which proteasomes from α1-RNAi transgenic flies would attract Ecm29. Ecm29 could specifically recognize conformations in either alternative assembly of CP or RP, or it might be able to recognize a specific signal at some integration point at the RP-CP interface. If Ecm29 were to recognize some misalignment between CP and RP, it would have the potential to be able to "sense" a variety of faulty proteasomes, even if the cause is from a different origin. Because Ecm29 has been reported to bind to the CP as well as the RP, one can imagine that subtle changes affecting the relative position of the two binding sites might function as a sensor of improper RP-CP alignment. As Rpt tails dock in pockets formed between α-subunits, substitution of a subunits might account for such mis-alignment. Additionally, alteration of the α subunits ring could manifest itself in different allosteric hindrances that might affect the proteasome affinity to chaperone. In support of this model Yashiroda and colleagues showed that deletion of

both Fub1 (PI31 yeast orthologue) and the 20S chaperone Pba4 is lethal (Yashiroda et al., 2015). This lethality is suppressed by deletion of α7 N-terminus. Crystal structures reveal that while in wild-type α7 N terminal region protrudes from the molecular surface of the α ring, when this region is deleted α1 N terminus protrudes instead.

Alternatively, since α1 is in short supply it could stall 20S assembly such that proteasome maturation is delayed. Lehmann et al. found that Ecm29 was enriched on proteasomes missing β3, moreover these proteasomes were abnormal in their immaturity, containing un-process β5 (Lehmann et al., 2010). In accordance Kusmierczyk et al. suggested that the arecheal chaperones PbaA-PbaB recognize immature 20S particles due to the presence of β subunits pro-peptides, implying their binding is regulated allosterically by changes that are initiated at distant sites (Kusmierczyk et al., 2011). Intuition suggests that active sites buried inside the CP should not be able to modify events occurring on the surface of the proteasome. Yet it was shown that that proteasome inhibitors can stabilize proteasomes by engagement of the proteolytic sites, suggesting some form of retrograde communication from the CP to the RP (Kleijnen et al., 2007). Since I observed robust hydrolytic activity of Ecm29-bound proteasomes (Figure 3.9) it seems unlikely that defects in active sites cause the recruitment of Ecm29. However, it is still possible that reduced levels of a CP subunit lead to immature species recognized by Ecm29. Incorporation of immature CP species into holoenzyme might reflect a relaxation in a checkpoint which prevents premature incorporation. The β6 subunit has a 19-residue N-terminal extension that is expected to be in close proximity to β7 before β6 processing in the precursor half proteasome (Groll et al., 1999). The β5 pro-peptide, the β6 N-terminal extension, and the β7 tail are key appendages in guiding assembly of the 20S (Li et al.,

2007). Especially intriguing is that the DTS5 mutation is located right adjacent to β6 NTE, and could possibly effect its interactions. Ump1 and the β5 pro-peptide have opposing functions in the joining and assembly of half-proteasome particles, with β5 pro-peptide driving it and Ump1 inhibiting stable dimerization until the rate-limiting insertion of the β7 subunit is completed. β5Δpro lethality is suppressed by deletion of the β6 NTE, suggesting β6 NTE collaborate with Ump1 in this assembly checkpoint. By passing the Ump1 checkpoint, perhaps due to the DTS5 mutation, could result in premature dimerization and immature proteasomes. This hypothesis can be tested with genetic analysis of mutants and assay proteasome maturity by observing β subunits processing.

5.2.4. Atrophy salvage by α1 knockdown correlates with altered localization of proteasomes

A striking feature of α1 knockdown effects under stress was re-distribution of proteasomes from primarily nuclear localization to the cytoplasm, both under DTS5 induced stress and DR related stress (section 3.3.2 and figure 4.5 D). Proteasomes cytosolic localization was primarily in peri-nuclear region known for the endoplasmic reticulum (ER) compartment which exhibits high level of ubiquitin-dependent proteolysis. It has long been established that this region is enriched in proteasomes especially when cells synthesize large amounts of abnormal proteins or when proteasomes are inhibited. This localization is presentation of the UPS function in mediating the ERAD (endoplasmic reticulum associated degradation), a critical pathway in the UPR for protein quality control

that clears un-folded and mis-folded proteins (Hampton, 2002; Kostova and Wolf, 2003; McCracken and Brodsky, 2003). The ERAD response involves retro-translocation of misfolded proteins from the ER back into the cytosol, where they are degraded by proteasomes. Interestingly, Ecm29 was also found localized in this area (Gorbea et al., 2004). Additionally, Ecm29 sequence is composed of domains which are characteristic of many other established adaptor proteins including HEAT repeats, VHS domain and potential clathrin-interacting domains (Bonifacino and Traub, 2003; Kajava et al., 2004; Lohi et al., 2002). Together with evidence linking Ecm29 to proteasomes trafficking (Gorbea et al., 2010; Hsu et al., 2015), these observations suggest that Ecm29 can function as an adaptor protein recruiting proteasomes to compartments of intense degradation thus aiding the response to proteotoxic stress. In fact, a role for Ecm29 in the ERAD pathway is indicated by overexpression of the protein in mutant CHO cells that exhibit increased ERAD activity (Gorbea et al., 2004). This hypothesis could assign a mechanistic significance to my data and present a functional role to proteasome localization in mitigating proteotoxic stress. However, localization of the proteasomes remained perinuclear whether DTS5 and α1-RNAi were expressed in a wild-type or mutant Ecm29 genetic background (data not shown). This result implies that Ecm29 is not involved in the localization changes in my model or that using a heterozygotes background of Ecm29 is not enough of a loss to modify localization. Another possible explanation is that re-localization results from altering accessibility of the nuclear localization signal of the proteasome as α1 bears one, though it still does not fully explain the stress context.

5.2.5 Summary

Cells have evolved numerous and often overlapping homeostatic pathways to adapt to changes in their environment and to survive under adverse conditions. Using a genetic screen of DTS5 impaired proteasomes I identified the collaborative mechanism of α1 knockdown and Ecm29 in mitigating proteotoxic stress through adaptation in proteasome assembly. Whereas much is known of proteasome stress response at the level of its expression, very little is known of adaptive responses through alternative assembly. My results suggest a new mechanism for proteasome stress adaption through modified assembly.

The most fascinating but puzzling feature of Ecm29 is its function through diverse mechanisms and versatile effects on the proteasome, at times even opposing effects. For example, its effects on gate opening are sometimes at odds (Kleijnen et al., 2007; Lee et al., 2011). Whereas Ecm29 often promotes a strong association between the RP and CP, it can also promote their dissociation such as under oxidative stress of the holoenzyme (Panasenko and Collart, 2011; Wang et al., 2010b). Likewise, under adverse conditions, Ecm29 mutations may either promote or antagonize resistance to stress. Depending on the conditions and mutants, Ecm29 can either suppress or enhance proteasome activity and resistance to stress. To better understand these conflicting observations, additional studies are essential to signify its physiological function at higher organisms. The detailed mechanism of action of Ecm29 and how exactly does it stabilize proteasomes are still unknown. This gap in knowledge could be addressed by conducting careful Ecm29-proteasme binding assays to understand the mechanism and stoichiometry of this

interaction. Such studies will address the question of whether the docking of one Ecm29 molecule between the 19S-20S interface is enough; or the binding of several molecules is needed, providing some form of a cap function. If Ecm29 functions as a cap it could also possibly modify rate of degradation or even recruitment of specific substrates. Some of these questions could be answered by piloting electron microscopy on purified proteasomes and Ecm29. These types of experiments could show how the addition of Ecm29 affects the association of individual complexes and do new types of proteasomes form. *In vitro* studies will also come useful in manipulating stoichiometry of the 20S subunits.

In summary, I find that Ecm29 functions as part of a large cellular response to the stress of compromised 20S assembly, but rather than compensating for aberrant proteasome output by simply enhancing proteasome activity, Ecm29 alters proteasome function by multiple mechanisms. Failed quality control mechanisms at protein level are typical preconditions of neurodegenerative disorders, cancer and aging. Therefore, understanding how the proteasome adapts to stress may help in identifying new therapeutic platforms. Existing drugs already encounter resistance in patients, hence exploring new sites of regulation as in assembly can be highly beneficial.

6 References

Adams, G.M., Falke, S., Goldberg, A.L., Slaughter, C.A., DeMartino, G.N., and Gogol, E.P. (1997). Structural and functional effects of PA700 and modulator protein on proteasomes. Journal of Molecular Biology *273*, 646–657.

Aiken, C.T., Kaake, R.M., Wang, X., and Huang, L. (2011). Oxidative stress-mediated regulation of proteasome complexes. Mol. Cell Proteomics *10*, R110.006924–R110.006924.

Alers, S., Wesselborg, S., and Stork, B. (2014). ATG13. Autophagy *10*, 944–956.

Arendt, C.S., and Hochstrasser, M. (1997). Identification of the yeast 20S proteasome catalytic centers and subunit interactions required for active-site formation. Proc. Natl. Acad. Sci. U.S.a. *94*, 7156–7161.

Arndt, V., Dick, N., Tawo, R., Dreiseidler, M., Wenzel, D., Hesse, M., Fürst, D.O., Saftig, P., Saint, R., Fleischmann, B.K., et al. (2010). Chaperone-Assisted Selective Autophagy Is Essential for Muscle Maintenance. Current Biology *20*, 143–148.

Bader, M., Benjamin, S., Wapinski, O.L., Smith, D.M., Goldberg, A.L., and Steller, H. (2011). A conserved F box regulatory complex controls proteasome activity in Drosophila. Cell *145*, 371–382.

Baehr, L.M., Furlow, J.D., and Bodine, S.C. (2011). Muscle sparing in muscle RING finger 1 null mice: response to synthetic glucocorticoids. The Journal of Physiology *589*, 4759–4776.

Bailey, J.L., Wang, X., England, B.K., Price, S.R., Ding, X., and Mitch, W.E. (1996). The acidosis of chronic renal failure activates muscle proteolysis in rats by augmenting transcription of genes encoding proteins of the ATP-dependent ubiquitin-proteasome pathway. J. Clin. Invest. *97*, 1447–1453.

Baracos, V.E., DeVivo, C., Hoyle, D.H., and Goldberg, A.L. (1995). Activation of the ATP-ubiquitin-proteasome pathway in skeletal muscle of cachectic rats bearing a hepatoma. Am. J. Physiol. *268*, E996–E1006.

Barthelme, D., and Sauer, R.T. (2012). Identification of the Cdc48bullet20S Proteasome as an Ancient AAA+ Proteolytic Machine. Science *337*, 843–846.

Bass, T.M., Grandison, R.C., Wong, R., Martinez, P., Partridge, L., and Piper, M.D.W. (2007). Optimization of dietary restriction protocols in Drosophila. J. Gerontol. a Biol. Sci. Med. Sci. *62*, 1071–1081.

Bate, M. (1990). The embryonic development of larval muscles in Drosophila. Development *110*, 791–804.

Baumeister, W., Walz, J., Zühl, F., and Seemüller, E. (1998). The proteasome: paradigm of a self-compartmentalizing protease. Cell *92*, 367–380.

Beckett, K., and Baylies, M.K. (2006). The development of the Drosophila larval body wall

muscles. Int. Rev. Neurobiol. *75*, 55–70.

Bedford, L., Hay, D., Devoy, A., Paine, S., Powe, D.G., Seth, R., Gray, T., Topham, I., Fone, K., Rezvani, N., et al. (2008). Depletion of 26S Proteasomes in Mouse Brain Neurons Causes Neurodegeneration and Lewy-Like Inclusions Resembling Human Pale Bodies. Journal of Neuroscience *28*, 8189–8198.

Bell, R.A.V., Al-Khalaf, M., and Megeney, L.A. (2016). The beneficial role of proteolysis in skeletal muscle growth and stress adaptation. Skeletal Muscle *6*, 16.

Belote, J.M., Miller, M., and Smyth, K.A. (1998). Evolutionary conservation of a testes-specific proteasome subunit gene in Drosophila. Gene *215*, 93–100.

Belote, J.M., and Fortier, E. (2002). Targeted expression of dominant negative proteasome mutants in Drosophila melanogaster. Genesis *34*, 80–82.

Bédard, N., Jammoul, S., Moore, T., Wykes, L., Hallauer, P.L., Hastings, K.E.M., Stretch, C., Baracos, V., Chevalier, S., Plourde, M., et al. (2015). Inactivation of the ubiquitin-specific protease 19 deubiquitinating enzyme protects against muscle wasting. Faseb J. *29*, 3889–3898.

Bilodeau, P.A., Coyne, E.S., and Wing, S.S. (2016). The ubiquitin proteasome system in atrophying skeletal muscle: roles and regulation. Am. J. Physiol., Cell Physiol. *311*, C392–C403.

Bingol, B., and Schuman, E.M. (2006). Activity-dependent dynamics and sequestration of proteasomes in dendritic spines. Nature *441*, 1144–1148.

Bischof, J., and Basler, K. (2008). Recombinases and their use in gene activation, gene inactivation, and transgenesis. Methods Mol. Biol. *420*, 175–195.

Bodine, S.C., Latres, E., Baumhueter, S., Lai, V.K., Nunez, L., Clarke, B.A., Poueymirou, W.T., Panaro, F.J., Na, E., Dharmarajan, K., et al. (2001). Identification of ubiquitin ligases required for skeletal muscle atrophy. Science *294*, 1704–1708.

Bonaldo, P., and Sandri, M. (2013). Cellular and molecular mechanisms of muscle atrophy. Dis Model Mech *6*, 25–39.

Bonifacino, J.S., and Traub, L.M. (2003). Signals for sorting of transmembrane proteins to endosomes and lysosomes. Annu. Rev. Biochem. *72*, 395–447.

Boveris, A. (1984). Determination of the production of superoxide radicals and hydrogen peroxide in mitochondria. Meth. Enzymol. *105*, 429–435.

Brand, A.H., and Perrimon, N. (1993). Targeted gene expression as a means of altering cell fates and generating dominant phenotypes. Development *118*, 401–415.

Breusing, N., and Grune, T. (2008). Regulation of proteasome-mediated protein degradation during oxidative stress and aging. Biol. Chem. *389*, 203–209.

Cai, D., Frantz, J.D., Tawa, N.E., Melendez, P.A., Oh, B.-C., Lidov, H.G.W., Hasselgren, P.-O., Frontera, W.R., Lee, J., Glass, D.J., et al. (2004). IKKbeta/NF-kappaB activation causes severe muscle wasting in mice. Cell *119*, 285–298.

Carmignac, V., Quéré, R., and Durbeej, M. (2011). Proteasome inhibition improves the muscle of laminin α2 chain-deficient mice. Hum. Mol. Genet. *20*, 541–552.

Cascio, P., Call, M., Petre, B.M., Walz, T., and Goldberg, A.L. (2002). Properties of the hybrid form of the 26S proteasome containing both 19S and PA28 complexes. The EMBO Journal *21*, 2636–2645.

Chai, Y., Shao, J., Miller, V.M., Williams, A., and Paulson, H.L. (2002). Live-cell imaging reveals divergent intracellular dynamics of polyglutamine disease proteins and supports a sequestration model of pathogenesis. Proc. Natl. Acad. Sci. U.S.a. *99*, 9310–9315.

Chen, J.C.J., and Goldhamer, D.J. (2003). Skeletal muscle stem cells. Reprod. Biol. Endocrinol. *1*, 101.

Chen, S., Wu, J., Lu, Y., Ma, Y.-B., Lee, B.-H., Yu, Z., Ouyang, Q., Finley, D.J., Kirschner, M.W., and Mao, Y. (2016). Structural basis for dynamic regulation of the human 26S proteasome. Proc. Natl. Acad. Sci. U.S.a. *113*, 12991–12996.

Chhangani, D., Joshi, A.P., and Mishra, A. (2012). E3 Ubiquitin Ligases in Protein Quality Control Mechanism. Molecular Neurobiology *45*, 571–585.

Chippindale, A.K., Leroi, A.M., Kim, S.B., and Rose, M.R. (2011). Phenotypic plasticity and selection in Drosophila life-history evolution. I. Nutrition and the cost of reproduction. In Methuselah Flies, (WORLD SCIENTIFIC), pp. 122–144.

Cho-Park, P.F., and Steller, H. (2013). Proteasome regulation by ADP-ribosylation. Cell *153*, 614–627.

Chondrogianni, N., Stratford, F.L.L., Trougakos, I.P., Friguet, B., Rivett, A.J., and Gonos, E.S. (2003). Central role of the proteasome in senescence and survival of human fibroblasts: induction of a senescence-like phenotype upon its inhibition and resistance to stress upon its activation. Journal of Biological Chemistry *278*, 28026–28037.

Chondrogianni, N., Tzavelas, C., Pemberton, A.J., Nezis, I.P., Rivett, A.J., and Gonos, E.S. (2005). Overexpression of proteasome beta5 assembled subunit increases the amount of proteasome and confers ameliorated response to oxidative stress and higher survival rates. Journal of Biological Chemistry *280*, 11840–11850.

Chou, A.P., Li, S., Fitzmaurice, A.G., and Bronstein, J.M. (2010). Mechanisms of rotenone-induced proteasome inhibition. Neurotoxicology *31*, 367–372.

Chuang, S.-M., and Madura, K. (2005). Saccharomyces cerevisiae Ub-conjugating enzyme Ubc4 binds the proteasome in the presence of translationally damaged proteins. Genetics *171*, 1477–1484.

Clarke, B.A., Drujan, D., Willis, M.S., Murphy, L.O., Corpina, R.A., Burova, E., Rakhilin, S.V., Stitt, T.N., Patterson, C., Latres, E., et al. (2007). The E3 Ligase MuRF1 Degrades Myosin Heavy Chain Protein in Dexamethasone-Treated Skeletal Muscle. Cell Metabolism *6*, 376–385.

Cohen, S., Brault, J.J., Gygi, S.P., Glass, D.J., Valenzuela, D.M., Gartner, C., Latres, E., and Goldberg, A.L. (2009). During muscle atrophy, thick, but not thin, filament components are degraded by MuRF1-dependent ubiquitylation. The Journal of Cell Biology *185*, 1083–1095.

Cohen, S., Zhai, B., Gygi, S.P., and Goldberg, A.L. (2012). Ubiquitylation by Trim32 causes coupled loss of desmin, Z-bands, and thin filaments in muscle atrophy. The Journal of Cell Biology *198*, 575–589.

Dange, T., Smith, D., Noy, T., Rommel, P.C., Jurzitza, L., Cordero, R.J.B., Legendre, A., Finley, D., Goldberg, A.L., and Schmidt, M. (2011). Blm10 protein promotes proteasomal substrate turnover by an active gating mechanism. J. Biol. Chem. *286*, 42830–42839.

Davies, K.J. (2001). Degradation of oxidized proteins by the 20S proteasome. Biochimie *83*, 301–310.

Davis, W.L., Jacoby, B.H., Jones, R.G., and Goodman, D.B. (1993). Superoxide formation preceding flight muscle histolysis in Solenopsis: fine structural cytochemistry and biochemistry. Histochem. J. *25*, 478–490.

Demontis, F., and Perrimon, N. (2010). FOXO/4E-BP signaling in Drosophila muscles regulates organism-wide proteostasis during aging. Cell *143*, 813–825.

Deng, H.-X., Chen, W., Hong, S.-T., Boycott, K.M., Gorrie, G.H., Siddique, N., Yang, Y., Fecto, F., Shi, Y., Zhai, H., et al. (2011). Mutations in UBQLN2 cause dominant X-linked juvenile and adult-onset ALS and ALS/dementia. Nature *477*, 211–215.

DeVorkin, L., Go, N.E., Hou, Y.-C.C., Moradian, A., Morin, G.B., and Gorski, S.M. (2014). The Drosophilaeffector caspase Dcp-1 regulates mitochondrial dynamics and autophagic flux via SesB. The Journal of Cell Biology *205*, 477–492.

Dey, D., Goldhamer, D.J., and Yu, P.B. (2015). Contributions of Muscle-Resident Progenitor Cells to Homeostasis and Disease. Current Molecular Biology Reports *1*, 175–188.

Dick, S.A., Chang, N.C., Dumont, N.A., Bell, R.A.V., Putinski, C., Kawabe, Y., Litchfield, D.W., Rudnicki, M.A., and Megeney, L.A. (2015). Caspase 3 cleavage of Pax7 inhibits self-renewal of satellite cells. Proc. Natl. Acad. Sci. U.S.a. *112*, E5246–E5252.

Ding, W.-X., Ni, H.-M., Gao, W., Yoshimori, T., Stolz, D.B., Ron, D., and Yin, X.-M. (2007). Linking of autophagy to ubiquitin-proteasome system is important for the regulation of endoplasmic reticulum stress and cell viability. Am. J. Pathol. *171*, 513–524.

Dobrowolny, G., Aucello, M., Rizzuto, E., Beccafico, S., Mammucari, C., Boncompagni, S., Bonconpagni, S., Belia, S., Wannenes, F., Nicoletti, C., et al. (2008). Skeletal muscle is a primary target of SOD1G93A-mediated toxicity. Cell Metabolism *8*, 425–436.

Dobson, C.M. (1999). Protein misfolding, evolution and disease. Trends Biochem. Sci. *24*, 329–332.

Dodd, S.L., Gagnon, B.J., Senf, S.M., Hain, B.A., and Judge, A.R. (2010). Ros-mediated activation of NF-ÎºB and Foxo during muscle disuse. Muscle & Nerve *41*, 110–113.

Du, J., Wang, X., Miereles, C., Bailey, J.L., Debigare, R., Zheng, B., Price, S.R., and Mitch, W.E. (2004). Activation of caspase-3 is an initial step triggering accelerated muscle proteolysis in catabolic conditions. J. Clin. Invest. *113*, 115–123.

Edström, E., Altun, M., Hägglund, M., and Ulfhake, B. (2006). Atrogin-1/MAFbx and MuRF1

are downregulated in aging-related loss of skeletal muscle. J. Gerontol. a Biol. Sci. Med. Sci. *61*, 663–674.

Ellgaard, L., and Helenius, A. (2003). Quality control in the endoplasmic reticulum. Nat. Rev. Mol. Cell Biol. *4*, 181–191.

Elsasser, S., Schmidt, M., and Finley, D. (2005). Characterization of the Proteasome Using Native Gel Electrophoresis. In Ubiquitin and Protein Degradation, Part A, (Elsevier), pp. 353–363.

Fernando, P., Kelly, J.F., Balazsi, K., Slack, R.S., and Megeney, L.A. (2002). Caspase 3 activity is required for skeletal muscle differentiation. Proc. Natl. Acad. Sci. U.S.a. *99*, 11025–11030.

Finkel, T., and Holbrook, N.J. (2000). Oxidants, oxidative stress and the biology of ageing. Nature *408*, 239–247.

Finley, D. (2009). Recognition and processing of ubiquitin-protein conjugates by the proteasome. Annu. Rev. Biochem. *78*, 477–513.

Firth, L.C., Li, W., Zhang, H., and Baker, N.E. (2006). Analyses of RAS Regulation of Eye Development in Drosophila melanogaster. In Regulators and Effectors of Small GTPases: Ras Family, (Elsevier), pp. 711–721.

Förster, A., Masters, E.I., Whitby, F.G., Robinson, H., and Hill, C.P. (2005). The 1.9 A structure of a proteasome-11S activator complex and implications for proteasome-PAN/PA700 interactions. Mol. Cell *18*, 589–599.

Freeman, M. (1996). Reiterative Use of the EGF Receptor Triggers Differentiation of All Cell Types in the Drosophila Eye. Cell *87*, 651–660.

Fuchs, Y., and Steller, H. (2011). Programmed cell death in animal development and disease. Cell *147*, 742–758.

Furuno, K., Goodman, M.N., and Goldberg, A.L. (1990). Role of different proteolytic systems in the degradation of muscle proteins during denervation atrophy. J. Biol. Chem. *265*, 8550–8557.

Fusco, C., Micale, L., Egorov, M., Monti, M., D'Addetta, E.V., Augello, B., Cozzolino, F., Calcagnì, A., Fontana, A., Polishchuk, R.S., et al. (2012). The E3-ubiquitin ligase TRIM50 interacts with HDAC6 and p62, and promotes the sequestration and clearance of ubiquitinated proteins into the aggresome. PLoS ONE *7*, e40440.

García-Prat, L., Martínez-Vicente, M., Perdiguero, E., Ortet, L., Rodríguez-Ubreva, J., Rebollo, E., Ruiz-Bonilla, V., Gutarra, S., Ballestar, E., Serrano, A.L., et al. (2016). Autophagy maintains stemness by preventing senescence. Nature *529*, 37–42.

Gerards, W.L., Enzlin, J., Häner, M., Hendriks, I.L., Aebi, U., Bloemendal, H., and Boelens, W. (1997). The human alpha-type proteasomal subunit HsC8 forms a double ringlike structure, but does not assemble into proteasome-like particles with the beta-type subunits HsDelta or HsBPROS26. J. Biol. Chem. *272*, 10080–10086.

Gerards, W.L.H., de Jong, W.W., Bloemendal, H., and Boelens, W. (1998). The human proteasomal subunit HsC8 induces ring formation of other α-type subunits. Journal of Molecular

Biology *275*, 113–121.

Gerlinger, U.M., Gückel, R., Hoffmann, M., Wolf, D.H., and Hilt, W. (1997). Yeast cycloheximide-resistant crl mutants are proteasome mutants defective in protein degradation. Mol. Biol. Cell *8*, 2487–2499.

Glickman, M.H., and Ciechanover, A. (2002). The ubiquitin-proteasome proteolytic pathway: destruction for the sake of construction. Physiol. Rev. *82*, 373–428.

Goldbaum, O., Vollmer, G., and Richter-Landsberg, C. (2006). Proteasome inhibition by MG-132 induces apoptotic cell death and mitochondrial dysfunction in cultured rat brain oligodendrocytes but not in astrocytes. Glia *53*, 891–901.

Goldberg, A.L. (1996). Importance of the ATP-Ubiquitin-Proteasome Pathway in the Degradation of Soluble and Myofibrillar Proteins in Rabbit Muscle Extracts. Journal of Biological Chemistry *271*, 26690–26697.

Goldberg, A.L. (2003). Protein degradation and protection against misfolded or damaged proteins. Nature *426*, 895–899.

Goldberg, A.L., Cascio, P., Saric, T., and Rock, K.L. (2002). The importance of the proteasome and subsequent proteolytic steps in the generation of antigenic peptides. Molecular Immunology *39*, 147–164.

Golic, K.G., and Lindquist, S. (1989). The FLP recombinase of yeast catalyzes site-specific recombination in the Drosophila genome. Cell *59*, 499–509.

Gomes, M.D., Lecker, S.H., Jagoe, R.T., Navon, A., and Goldberg, A.L. (2001). Atrogin-1, a muscle-specific F-box protein highly expressed during muscle atrophy. Proc. Natl. Acad. Sci. U.S.a. *98*, 14440–14445.

Gorbea, C., Goellner, G.M., Teter, K., Holmes, R.K., and Rechsteiner, M. (2004). Characterization of mammalian Ecm29, a 26 S proteasome-associated protein that localizes to the nucleus and membrane vesicles. Journal of Biological Chemistry *279*, 54849–54861.

Gorbea, C., Pratt, G., Ustrell, V., Bell, R., Sahasrabudhe, S., Hughes, R.E., and Rechsteiner, M. (2010). A protein interaction network for Ecm29 links the 26 S proteasome to molecular motors and endosomal components. J. Biol. Chem. *285*, 31616–31633.

Greene, J.C., Whitworth, A.J., Kuo, I., Andrews, L.A., Feany, M.B., and Pallanck, L.J. (2003). Mitochondrial pathology and apoptotic muscle degeneration in Drosophila parkin mutants. Proc. Natl. Acad. Sci. U.S.a. *100*, 4078–4083.

Groettrup, M., Soza, A., Eggers, M., Kuehn, L., Dick, T.P., Schild, H., Rammensee, H.-G., Koszinowski, U.H., and Kloetzel, P.-M. (1996). A role for the proteasome regulator PA28α in antigen presentation. Nature *381*, 166–168.

Groll, M., Bajorek, M., Kohler, A., Moroder, L., Rubin, D.M., Huber, R., Glickman, M.H., and Finley, D. (2000). A GATED CHANNEL INTO THE PROTEASOME CORE PARTICLE.

Groll, M., Heinemeyer, W., Jäger, S., Ullrich, T., Bochtler, M., Wolf, D.H., and Huber, R. (1999). The catalytic sites of 20S proteasomes and their role in subunit maturation: a mutational

and crystallographic study. Proc. Natl. Acad. Sci. U.S.a. *96*, 10976–10983.

Groll, M., Ditzel, L., Löwe, J., Stock, D., Bochtler, M., Bartunik, H.D., and Huber, R. (1997). Structure of 20S proteasome from yeast at 2.4Å resolution. Nature *386*, 463–471.

Grumati, P., Coletto, L., Schiavinato, A., Castagnaro, S., Bertaggia, E., Sandri, M., and Bonaldo, P. (2011). Physical exercise stimulates autophagy in normal skeletal muscles but is detrimental for collagen VI-deficient muscles. Autophagy *7*, 1415–1423.

Guterman, A., and Glickman, M.H. (2004). Deubiquitinating Enzymes are IN(Trinsic to Proteasome Function). Current Protein and Peptide Science *5*, 201–210.

Haas, K.F., Woodruff, E., and Broadie, K. (2007). Proteasome function is required to maintain muscle cellular architecture. Biol. Cell *99*, 615–626.

Hampton, R.Y. (2002). ER-associated degradation in protein quality control and cellular regulation. Current Opinion in Cell Biology *14*, 476–482.

Hanna, J., Meides, A., Zhang, D.P., and Finley, D. (2007). A Ubiquitin Stress Response Induces Altered Proteasome Composition. Cell *129*, 747–759.

Haratake, K., Sato, A., Tsuruta, F., and Chiba, T. (2016). KIAA0368-deficiency affects disassembly of 26S proteasome under oxidative stress condition. Journal of Biochemistry *159*, 609–618.

Harrison, D.A., and Perrimon, N. (1993). Simple and efficient generation of marked clones in Drosophila. Curr. Biol. *3*, 424–433.

Hartl, F.U., and Hayer-Hartl, M. (2009). Converging concepts of protein folding in vitro and in vivo. Nature Structural & Molecular Biology *16*, 574–581.

He, C., Bassik, M.C., Moresi, V., Sun, K., Wei, Y., Zou, Z., An, Z., Loh, J., Fisher, J., Sun, Q., et al. (2012). Exercise-induced BCL2-regulated autophagy is required for muscle glucose homeostasis. Nature *481*, 511–515.

Henchoz, S., De Rubertis, F., Pauli, D., and Spierer, P. (1996). The dose of a putative ubiquitin-specific protease affects position-effect variegation in Drosophila melanogaster. Mol. Cell. Biol. *16*, 5717–5725.

Hendil, K.B., Hartmann-Petersen, R., and Tanaka, K. (2002). 26 S proteasomes function as stable entities. Journal of Molecular Biology *315*, 627–636.

Hendil, K.B., Kriegenburg, F., Tanaka, K., Murata, S., Lauridsen, A.-M.B., Johnsen, A.H., and Hartmann-Petersen, R. (2009). The 20S proteasome as an assembly platform for the 19S regulatory complex. Journal of Molecular Biology *394*, 320–328.

Herskowitz, I. (1987). Functional inactivation of genes by dominant negative mutations. Nature *329*, 219–222.

Hériché, J.-K., Ang, D., Bier, E., and O'Farrell, P.H. (2003). Involvement of an SCFSlmb complex in timely elimination of E2F upon initiation of DNA replication in Drosophila. BMC Genet. *4*, 9.

Hirano, Y., Hendil, K.B., Yashiroda, H., Iemura, S.-I., Nagane, R., Hioki, Y., Natsume, T., Tanaka, K., and Murata, S. (2005). A heterodimeric complex that promotes the assembly of mammalian 20S proteasomes. Nature *437*, 1381–1385.

Hirano, Y., Kaneko, T., Okamoto, K., Bai, M., Yashiroda, H., Furuyama, K., Kato, K., Tanaka, K., and Murata, S. (2008). Dissecting beta-ring assembly pathway of the mammalian 20S proteasome. The EMBO Journal *27*, 2204–2213.

Holden, J.J., and Suzuki, D.T. (1973). Temperature-sensitive mutations in Drosophila melanogaster. XII. The genetic and developmental effects of dominant lethals on chromosome 3. Genetics *73*, 445–458.

Hsu, M.-T., Guo, C.-L., Liou, A.Y., Chang, T.-Y., Ng, M.-C., Florea, B.I., Overkleeft, H.S., Wu, Y.-L., Liao, J.-C., and Cheng, P.-L. (2015). Stage-Dependent Axon Transport of Proteasomes Contributes to Axon Development. Dev. Cell *35*, 418–431.

Huang, S.-M.A., Mishina, Y.M., Liu, S., Cheung, A., Stegmeier, F., Michaud, G.A., Charlat, O., Wiellette, E., Zhang, Y., Wiessner, S., et al. (2009). Tankyrase inhibition stabilizes axin and antagonizes Wnt signalling. Nature *461*, 614–620.

Huang, X., Luan, B., Wu, J., and Shi, Y. (2016). An atomic structure of the human 26S proteasome. Nature Structural & Molecular Biology *23*, 778–785.

Huber, E.M., and Groll, M. (2016). Yeast 20S proteasome at 2.3 A resolution.

Huh, W.-K., Falvo, J.V., Gerke, L.C., Carroll, A.S., Howson, R.W., Weissman, J.S., and O'Shea, E.K. (2003). Global analysis of protein localization in budding yeast. Nature *425*, 686–691.

Hwang, P.M., and Sykes, B.D. (2015). Targeting the sarcomere to correct muscle function. Nat Rev Drug Discov *14*, 313–328.

Isono, E., Nishihara, K., Saeki, Y., Yashiroda, H., Kamata, N., Ge, L., Ueda, T., Kikuchi, Y., Tanaka, K., Nakano, A., et al. (2007). The assembly pathway of the 19S regulatory particle of the yeast 26S proteasome. Mol. Biol. Cell *18*, 569–580.

Iwanczyk, J., Sadre-Bazzaz, K., Ferrell, K., Kondrashkina, E., Formosa, T., Hill, C.P., and Ortega, J. (2006). Structure of the Blm10-20 S proteasome complex by cryo-electron microscopy. Insights into the mechanism of activation of mature yeast proteasomes. Journal of Molecular Biology *363*, 648–659.

Jamart, C., Benoit, N., Raymackers, J.-M., Kim, H.J., Kim, C.K., and Francaux, M. (2012a). Autophagy-related and autophagy-regulatory genes are induced in human muscle after ultraendurance exercise. Eur. J. Appl. Physiol. *112*, 3173–3177.

Jamart, C., Francaux, M., Millet, G.Y., Deldicque, L., Frère, D., and Féasson, L. (2012b). Modulation of autophagy and ubiquitin-proteasome pathways during ultra-endurance running. J. Appl. Physiol. *112*, 1529–1537.

Jang, Y.C., and Van Remmen, H. (2011). Age-associated alterations of the neuromuscular junction. Exp. Gerontol. *46*, 193–198.

Jung, T., and Grune, T. (2008). The proteasome and its role in the degradation of oxidized

proteins. IUBMB Life *60*, 743–752.

Kageyama, S., Sou, Y.-S., Uemura, T., Kametaka, S., Saito, T., Ishimura, R., Kouno, T., Bedford, L., Mayer, R.J., Lee, M.-S., et al. (2014). Proteasome dysfunction activates autophagy and the Keap1-Nrf2 pathway. J. Biol. Chem. *289*, 24944–24955.

Kajava, A.V., Gorbea, C., Ortega, J., Rechsteiner, M., and Steven, A.C. (2004). New HEAT-like repeat motifs in proteins regulating proteasome structure and function. J. Struct. Biol. *146*, 425–430.

Kandarian, S.C., and Jackman, R.W. (2006). Intracellular signaling during skeletal muscle atrophy. Muscle & Nerve *33*, 155–165.

Kedar, V., McDonough, H., Arya, R., Li, H.H., Rockman, H.A., and Patterson, C. (2004). Muscle-specific RING finger 1 is a bona fide ubiquitin ligase that degrades cardiac troponin I. Proc. Natl. Acad. Sci. U.S.a. *101*, 18135–18140.

Kee, A.J., Combaret, L., Tilignac, T., Souweine, B., Aurousseau, E., Dalle, M., Taillandier, D., and Attaix, D. (2003). Ubiquitin-proteasome-dependent muscle proteolysis responds slowly to insulin release and refeeding in starved rats. The Journal of Physiology *546*, 765–776.

Khor, B., Bredemeyer, A.L., Huang, C.-Y., Turnbull, I.R., Evans, R., Maggi, L.B., White, J.M., Walker, L.M., Carnes, K., Hess, R.A., et al. (2006). Proteasome activator PA200 is required for normal spermatogenesis. Mol. Cell. Biol. *26*, 2999–3007.

Kiffin, R., Christian, C., Knecht, E., and Cuervo, A.M. (2004). Activation of chaperone-mediated autophagy during oxidative stress. Mol. Biol. Cell *15*, 4829–4840.

Kim, Y.A., Kim, Y.S., and Song, W. (2012). Autophagic response to a single bout of moderate exercise in murine skeletal muscle. J. Physiol. Biochem. *68*, 229–235.

Kim, Y.-C., and DeMartino, G.N. (2011). C termini of proteasomal ATPases play nonequivalent roles in cellular assembly of mammalian 26 S proteasome. J. Biol. Chem. *286*, 26652–26666.

Kimura, A., Kato, Y., and Hirano, H. (2012). N-myristoylation of the Rpt2 subunit regulates intracellular localization of the yeast 26S proteasome. Biochemistry *51*, 8856–8866.

Kitajima, Y., Tashiro, Y., Suzuki, N., Warita, H., Kato, M., Tateyama, M., Ando, R., Izumi, R., Yamazaki, M., Abe, M., et al. (2014). Proteasome dysfunction induces muscle growth defects and protein aggregation. J. Cell. Sci. *127*, 5204–5217.

Kleijnen, M.F., Roelofs, J., Park, S., Hathaway, N.A., Glickman, M., King, R.W., and Finley, D. (2007). Stability of the proteasome can be regulated allosterically through engagement of its proteolytic active sites. Nature Structural & Molecular Biology *14*, 1180–1188.

Kloetzel, P.-M. (2004). Generation of major histocompatibility complex class I antigens: functional interplay between proteasomes and TPPII. Nature Immunology *5*, 661–669.

Knöll, R., and Marston, S. (2012). On mechanosensation, acto/myosin interaction, and hypertrophy. Trends Cardiovasc. Med. *22*, 17–22.

Koncarevic, A., Jackman, R.W., and Kandarian, S.C. (2007). The ubiquitin-protein ligase Nedd4

targets Notch1 in skeletal muscle and distinguishes the subset of atrophies caused by reduced muscle tension. Faseb J. *21*, 427–437.

Kostova, Z., and Wolf, D.H. (2003). For whom the bell tolls: protein quality control of the endoplasmic reticulum and the ubiquitin-proteasome connection. The EMBO Journal *22*, 2309–2317.

Koushika, S.P., Lisbin, M.J., and White, K. (1996). ELAV, a Drosophila neuron-specific protein, mediates the generation of an alternatively spliced neural protein isoform. Curr. Biol. *6*, 1634–1641.

Krogan, N.J., Lam, M.H.Y., Fillingham, J., Keogh, M.-C., Gebbia, M., Li, J., Datta, N., Cagney, G., Buratowski, S., Emili, A., et al. (2004). Proteasome involvement in the repair of DNA double-strand breaks. Mol. Cell *16*, 1027–1034.

Kudryashova, E., Kramerova, I., and Spencer, M.J. (2012). Satellite cell senescence underlies myopathy in a mouse model of limb-girdle muscular dystrophy 2H. J. Clin. Invest. *122*, 1764–1776.

Kunjappu, M.J., and Hochstrasser, M. (2014). Assembly of the 20S proteasome. Biochimica Et Biophysica Acta (BBA) - Molecular Cell Research *1843*, 2–12.

Kusmierczyk, A.R., Kunjappu, M.J., Funakoshi, M., and Hochstrasser, M. (2008). A multimeric assembly factor controls the formation of alternative 20S proteasomes. Nature Structural & Molecular Biology *15*, 237–244.

Kusmierczyk, A.R., Kunjappu, M.J., Kim, R.Y., and Hochstrasser, M. (2011). A conserved 20S proteasome assembly factor requires a C-terminal HbYX motif for proteasomal precursor binding. Nature Structural & Molecular Biology *18*, 622–629.

La Mota-Peynado, De, A., Lee, S.Y.-C., Pierce, B.M., Wani, P., Singh, C.R., and Roelofs, J. (2013). The proteasome-associated protein Ecm29 inhibits proteasomal ATPase activity and in vivo protein degradation by the proteasome. J. Biol. Chem. *288*, 29467–29481.

Lagirand-Cantaloube, J., Offner, N., Csibi, A., Leibovitch, M.P., Batonnet-Pichon, S., Tintignac, L.A., Segura, C.T., and Leibovitch, S.A. (2008). The initiation factor eIF3-f is a major target for atrogin1/MAFbx function in skeletal muscle atrophy. The EMBO Journal *27*, 1266–1276.

Lam, Y.A., Xu, W., DeMartino, G.N., and Cohen, R.E. (1997). Editing of ubiquitin conjugates by an isopeptidase in the 26S proteasome. Nature *385*, 737–740.

Lang-Rollin, I., Vekrellis, K., Wang, Q., Rideout, H.J., and Stefanis, L. (2004). Application of proteasomal inhibitors to mouse sympathetic neurons activates the intrinsic apoptotic pathway. J. Neurochem. *90*, 1511–1520.

Laporte, D., Salin, B., Daignan-Fornier, B., and Sagot, I. (2008). Reversible cytoplasmic localization of the proteasome in quiescent yeast cells. The Journal of Cell Biology *181*, 737–745.

Le Tallec, B., Barrault, M.-B., Courbeyrette, R., Guérois, R., Marsolier-Kergoat, M.-C., and Peyroche, A. (2007). 20S proteasome assembly is orchestrated by two distinct pairs of chaperones in yeast and in mammals. Mol. Cell *27*, 660–674.

Leach, J.K., Van Tuyle, G., Lin, P.S., Schmidt-Ullrich, R., and Mikkelsen, R.B. (2001). Ionizing radiation-induced, mitochondria-dependent generation of reactive oxygen/nitrogen. Cancer Res. *61*, 3894–3901.

Lecker, S.H., Goldberg, A.L., and Mitch, W.E. (2006). Protein degradation by the ubiquitin-proteasome pathway in normal and disease states. J. Am. Soc. Nephrol. *17*, 1807–1819.

Lecker, S.H., Jagoe, R.T., Gilbert, A., Gomes, M., Baracos, V., Bailey, J., Price, S.R., Mitch, W.E., and Goldberg, A.L. (2004). Multiple types of skeletal muscle atrophy involve a common program of changes in gene expression. Faseb J. *18*, 39–51.

Lee, C.S., Yi, J.-S., Jung, S.-Y., Kim, B.-W., Lee, N.-R., Choo, H.-J., Jang, S.-Y., Han, J., Chi, S.-G., Park, M., et al. (2010). TRIM72 negatively regulates myogenesis via targeting insulin receptor substrate-1. Cell Death Differ. *17*, 1254–1265.

Lee, D.H., and Goldberg, A.L. (1998). Proteasome inhibitors: valuable new tools for cell biologists. Trends Cell Biol. *8*, 397–403.

Lee, J., Giordano, S., and Zhang, J. (2012a). Autophagy, mitochondria and oxidative stress: cross-talk and redox signalling. Biochem. J. *441*, 523–540.

Lee, S.H., Moon, J.H., Yoon, S.K., and Yoon, J.B. (2012b). Stable Incorporation of ATPase Subunits into 19 S Regulatory Particle of Human Proteasome Requires Nucleotide Binding and C-terminal Tails. Journal of Biological Chemistry *287*, 9269–9279.

Lee, S.Y.-C., La Mota-Peynado, De, A., and Roelofs, J. (2011). Loss of Rpt5 protein interactions with the core particle and Nas2 protein causes the formation of faulty proteasomes that are inhibited by Ecm29 protein. J. Biol. Chem. *286*, 36641–36651.

Leggett, D.S., Hanna, J., Borodovsky, A., Crosas, B., Schmidt, M., Baker, R.T., Walz, T., Ploegh, H., and Finley, D. (2002). Multiple Associated Proteins Regulate Proteasome Structure and Function. Mol. Cell *10*, 495–507.

Lehmann, A., Janek, K., Braun, B., Kloetzel, P.-M., and Enenkel, C. (2002). 20 S proteasomes are imported as precursor complexes into the nucleus of yeast. Journal of Molecular Biology *317*, 401–413.

Lehmann, A., Jechow, K., and Enenkel, C. (2008). Blm10 binds to pre-activated proteasome core particles with open gate conformation. EMBO Rep. *9*, 1237–1243.

Lehmann, A., Niewienda, A., Jechow, K., Janek, K., and Enenkel, C. (2010). Ecm29 Fulfils Quality Control Functions in Proteasome Assembly. Mol. Cell *38*, 879–888.

Li, X., Kusmierczyk, A.R., Wong, P., Emili, A., and Hochstrasser, M. (2007). beta-Subunit appendages promote 20S proteasome assembly by overcoming an Ump1-dependent checkpoint. The EMBO Journal *26*, 2339–2349.

Li, X., Matilainen, O., Jin, C., Glover-Cutter, K.M., Holmberg, C.I., and Blackwell, T.K. (2011). Specific SKN-1/Nrf stress responses to perturbations in translation elongation and proteasome activity. PLoS Genet. *7*, e1002119.

Lira, V.A., Okutsu, M., Akhtar, Y.N., Zhang, M., and Yan, Z. (2010). Autophagy in Skeletal

Muscle is Required for Exercise Training-Induced Improvement in Glucose Tolerance. Medicine & Science in Sports & Exercise *42*, 8.

Liu, C.-C., Lin, Y.-C., Chen, Y.-H., Chen, C.-M., Pang, L.-Y., Chen, H.-A., Wu, P.-R., Lin, M.-Y., Jiang, S.-T., Tsai, T.-F., et al. (2016). Cul3-KLHL20 Ubiquitin Ligase Governs the Turnover of ULK1 and VPS34 Complexes to Control Autophagy Termination. Mol. Cell *61*, 84–97.

Lohi, O., Poussu, A., Mao, Y., Quiocho, F., and Lehto, V.P. (2002). VHS domain -- a longshoreman of vesicle lines. FEBS Letters *513*, 19–23.

London, M.K., Keck, B.I., Ramos, P.C., and Dohmen, R.J. (2004). Regulatory mechanisms controlling biogenesis of ubiquitin and the proteasome. FEBS Letters *567*, 259–264.

Lopez, A.D., Tar, K., Krügel, U., Dange, T., Ros, I.G., and Schmidt, M. (2011). Proteasomal degradation of Sfp1 contributes to the repression of ribosome biogenesis during starvation and is mediated by the proteasome activator Blm10. Mol. Biol. Cell *22*, 528–540.

Lundgren, J., Masson, P., Mirzaei, Z., and Young, P. (2005). Identification and characterization of a Drosophila proteasome regulatory network. Mol. Cell. Biol. *25*, 4662–4675.

Lundgren, J., Masson, P., Realini, C.A., and Young, P. (2003). Use of RNA interference and complementation to study the function of the Drosophila and human 26S proteasome subunit S13. Mol. Cell. Biol. *23*, 5320–5330.

Ma, J., Katz, E., and Belote, J.M. (2002). Expression of proteasome subunit isoforms during spermatogenesis in Drosophila melanogaster. Insect Mol. Biol. *11*, 627–639.

Ma, M., and Liu, Z.L. (2010). Comparative transcriptome profiling analyses during the lag phase uncover YAP1, PDR1, PDR3, RPN4, and HSF1 as key regulatory genes in genomic adaptation to the lignocellulose derived inhibitor HMF for Saccharomyces cerevisiae. BMC Genomics *11*, 660.

Machiels, B.M., Henfling, M.E., Broers, J.L., Hendil, K.B., and Ramaekers, F.C. (1995). Changes in immunocytochemical detectability of proteasome epitopes depending on cell growth and fixation conditions of lung cancer cell lines. Eur. J. Cell Biol. *66*, 282–292.

Madura, K. (2004). Rad23 and Rpn10: perennial wallflowers join the melee. Trends Biochem. Sci. *29*, 637–640.

Mair, W., Piper, M.D.W., and Partridge, L. (2005). Calories do not explain extension of life span by dietary restriction in Drosophila. PLoS Biol. *3*, e223.

Malicdan, M.C., Noguchi, S., Nonaka, I., Saftig, P., and Nishino, I. (2008). Lysosomal myopathies: An excessive build-up in autophagosomes is too much to handle. Neuromuscular Disorders *18*, 521–529.

Mallik, M., and Lakhotia, S.C. (2009). The developmentally active and stress-inducible noncoding hsromega gene is a novel regulator of apoptosis in Drosophila. Genetics *183*, 831–852.

Mallik, M., and Lakhotia, S.C. (2014). RNAi for the large non-coding hsrω transcripts suppresses polyglutamine pathogenesis in Drosophilamodels. RNA Biology *6*, 464–478.

Mammucari, C., Milan, G., Romanello, V., Masiero, E., Rudolf, R., Del Piccolo, P., Burden, S.J.,

Di Lisi, R., Sandri, C., Zhao, J., et al. (2007). FoxO3 Controls Autophagy in Skeletal Muscle In Vivo. Cell Metabolism *6*, 458–471.

Mannhaupt, G., Schnall, R., Karpov, V., Vetter, I., and Feldmann, H. (1999). Rpn4p acts as a transcription factor by binding to PACE, a nonamer box found upstream of 26S proteasomal and other genes in yeast. FEBS Letters *450*, 27–34.

Martin, J.B. (1999). Molecular basis of the neurodegenerative disorders. N. Engl. J. Med. *340*, 1970–1980.

Masiero, E., Agatea, L., Mammucari, C., Blaauw, B., Loro, E., Komatsu, M., Metzger, D., Reggiani, C., Schiaffino, S., and Sandri, M. (2009). Autophagy is required to maintain muscle mass. Cell Metabolism *10*, 507–515.

Masson, P., Andersson, O., Petersen, U.M., and Young, P. (2001). Identification and Characterization of a DrosophilaNuclear Proteasome Regulator: A HOMOLOG OF HUMAN 11 S REG (PA28). Journal of Biological Chemistry *276*, 1383–1390.

McCracken, A.A., and Brodsky, J.L. (2003). Evolving questions and paradigm shifts in endoplasmic-reticulum-associated degradation (ERAD). BioEssays *25*, 868–877.

McLeod, M., Craft, S., and Broach, J.R. (1986). Identification of the crossover site during FLP-mediated recombination in the Saccharomyces cerevisiae plasmid 2 microns circle. Mol. Cell. Biol. *6*, 3357–3367.

McNaught, K.S.P., Belizaire, R., Isacson, O., Jenner, P., and Olanow, C.W. (2003). Altered proteasomal function in sporadic Parkinson's disease. Exp. Neurol. *179*, 38–46.

Medina, R., Wing, S.S., and Goldberg, A.L. (1995). Increase in levels of polyubiquitin and proteasome mRNA in skeletal muscle during starvation and denervation atrophy. Biochem. J. *307 (Pt 3)*, 631–637.

Medina, R., Wing, S.S., Haas, A., and Goldberg, A.L. (1991). Activation of the ubiquitin-ATP-dependent proteolytic system in skeletal muscle during fasting and denervation atrophy. Biomed. Biochim. Acta *50*, 347–356.

Meiners, S., Heyken, D., Weller, A., Ludwig, A., Stangl, K., Kloetzel, P.-M., and Krüger, E. (2003). Inhibition of proteasome activity induces concerted expression of proteasome genes and de novo formation of Mammalian proteasomes. J. Biol. Chem. *278*, 21517–21525.

Milan, G., Romanello, V., Pescatore, F., Armani, A., Paik, J.-H., Frasson, L., Seydel, A., Zhao, J., Abraham, R., Goldberg, A.L., et al. (2015). Regulation of autophagy and the ubiquitin-proteasome system by the FoxO transcriptional network during muscle atrophy. Nat Commun *6*, 6670.

Mitch, W.E., and Goldberg, A.L. (1996). Mechanisms of muscle wasting. The role of the ubiquitin-proteasome pathway. N. Engl. J. Med. *335*, 1897–1905.

Mitch, W.E., Medina, R., Grieber, S., May, R.C., England, B.K., Price, S.R., Bailey, J.L., and Goldberg, A.L. (1994). Metabolic acidosis stimulates muscle protein degradation by activating the adenosine triphosphate-dependent pathway involving ubiquitin and proteasomes. J. Clin. Invest. *93*, 2127–2133.

Mitsiades, N., Mitsiades, C.S., Poulaki, V., Chauhan, D., Fanourakis, G., Gu, X., Bailey, C., Joseph, M., Libermann, T.A., Treon, S.P., et al. (2002). Molecular sequelae of proteasome inhibition in human multiple myeloma cells. Proc. Natl. Acad. Sci. U.S.a. *99*, 14374–14379.

Mizushima, N., and Komatsu, M. (2011). Autophagy: renovation of cells and tissues. Cell *147*, 728–741.

Mizushima, N., Yamamoto, A., Matsui, M., Yoshimori, T., and Ohsumi, Y. (2004). In vivo analysis of autophagy in response to nutrient starvation using transgenic mice expressing a fluorescent autophagosome marker. Mol. Biol. Cell *15*, 1101–1111.

Morris, E.J., Michaud, W.A., Ji, J.-Y., Moon, N.-S., Rocco, J.W., and Dyson, N.J. (2006). Functional identification of Api5 as a suppressor of E2F-dependent apoptosis in vivo. PLoS Genet. *2*, e196.

Moylan, J.S., and Reid, M.B. (2007). Oxidative stress, chronic disease, and muscle wasting. Muscle & Nerve *35*, 411–429.

Muller, F.L., Song, W., Liu, Y., Chaudhuri, A., Pieke-Dahl, S., Strong, R., Huang, T.-T., Epstein, C.J., Roberts, L.J., Csete, M., et al. (2006). Absence of CuZn superoxide dismutase leads to elevated oxidative stress and acceleration of age-dependent skeletal muscle atrophy. Free Radic. Biol. Med. *40*, 1993–2004.

Murata, S., Sasaki, K., Kishimoto, T., Niwa, S.-I., Hayashi, H., Takahama, Y., and Tanaka, K. (2007). Regulation of CD8+ T cell development by thymus-specific proteasomes. Science *316*, 1349–1353.

Murata, S., Takahama, Y., and Tanaka, K. (2008). Thymoproteasome: probable role in generating positively selecting peptides. Curr. Opin. Immunol. *20*, 192–196.

Murata, S., Yashiroda, H., and Tanaka, K. (2009). Molecular mechanisms of proteasome assembly. Nat. Rev. Mol. Cell Biol. *10*, 104–115.

Murray, T.V.A., McMahon, J.M., Howley, B.A., Stanley, A., Ritter, T., Mohr, A., Zwacka, R., and Fearnhead, H.O. (2008). A non-apoptotic role for caspase-9 in muscle differentiation. J. Cell. Sci. *121*, 3786–3793.

Møller, A.B., Vendelbo, M.H., Christensen, B., Clasen, B.F., Bak, A.M., Jørgensen, J.O.L., Møller, N., and Jessen, N. (2015). Physical exercise increases autophagic signaling through ULK1 in human skeletal muscle. J. Appl. Physiol. *118*, 971–979.

Nakao, R., Hirasaka, K., Goto, J., Ishidoh, K., Yamada, C., Ohno, A., Okumura, Y., Nonaka, I., Yasutomo, K., Baldwin, K.M., et al. (2009). Ubiquitin ligase Cbl-b is a negative regulator for insulin-like growth factor 1 signaling during muscle atrophy caused by unloading. Mol. Cell. Biol. *29*, 4798–4811.

Narwal, M., Venkannagari, H., and Lehtiö, L. (2012). Structural basis of selective inhibition of human tankyrases. J. Med. Chem. *55*, 1360–1367.

Nederlof, P.M., Wang, H.R., and Baumeister, W. (1995). Nuclear localization signals of human and Thermoplasma proteasomal alpha subunits are functional in vitro. Proc. Natl. Acad. Sci. U.S.a. *92*, 12060–12064.

Neuburger, P.J., Saville, K.J., Zeng, J., Smyth, K.-A., and Belote, J.M. (2006). A genetic suppressor of two dominant temperature-sensitive lethal proteasome mutants of Drosophila melanogaster is itself a mutated proteasome subunit gene. Genetics *173*, 1377–1387.

Nie, J., Wu, M., Wang, J., Xing, G., He, F., and Zhang, L. (2010). REGγ proteasome mediates degradation of the ubiquitin ligase Smurf1. FEBS Letters *584*, 3021–3027.

Nucifora, F.C., Jr (2001). Interference by Huntingtin and Atrophin-1 with CBP-Mediated Transcription Leading to Cellular Toxicity. Science *291*, 2423–2428.

Olzscha, H., Schermann, S.M., Woerner, A.C., Pinkert, S., Hecht, M.H., Tartaglia, G.G., Vendruscolo, M., Hayer-Hartl, M., Hartl, F.U., and Vabulas, R.M. (2011). Amyloid-like aggregates sequester numerous metastable proteins with essential cellular functions. Cell *144*, 67–78.

Osmulski, P.A., Hochstrasser, M., and Gaczynska, M. (2009). A tetrahedral transition state at the active sites of the 20S proteasome is coupled to opening of the alpha-ring channel. Structure *17*, 1137–1147.

Osterwalder, T., Yoon, K.S., White, B.H., and Keshishian, H. (2001). A conditional tissue-specific transgene expression system using inducible GAL4. Proc. Natl. Acad. Sci. U.S.a. *98*, 12596–12601.

Padmanabhan, A., Vuong, S.A.-T., and Hochstrasser, M. (2016). Assembly of an Evolutionarily Conserved Alternative Proteasome Isoform in Human Cells. Cell Rep *14*, 2962–2974.

Page, M.M., Robb, E.L., Salway, K.D., and Stuart, J.A. (2010). Mitochondrial redox metabolism: Aging, longevity and dietary effects. Mech. Ageing Dev. *131*, 242–252.

Paik, D., Jang, Y.G., Lee, Y.E., Lee, Y.N., Yamamoto, R., Gee, H.Y., Yoo, S., Bae, E., Min, K.-J., Tatar, M., et al. (2012). Misexpression screen delineates novel genes controlling Drosophila lifespan. Mech. Ageing Dev. *133*, 234–245.

Pan, T., Kondo, S., Zhu, W., Xie, W., Jankovic, J., and Le, W. (2008). Neuroprotection of rapamycin in lactacystin-induced neurodegeneration via autophagy enhancement. Neurobiol. Dis. *32*, 16–25.

Panasenko, O.O., and Collart, M.A. (2011). Not4 E3 ligase contributes to proteasome assembly and functional integrity in part through Ecm29. Mol. Cell. Biol. *31*, 1610–1623.

Pandey, U.B., Batlevi, Y., Baehrecke, E.H., and Taylor, J.P. (2007). HDAC6 at the Intersection of Autophagy, the Ubiquitin-proteasome System, and Neurodegeneration. Autophagy *3*, 643–645.

Park, S., Kim, W., Tian, G., Gygi, S.P., and Finley, D. (2011). Structural Defects in the Regulatory Particle-Core Particle Interface of the Proteasome Induce a Novel Proteasome Stress Response. J. Biol. Chem. *286*, 36652–36666.

Park, S., Roelofs, J., Kim, W., Robert, J., Schmidt, M., Gygi, S.P., and Finley, D. (2009). Hexameric assembly of the proteasomal ATPases is templated through their C termini. Nature *459*, 866–870.

Park, S., Tian, G., Roelofs, J., and Finley, D. (2010). Assembly manual for the proteasome

regulatory particle: the first draft. Biochem. Soc. Trans. *38*, 6–13.

Partridge, L., Piper, M.D.W., and Mair, W. (2005). Dietary restriction in Drosophila. Mech. Ageing Dev. *126*, 938–950.

Paul, P.K., Bhatnagar, S., Mishra, V., Srivastava, S., Darnay, B.G., Choi, Y., and Kumar, A. (2012). The E3 Ubiquitin Ligase TRAF6 Intercedes in Starvation-Induced Skeletal Muscle Atrophy through Multiple Mechanisms. Mol. Cell. Biol. *32*, 1248–1259.

Paul, P.K., Gupta, S.K., Bhatnagar, S., Panguluri, S.K., Darnay, B.G., Choi, Y., and Kumar, A. (2010). Targeted ablation of TRAF6 inhibits skeletal muscle wasting in mice. The Journal of Cell Biology *191*, 1395–1411.

Piterman, R., Braunstein, I., Isakov, E., Ziv, T., Navon, A., Cohen, S., and Stanhill, A. (2014). VWA domain of S5a restricts the ability to bind ubiquitin and Ubl to the 26S proteasome. Mol. Biol. Cell *25*, 3988–3998.

Polge, C., Heng, A.-E., Jarzaguet, M., Ventadour, S., Claustre, A., Combaret, L., Béchet, D., Matondo, M., Uttenweiler-Joseph, S., Monsarrat, B., et al. (2011). Muscle actin is polyubiquitinylated in vitro and in vivo and targeted for breakdown by the E3 ligase MuRF1. Faseb J. *25*, 3790–3802.

Raben, N., Schreiner, C., Baum, R., Takikita, S., Xu, S., Xie, T., Myerowitz, R., Komatsu, M., Van der Meulen, J.H., Nagaraju, K., et al. (2010). Suppression of autophagy permits successful enzyme replacement therapy in a lysosomal storage disorder--murine Pompe disease. Autophagy *6*, 1078–1089.

Rabl, J., Smith, D.M., Yu, Y., Chang, S.-C., Goldberg, A.L., and Cheng, Y. (2008). Mechanism of gate opening in the 20S proteasome by the proteasomal ATPases. Mol. Cell *30*, 360–368.

Radhakrishnan, S.K., Lee, C.S., Young, P., Beskow, A., Chan, J.Y., and Deshaies, R.J. (2010). Transcription factor Nrf1 mediates the proteasome recovery pathway after proteasome inhibition in mammalian cells. Mol. Cell *38*, 17–28.

Ramos, P.C. (2004). Role of C-terminal Extensions of Subunits 2 and 7 in Assembly and Activity of Eukaryotic Proteasomes. Journal of Biological Chemistry *279*, 14323–14330.

Ramos, P.C., Höckendorff, J., Johnson, E.S., Varshavsky, A., and Dohmen, R.J. (1998). Ump1p Is Required for Proper Maturation of the 20S Proteasome and Becomes Its Substrate upon Completion of the Assembly. Cell *92*, 489–499.

Ray, M., and Lakhotia, S.C. (2015). The commonly used eye-specific sev-GAL4 and GMR-GAL4 drivers in Drosophila melanogaster are expressed in tissues other than eyes also. J. Genet. *94*, 407–416.

Reinke, R., Krantz, D.E., Yen, D., and Zipursky, S.L. (1988). Chaoptin, a cell surface glycoprotein required for Drosophila photoreceptor cell morphogenesis, contains a repeat motif found in yeast and human. Cell *52*, 291–301.

Reinstein, E., and Ciechanover, A. (2006). Narrative review: protein degradation and human diseases: the ubiquitin connection. Ann. Intern. Med. *145*, 676–684.

Reits, E.A., Benham, A.M., Plougastel, B., Neefjes, J., and Trowsdale, J. (1997). Dynamics of proteasome distribution in living cells. The EMBO Journal *16*, 6087–6094.

Rock, K.L., Gramm, C., Rothstein, L., Clark, K., Stein, R., Dick, L., Hwang, D., and Goldberg, A.L. (1994). Inhibitors of the proteasome block the degradation of most cell proteins and the generation of peptides presented on MHC class I molecules. Cell *78*, 761–771.

Rock, K.L., York, I.A., and Goldberg, A.L. (2004). Post-proteasomal antigen processing for major histocompatibility complex class I presentation. Nature Immunology *5*, 670–677.

Roelofs, J., Park, S., Haas, W., Tian, G., McAllister, F.E., Huo, Y., Lee, B.-H., Zhang, F., Shi, Y., Gygi, S.P., et al. (2009). Chaperone-mediated pathway of proteasome regulatory particle assembly. Nature *459*, 861–865.

Rubinsztein, D.C. (2006). The roles of intracellular protein-degradation pathways in neurodegeneration. Nature *443*, 780–786.

Sakata, E., Yamaguchi, Y., Kurimoto, E., Kikuchi, J., Yokoyama, S., Yamada, S., Kawahara, H., Yokosawa, H., Hattori, N., Mizuno, Y., et al. (2003). Parkin binds the Rpn10 subunit of 26S proteasomes through its ubiquitin-like domain. EMBO Rep. *4*, 301–306.

Sancak, Y., Bar-Peled, L., Zoncu, R., Markhard, A.L., Nada, S., and Sabatini, D.M. (2010). Ragulator-Rag complex targets mTORC1 to the lysosomal surface and is necessary for its activation by amino acids. Cell *141*, 290–303.

Sandri, M., Sandri, C., Gilbert, A., Skurk, C., Calabria, E., Picard, A., Walsh, K., Schiaffino, S., Lecker, S.H., and Goldberg, A.L. (2004). Foxo transcription factors induce the atrophy-related ubiquitin ligase atrogin-1 and cause skeletal muscle atrophy. Cell *117*, 399–412.

Sartori, R., Schirwis, E., Blaauw, B., Bortolanza, S., Zhao, J., Enzo, E., Stantzou, A., Mouisel, E., Toniolo, L., Ferry, A., et al. (2013). BMP signaling controls muscle mass. Nat. Genet. *45*, 1309–1318.

Satoo, K., Noda, N.N., Kumeta, H., Fujioka, Y., Mizushima, N., Ohsumi, Y., and Inagaki, F. (2009). The structure of Atg4B-LC3 complex reveals the mechanism of LC3 processing and delipidation during autophagy. The EMBO Journal *28*, 1341–1350.

Saville, K.J., and Belote, J.M. (1993). Identification of an essential gene, l(3)73Ai, with a dominant temperature-sensitive lethal allele, encoding a Drosophila proteasome subunit. Proc. Natl. Acad. Sci. U.S.a. *90*, 8842–8846.

Schmidt, M., Haas, W., Crosas, B., Santamaria, P.G., Gygi, S.P., Walz, T., and Finley, D. (2005a). The HEAT repeat protein Blm10 regulates the yeast proteasome by capping the core particle. Nature Structural & Molecular Biology *12*, 294–303.

Schmidt, M., Hanna, J., Elsasser, S., and Finley, D. (2005b). Proteasome-associated proteins: regulation of a proteolytic machine. Biol. Chem. *386*, 725–737.

Schulz, C., Kiger, A.A., Tazuke, S.I., Yamashita, Y.M., Pantalena-Filho, L.C., Jones, D.L., Wood, C.G., and Fuller, M.T. (2004). A misexpression screen reveals effects of bag-of-marbles and TGF beta class signaling on the Drosophila male germ-line stem cell lineage. Genetics *167*, 707–723.

Schwalm, C., Jamart, C., Benoit, N., Naslain, D., Prémont, C., Prévet, J., Van Thienen, R., Deldicque, L., and Francaux, M. (2015). Activation of autophagy in human skeletal muscle is dependent on exercise intensity and AMPK activation. Faseb J. *29*, 3515–3526.

Schweisguth, F. (1999). Dominant-negative mutation in the beta2 and beta6 proteasome subunit genes affect alternative cell fate decisions in the Drosophila sense organ lineage. Proc. Natl. Acad. Sci. U.S.a. *96*, 11382–11386.

Schweitzer, A., Aufderheide, A., Rudack, T., Beck, F., Pfeifer, G., Plitzko, J.M., Sakata, E., Schulten, K., Förster, F., and Baumeister, W. (2016). Structure of the human 26S proteasome at a resolution of 3.9 Å. Proc. Natl. Acad. Sci. U.S.a. *113*, 7816–7821.

Scott, S.V., and Klionsky, D.J. (1998). Delivery of proteins and organelles to the vacuole from the cytoplasm. Current Opinion in Cell Biology *10*, 523–529.

Seeger, M., Hartmann-Petersen, R., Wilkinson, C.R.M., Wallace, M., Samejima, I., Taylor, M.S., and Gordon, C. (2003). Interaction of the Anaphase-promoting Complex/Cyclosome and Proteasome Protein Complexes with Multiubiquitin Chain-binding Proteins. Journal of Biological Chemistry *278*, 16791–16796.

Seo, H., Sonntag, K.-C., and Isacson, O. (2004). Generalized brain and skin proteasome inhibition in Huntington's disease. Ann. Neurol. *56*, 319–328.

Shi, J., Luo, L., Eash, J., Ibebunjo, C., and Glass, D.J. (2011). The SCF-Fbxo40 complex induces IRS1 ubiquitination in skeletal muscle, limiting IGF1 signaling. Dev. Cell *21*, 835–847.

Shibatani, T., Carlson, E.J., Larabee, F., McCormack, A.L., Früh, K., and Skach, W.R. (2006). Global organization and function of mammalian cytosolic proteasome pools: Implications for PA28 and 19S regulatory complexes. Mol. Biol. Cell *17*, 4962–4971.

Smith, C.D., Carney, J.M., Starke-Reed, P.E., Oliver, C.N., Stadtman, E.R., Floyd, R.A., and Markesbery, W.R. (1991). Excess brain protein oxidation and enzyme dysfunction in normal aging and in Alzheimer disease. Proc. Natl. Acad. Sci. U.S.a. *88*, 10540–10543.

Smith, D.M., Chang, S.-C., Park, S., Finley, D., Cheng, Y., and Goldberg, A.L. (2007). Docking of the Proteasomal ATPases“ Carboxyl Termini in the 20S Proteasome”s α Ring Opens the Gate for Substrate Entry. Mol. Cell *27*, 731–744.

Smith, S., Giriat, I., Schmitt, A., and de Lange, T. (1998). Tankyrase, a poly(ADP-ribose) polymerase at human telomeres. Science *282*, 1484–1487.

Smyth, K.A., and Belote, J.M. (1999). The dominant temperature-sensitive lethal DTS7 of Drosophila melanogaster encodes an altered 20S proteasome beta-type subunit. Genetics *151*, 211–220.

Speese, S.D., Trotta, N., Rodesch, C.K., Aravamudan, B., and Broadie, K. (2003). The ubiquitin proteasome system acutely regulates presynaptic protein turnover and synaptic efficacy. Curr. Biol. *13*, 899–910.

Stadtmueller, B.M., and Hill, C.P. (2011). Proteasome activators. Mol. Cell *41*, 8–19.

Steffan, J.S., Kazantsev, A., Spasic-Boskovic, O., Greenwald, M., Zhu, Y.Z., Gohler, H.,

Wanker, E.E., Bates, G.P., Housman, D.E., and Thompson, L.M. (2000). The Huntington's disease protein interacts with p53 and CREB-binding protein and represses transcription. Proc. Natl. Acad. Sci. U.S.a. *97*, 6763–6768.

Steffen, J., Seeger, M., Koch, A., and Krüger, E. (2010). Proteasomal degradation is transcriptionally controlled by TCF11 via an ERAD-dependent feedback loop. Mol. Cell *40*, 147–158.

Stitt, T.N., Drujan, D., Clarke, B.A., Panaro, F., Timofeyva, Y., Kline, W.O., Gonzalez, M., Yancopoulos, G.D., and Glass, D.J. (2004). The IGF-1/PI3K/Akt pathway prevents expression of muscle atrophy-induced ubiquitin ligases by inhibiting FOXO transcription factors. Mol. Cell *14*, 395–403.

Strehl, B., Seifert, U., Krüger, E., Heink, S., Kuckelkorn, U., and Kloetzel, P.-M. (2005). Interferon-gamma, the functional plasticity of the ubiquitin-proteasome system, and MHC class I antigen processing. Immunological Reviews *207*, 19–30.

Sun, H., Gong, Y., Qiu, J., Chen, Y., Ding, F., and Zhao, Q. (2014). TRAF6 inhibition rescues dexamethasone-induced muscle atrophy. Int J Mol Sci *15*, 11126–11141.

Sundaram, P., Pang, Z., Miao, M., Yu, L., and Wing, S.S. (2009). USP19-deubiquitinating enzyme regulates levels of major myofibrillar proteins in L6 muscle cells. Am. J. Physiol. Endocrinol. Metab. *297*, E1283–E1290.

Suzuki, R., Moriishi, K., Fukuda, K., Shirakura, M., Ishii, K., Shoji, I., Wakita, T., Miyamura, T., Matsuura, Y., and Suzuki, T. (2009). Proteasomal turnover of hepatitis C virus core protein is regulated by two distinct mechanisms: a ubiquitin-dependent mechanism and a ubiquitin-independent but PA28gamma-dependent mechanism. J. Virol. *83*, 2389–2392.

Szlanka, T., Haracska, L., Kiss, I., Deák, P., Kurucz, E., Andó, I., Virágh, E., and Udvardy, A. (2003). Deletion of proteasomal subunit S5a/Rpn10/p54 causes lethality, multiple mitotic defects and overexpression of proteasomal genes in Drosophila melanogaster. J. Cell. Sci. *116*, 1023–1033.

Tanahashi, N., Murakami, Y., Minami, Y., Shimbara, N., Hendil, K.B., and Tanaka, K. (2000). Hybrid proteasomes. Induction by interferon-gamma and contribution to ATP-dependent proteolysis. Journal of Biological Chemistry *275*, 14336–14345.

Tanaka, K., and Kasahara, M. (1998). The MHC class I ligand-generating system: roles of immunoproteasomes and the interferon-gamma-inducible proteasome activator PA28. Immunological Reviews *163*, 161–176.

Tanaka, K., Yoshimura, T., Tamura, T., Fujiwara, T., Kumatori, A., and Ichihara, A. (1990). Possible mechanism of nuclear translocation of proteasomes. FEBS Letters *271*, 41–46.

Tang, A.H., and Rando, T.A. (2014). Induction of autophagy supports the bioenergetic demands of quiescent muscle stem cell activation. The EMBO Journal *33*, 2782–2797.

Tawa, N.E., Odessey, R., and Goldberg, A.L. (1997). Inhibitors of the proteasome reduce the accelerated proteolysis in atrophying rat skeletal muscles. J. Clin. Invest. *100*, 197–203.

Taylor, J.P., Hardy, J., and Fischbeck, K.H. (2002). Toxic proteins in neurodegenerative disease.

Science *296*, 1991–1995.

Thrower, J.S., Hoffman, L., Rechsteiner, M., and Pickart, C.M. (2000). Recognition of the polyubiquitin proteolytic signal. The EMBO Journal *19*, 94–102.

Tian, G., Park, S., Lee, M.J., Huck, B., McAllister, F., Hill, C.P., Gygi, S.P., and Finley, D. (2011). An asymmetric interface between the regulatory and core particles of the proteasome. Nature Structural & Molecular Biology *18*, 1259–1267.

Tiao, G., Fagan, J.M., Samuels, N., James, J.H., Hudson, K., Lieberman, M., Fischer, J.E., and Hasselgren, P.O. (1994). Sepsis stimulates nonlysosomal, energy-dependent proteolysis and increases ubiquitin mRNA levels in rat skeletal muscle. J. Clin. Invest. *94*, 2255–2264.

Tintignac, L.A., Lagirand, J., Batonnet, S., Sirri, V., Leibovitch, M.P., and Leibovitch, S.A. (2005). Degradation of MyoD mediated by the SCF (MAFbx) ubiquitin ligase. J. Biol. Chem. *280*, 2847–2856.

Tsvetkov, P., Mendillo, M.L., Zhao, J., Carette, J.E., Merrill, P.H., Cikes, D., Varadarajan, M., van Diemen, F.R., Penninger, J.M., Goldberg, A.L., et al. (2015). Compromising the 19S proteasome complex protects cells from reduced flux through the proteasome. Elife *4*, 109.

Tsvetkov, P., Sokol, E., Jin, D., Brune, Z., Thiru, P., Ghandi, M., Garraway, L.A., Gupta, P.B., Santagata, S., Whitesell, L., et al. (2017). Suppression of 19S proteasome subunits marks emergence of an altered cell state in diverse cancers. Proc. Natl. Acad. Sci. U.S.a. *114*, 382–387.

Turrens, J.F., and Boveris, A. (1980). Generation of superoxide anion by the NADH dehydrogenase of bovine heart mitochondria. Biochem. J. *191*, 421–427.

Ugrankar, R., Berglund, E., Akdemir, F., Tran, C., Kim, M.S., Noh, J., Schneider, R., Ebert, B., and Graff, J.M. (2015). Drosophila glucome screening identifies Ck1alpha as a regulator of mammalian glucose metabolism. Nat Commun *6*, 7102.

Unno, M., Mizushima, T., Morimoto, Y., Tomisugi, Y., Tanaka, K., Yasuoka, N., and Tsukihara, T. (2002). The structure of the mammalian 20S proteasome at 2.75 A resolution. Structure *10*, 609–618.

Ustrell, V., Hoffman, L., Pratt, G., and Rechsteiner, M. (2002). PA200, a nuclear proteasome activator involved in DNA repair. The EMBO Journal *21*, 3516–3525.

Velichutina, I., Connerly, P.L., Arendt, C.S., Li, X., and Hochstrasser, M. (2004). Plasticity in eucaryotic 20S proteasome ring assembly revealed by a subunit deletion in yeast. The EMBO Journal *23*, 500–510.

Voisin, L., Breuillé, D., Combaret, L., Pouyet, C., Taillandier, D., Aurousseau, E., Obled, C., and Attaix, D. (1996). Muscle wasting in a rat model of long-lasting sepsis results from the activation of lysosomal, Ca2+ -activated, and ubiquitin-proteasome proteolytic pathways. J. Clin. Invest. *97*, 1610–1617.

Wang, X.H., Zhang, L., Mitch, W.E., LeDoux, J.M., Hu, J., and Du, J. (2010a). Caspase-3 cleaves specific 19 S proteasome subunits in skeletal muscle stimulating proteasome activity. J. Biol. Chem. *285*, 21249–21257.

Wang, X., Yen, J., Kaiser, P., and Huang, L. (2010b). Regulation of the 26S proteasome complex during oxidative stress. Sci Signal *3*, ra88–ra88.

Wang, X., Blagden, C., Fan, J., Nowak, S.J., Taniuchi, I., Littman, D.R., and Burden, S.J. (2005). Runx1 prevents wasting, myofibrillar disorganization, and autophagy of skeletal muscle. Genes Dev. *19*, 1715–1722.

Watanabe, Y., Suzuki, O., Haruyama, T., and Akaike, T. (2003). Interferon-gamma induces reactive oxygen species and endoplasmic reticulum stress at the hepatic apoptosis. J. Cell. Biochem. *89*, 244–253.

Wendler, P., Lehmann, A., Janek, K., Baumgart, S., and Enenkel, C. (2004). The bipartite nuclear localization sequence of Rpn2 is required for nuclear import of proteasomal base complexes via karyopherin alphabeta and proteasome functions. Journal of Biological Chemistry *279*, 37751–37762.

Wesley, C.S., and Saez, L. (2000). Analysis of notch lacking the carboxyl terminus identified in Drosophila embryos. The Journal of Cell Biology *149*, 683–696.

Whitby, F.G., Masters, E.I., Kramer, L., Knowlton, J.R., Yao, Y., Wang, C.C., and Hill, C.P. (2000). Structural basis for the activation of 20S proteasomes by 11S regulators. Nature *408*, 115–120.

Wiles, B., Miao, M., Coyne, E., Larose, L., Cybulsky, A.V., and Wing, S.S. (2015). USP19 deubiquitinating enzyme inhibits muscle cell differentiation by suppressing unfolded-protein response signaling. Mol. Biol. Cell *26*, 913–923.

Wilkinson, C.R., Wallace, M., Morphew, M., Perry, P., Allshire, R., Javerzat, J.P., McIntosh, J.R., and Gordon, C. (1998). Localization of the 26S proteasome during mitosis and meiosis in fission yeast. The EMBO Journal *17*, 6465–6476.

Wing, S.S., and Goldberg, A.L. (1993). Glucocorticoids activate the ATP-ubiquitin-dependent proteolytic system in skeletal muscle during fasting. Am. J. Physiol. *264*, E668–E676.

Witt, E., Zantopf, D., Schmidt, M., Kraft, R., Kloetzel, P.-M., and Krüger, E. (2000). Characterisation of the newly identified human Ump1 homologue POMP and analysis of LMP7(β5i) incorporation into 20 S proteasomes. Journal of Molecular Biology *301*, 1–9.

Wójcik, C., and DeMartino, G.N. (2002). Analysis of Drosophila 26 S proteasome using RNA interference. Journal of Biological Chemistry *277*, 6188–6197.

Xie, Y., and Varshavsky, A. (2001). RPN4 is a ligand, substrate, and transcriptional regulator of the 26S proteasome: A negative feedback circuit. Proc. Natl. Acad. Sci. U.S.a. *98*, 3056–3061.

Xie, Y., and Varshavsky, A. (2002). UFD4 lacking the proteasome-binding region catalyses ubiquitination but is impaired in proteolysis. Nat. Cell Biol. *4*, 1003–1007.

YAO, Y., TOTH, C.R., Huang, L., WONG, M.-L., DIAS, P., BURLINGAME, A.L., COFFINO, P., and WANG, C.C. (1999). α5 subunit in Trypanosoma brucei proteasome can self-assemble to form a cylinder of four stacked heptamer rings. Biochem. J. *344*, 349–358.

Yashiroda, H., Toda, Y., Otsu, S., Takagi, K., Mizushima, T., and Murata, S. (2015). N-terminal

α7 deletion of the proteasome 20S core particle substitutes for yeast PI31 function. Mol. Cell. Biol. *35*, 141–152.

Yu, Y., Smith, D.M., Kim, H.M., Rodriguez, V., Goldberg, A.L., and Cheng, Y. (2010). Interactions of PAN's C-termini with archaeal 20S proteasome and implications for the eukaryotic proteasome-ATPase interactions. The EMBO Journal *29*, 692–702.

Zhang, Y., Nicholatos, J., Dreier, J.R., Ricoult, S.J.H., Widenmaier, S.B., Hotamisligil, G.S., Kwiatkowski, D.J., and Manning, B.D. (2014). Coordinated regulation of protein synthesis and degradation by mTORC1. Nature *513*, 440–443.

Zhao, J., Brault, J.J., Schild, A., and Goldberg, A.L. (2014). Coordinate activation of autophagy and the proteasome pathway by FoxO transcription factor. Autophagy *4*, 378–380.

Zhao, J., Brault, J.J., Schild, A., Cao, P., Sandri, M., Schiaffino, S., Lecker, S.H., and Goldberg, A.L. (2007). FoxO3 coordinately activates protein degradation by the autophagic/lysosomal and proteasomal pathways in atrophying muscle cells. Cell Metabolism *6*, 472–483.

Zhao, J., Zhai, B., Gygi, S.P., and Goldberg, A.L. (2015). mTOR inhibition activates overall protein degradation by the ubiquitin proteasome system as well as by autophagy. Proc. Natl. Acad. Sci. U.S.a. *112*, 15790–15797.

Zhong, L., and Belote, J.M. (2007). The testis-specific proteasome subunit Pros 6T of D. melanogaster is required for individualization and nuclear maturation during spermatogenesis. Development *134*, 3517–3525.

Zirin, J., Nieuwenhuis, J., Samsonova, A., Tao, R., and Perrimon, N. (2015). Regulators of autophagosome formation in Drosophila muscles. PLoS Genet. *11*, e1005006.

Zwickl, P., Kleinz, J., and Baumeister, W. (1994). Critical elements in proteasome assembly. Nat. Struct. Biol. *1*, 765–770.